ENGINEERING RESEARCH INSTITUTE
UNIVERSITY OF MICHIGAN
ANN ARBOR

Technical Report No. 2

PLASMA FLUCTUATIONS IN CROSSED ELECTRIC AND MAGNETIC FIELDS

by
(Hugh Wallace)
Hugh W. Batten
Harold C. Early

Approved by: The Czar

Professor W. G. Dow
Dept. of Electrical
Engineering

OFFICE OF ORDNANCE RESEARCH
ORDNANCE CORPS, U.S. ARMY
CONTRACT NO. DA-20-018 ORD-11913
Dept. of Army Proj. No. 599-16-005
Ordnance R & D Project No. TB3-0001
OOR Proj. No. 146

Contract Title: "Electrical Means of
Producing High Velocity Wind"

May, 1954

UMM 278

RESUME OF PREVIOUS WORK ON THE CONTRACT

The study of plasma fluctuations in crossed electric and magnetic fields is an outgrowth of a previous investigation of "Electrical Means of Producing High Velocity Wind." This earlier research was concerned with various mechanisms by which electrical and magnetic forces could be used to produce directed momentum in a low density ionized gas. Summary Report #1 (Electrical Wind Phenomena; November, 1952) describes several types of electrical wind generators, but emphasizes the wind generated by a discharge transverse to a strong magnetic field.

A quantitative study of wind effects requires means of determining the temperature and velocity of a high temperature ionized gas. Suitable techniques for measuring the electrical properties of the plasma are also essential. Therefore, a substantial part of this research program has been concerned with the evaluation of existing methods of instrumentation and in devising new techniques.

Most of the experimental difficulties encountered in measuring the plasma properties are caused by the violent electrical fluctuations. These fluctuations are several orders of magnitude larger than those in conventional discharges and they completely mask the data usually obtainable by probe measurements. Such electrical fluctuations are an outstanding feature of this type of discharge, and so little information has been published on this subject that a thorough study seemed warranted. Accordingly, an investigation of the noise fluctuations was undertaken in January, 1953. The present report summarizes that activity.

TABLE OF CONTENTS

LIST OF ILLUSTRATIONS

ABSTRACT

This study is an investigation of the electrical fluctuations associated with a gas discharge in a magnetic field. The study is both theoretical and experimental. The theory is divided into two parts: a study of the ion fluctuations and a study of the electron fluctuations. The theory on ion fluctuations is a natural generalization of the work by Tonks and Langmuir; it extends their work to include the presence of a magnetic field, ion drift, and ion collisions. A dispersion relation is derived, and such quantities in the solution as the velocity and path of the ions, the electric field, and the space-charge densities are studied. It is shown that: (1) the plane waves in the plasma are polarized in the direction of propagation, (2) the ion orbit in velocity space is an ellipse, (3) the fluctuations introduce a mobility, and (4) there is no electric field associated with waves at the ion cyclotron frequency.

The theoretical study of electronic disturbances is not as extensively treated as the ionic disturbances since the former has been more completely covered in the literature. However, the low-frequency waves propagating normally to the magnetic field are studied in some detail. It is shown that these waves can grow as they propagate, that they tend to propagate in the direction of electron drift, and that their velocity of propagation approximates the velocity of electron drift. These arguments are in agreement with the experiments.

The experimental studies were undertaken in an especially designed diode. Probes were introduced into the plasma region of the glow discharge in this diode, and the fluctuating electrical signals on the probes were studied. The parameters that were varied included the type of gas, pressure in the discharge, magnetic field, power input, type of probe, and probe location. The power spectrum of the fluctuations was studied over a broad frequency range, and the correlation between the fluctuations on neighboring probes in the discharge was investigated. The power spectrum shows a high level continuous amplitude over the entire frequency range studied (0.5 to 4,000 megacycles per second in some cases). A careful study of discharges in hydrogen and helium near the ion cyclotron frequency showed a sharp dip in the spectrum at that frequency. The amplitude of the power spectrum increases at all frequencies with a decrease in pressure; the low-frequency amplitude increases with an increase in magnetic field.

The experimental data taken to correlate the fluctuations on two neighboring probes show that the fluctuations on the "downstream" probe are delayed in time with respect to the "upstream" probe. This delay is determined by cross-correlating the fluctuations on the two probes. The velocity and direction of propagation for the low-frequency fluctuations are determined in this way. The results show that the direction of propagation is approximately that of the electron drift, and the velocity of propagation is somewhat less than the Lorentz drift velocity.

HISTORICAL NOTE

Electrical fluctuations in a gas discharge tube were first reported in 1863,[1] but little progress was made in the investigation of these fluctuations until twenty-five years ago when the classic article of Tonks and Langmuir was published.[2] This article set the pattern both theoretically and experimentally for most of the work that followed. The experimental work of Tonks and Langmuir was a probe study in which the probe was a part of a parallel resonant circuit. The frequencies of oscillations in the plasma could be determined by varying the resonant frequency of the circuit and detecting the voltage across the circuit terminals. Tonks and Langmuir observed a set of discrete frequencies using this technique, some of which they identified with electron vibrations in the plasma, others with ion vibrations in accordance with their theories.

Theoretically the Tonks-Langmuir point of view was this: imagine the frequency scale divided up into "low frequencies" and "high frequencies;" the oscillations in the low-frequency range are caused by ion vibrations and the electrons are sufficiently mobile so that they are in thermal equilibrium with the electric potential established by such vibrations. The high-frequency oscillations are attributed to electron vibrations, the ions being relatively so heavy that they

---

[1] See Reference 57. The references are found in Appendix 1.

[2] Reference 59.

remain immobile.

This argument of Tonks and Langmuir led them to a set of differential equations for the high-frequency disturbances and a set of differential equations for low-frequency disturbances. The dependent variables in these equations included the density of charged particles, the electric potential, the particle velocity, etc.; the independent variables in their study were time and displacement (in one dimension). The authors, assuming that the oscillations were small, linearized the differential equations and looked for solutions in which the dependent variables had the form

$$be^{i(\omega t-\beta z)}$$

where b, ω, and β are constants; t is time and z represents the displacement. The differential equations in this type of problem are homogeneous, and the existence of solutions in this form requires that the frequency ω and the propagation constant β be related by an equation

$$\beta = \beta(\omega)$$

called the dispersion relation. The goal of Tonks and Langmuir, and most other theoretical investigators, was to obtain this function for certain assumed conditions, and by examining it, interpret and predict experimental results. Tonks and Langmuir obtained two dispersion relations for the electron vibrations, the one applying when the electron direction of vibration and the direction of propagation are

collinear (longitudinal propagation), the other appropriate when the electrons vibrate normally to the propagating direction (transverse propagation). They derived a single dispersion relation for the ions corresponding to longitudinal propagation. These theoretical studies of Tonks and Langmuir were of limited generality; they allowed for no magnetic field; they neglected particle drift velocity, collisions between particles, and the temperature of the vibrating particles.

Parallel with the work of Tonks and Langmuir, and others such as J. J. Thomson,[1] who were investigating the electrical fluctuations in gas-discharge tubes, there developed an interest in the propagation properties of the ionosphere. The theoretical work on this subject by Hartree, Appleton and Builder, von Lassen, and others was largely a derivation of the dispersion relation for the medium.[2] The assumptions involved were just those applied by Tonks and Langmuir to their electron vibrations except that the derivation was generalized to account for collisions and the presence of a magnetic field.

In 1945 Cobine and Gallagher published an impressive experimental study on electrical fluctuations in hot-cathode arcs.[3] Their work was an investigation of the power spectrum of the fluctuations, i.e. the distribution of the fluctuating

---

[1]Reference 57.

[2]References 1, 2, 30, and 62.

[3]Reference 16 and References 17 and 18.

power with frequency. This study covered a frequency range from twenty-five cycles per second to nine megacycles per second, pressures from one hundredth to two millimeters of mercury, and magnetic field strengths from zero to nine hundred gauss. They explained the continuous power spectrum they observed on the basis of the Tonks-Langmuir ion theory. For low magnetic fields they also noted a resonance that could not be identified with the plasma and apparently belonged to ions oscillating in a potential minimum at the cathode.[1]

Bailey submitted a generalized theory on electron vibrations in 1948.[2] This theory was a derivation of a still more general dispersion relation which included the influence of a drift velocity for the electrons. Perhaps more important than the generalized theory was Bailey's interpretation of the dispersion relation. Before Bailey it was assumed that the frequency components in the fluctuations were those prescribed by the dispersion relation for real values of the propagation constant. Bailey asserted that the frequency components in the fluctuations were precisely those that increased in amplitude as the fluctuations propagated in the medium; consequently he examined the dispersion relation for those real frequencies which determined a complex propagation constant with a positive imaginary part. On this basis he

---

[1]The recognition and identification of this oscillation is apparently due to Ballantine, Reference 10.

[2]Reference 4 and also References 5, 6, 7, and 8.

determined that there were three frequency bands in which electron fluctuations would occur.

These comments on the fluctuation studies are brief; they omit the important work of Bohm and Gross who introduced electron temperature into the longitudinal electron dispersion relation and made other important contributions; they omit the work of Wehner who has developed a plasma electron oscillator tube and the important related work in electron beam tubes. The intention of this historical note is to leave these impressions: (a) the theoretical studies on the electrical fluctuations are usually a derivation of a dispersion relation for the medium; (b) the experimental studies are largely an examination of the distribution of noise power with frequency; and (c) neither the argument of Bailey which identifies the continuous electrical noise spectrum with amplified electronic disturbances nor the argument of Cobine who credited the frequencies of this spectrum below nine megacycles to unamplified ion vibrations has been proven experimentally.

OUTLINE OF THE STUDY

The various electrical fluctuations of an ionized gas have usually been explained in one of four ways depending on the motion of the charged particles responsible for the fluctuations. They are identified (1) with plasma ion oscillations, (2) with plasma electron oscillations, (3) with ions vibrating in a potential minimum at the cathode, and (4) with the thermal motion of charged particles. The first three of these categories represent the organized motion of large groups of charged particles displaced from their equilibrium. For those frequencies where such group fluctuations are present the thermal spectrum is obscured, but thermal noise has been observed in gas discharges.[1] Indeed Knol has shown that the thermal noise spectrum can be used to measure the electron temperature in the plasma.

The high-intensity plasma fluctuations are of principal interest in the present study. These fluctuations are usually ascribed to either plasma ion or plasma electron oscillations. They always seem to be present in gas-discharge tubes, playing an important role in the scattering, diffusion, and ionization processes of the gas. Plasma fluctuations reach especially high intensity in a static magnetic field, and the experimental work of this paper concerns these fluctuations in the presence of a strong magnetic field.

---

[1]References 36 and 44.

In this study little attention is given to the source of energy responsible for the plasma disturbances although it is speculated that cathode sputtering probably initiates the fluctuations.

Chapters I and II are theoretical investigations of ion and electron oscillations. These investigations are developed assuming an idealized plasma with smooth properties so that the discrete nature of the charged particles can be ignored. Chapter I is a generalization of the Tonks-Langmuir theory on ion fluctuations. Their work is extended to include the influence of a magnetic field, a drift velocity for the ions, and ion collisions. A dispersion relation is derived, and using the dispersion relation in the differential equations such quantities as the ion and electron space-charge densities, the electric field, and the particle motion are derived and studied.

Chapter II represents a similar study for the electrons. A general "stream" theory due to Gabor is presented. It is shown that many familiar electron dispersion relations can be derived from this theory. A derivation of the dispersion relation for transverse propagation which includes the electron temperature is given. The velocity and gain of low-frequency propagation normal to the magnetic field are studied.

Chapter III is an experimental study of the power spectrum of the fluctuating potential. Data are presented for a frequency range from half a megacycle to three thousand megacycles per second.

Various pressures, gases, and magnetic fields are considered. Data for two kinds of probes, various locations of the probes, and different power levels are given. In Chapter IV the group velocity and gain for low-frequency noise fluctuations are investigated experimentally. The dependence of this group velocity on power, magnetic field, and pressure is shown.

Chapter V presents a comparison between the theoretical and the experimental work. The work of other investigators is brought in at this point and an attempt is made to explain the fluctuations.

Chapter I

A THEORY OF ION FLUCTUATIONS

The theory presented in this section is a natural generalization of the work of Tonks and Langmuir.[1] An extension of their theory is made by including the influences of a magnetic field, drift velocity in the ion stream, and ion collisions. The generalization is carried through without the burden of any additional assumptions not already present in the Tonks-Langmuir argument. Since the equations and their graphical representation become very unwieldy, much of the theory presented is limited to considering the influence of the magnetic field, neglecting ion drift and ion collisions.

1.1 The general differential equations

The following equations are taken from electromagnetic field theory:[2]

the electric divergence relation,

$$\nabla \cdot \vec{E} = \frac{e}{\epsilon_0} (N_p - N_e) \quad ; \qquad (1.1)$$

where $\vec{E}$ is the electric field strength, e the fundamental charge, ϵ_0 the free-space dielectric constant, and N_p and N_e the density of ions and electrons, respectively,

---

[1] Reference 59.

[2] Symbols are defined where they are first introduced in the report. In addition, a list of symbols is given in Appendix 2. The MKS system of units is used throughout this paper.

continuity for the ions,

$$\frac{\partial N_p}{\partial t} + \nabla . (N_p \vec{v}_p) = 0 ; \qquad (1.2)$$

where $\vec{v}_p$ is the velocity of the ions, and

the Lorentz force law for an ion,

$$\frac{e}{m_p} (\vec{E} + \vec{v}_p \times \vec{B}_o) = \frac{d\vec{v}_p}{dt} + \nu \vec{v}_p ; \qquad (1.3)$$

where m_p is the ion mass, $\vec{B}_o$ the magnetic flux density, and υ a damping constant approximately equal to the ion collision frequency.

In addition to these equations, the hypothesis is added that any fluctuations in the gas are sufficiently slow that the electrons remain in thermal equilibrium, and therefore satisfy the Maxwell-Boltzmann law for spatial distribution,

$$N_e = A \exp \left(\frac{e\Phi}{kT} \right) , \qquad (1.4)$$

where A is a constant, Φ is the electric potential, T is the electron temperature, and k is the Boltzmann constant. The addition of the familiar approximation

$$\vec{E} = - \nabla \Phi \qquad (1.5)$$

to the system of equations above expresses the mathematical problem in terms of nine equations in nine variables.

1.2 The perturbation form of the differential equations

This general system of equations is far too complicated for a general solution, but treating the disturbances that

are responsible for the electrical fluctuations as small changes in such a solution provides a linear system of differential equations that is more tractable. Thus the procedure is to examine the perturbation equations corresponding to relations (1.1-1.5). Denoting the undisturbed variables by the subscript zero, the perturbed variables can be written:

$$\begin{aligned} \vec{\xi} &= \vec{E} - \vec{E}_0 , \\ n_p &= N_p - N_0 , \\ n_e &= N_e - N_0 , \\ \vec{u} &= \vec{v}_p - \vec{v}_{p_0} , \\ \text{and } \phi &= \Phi - \Phi_0 . \end{aligned} \tag{1.6}$$

In writing these expressions it has already been assumed that the undisturbed electron and ion densities are equal constants, corresponding to a plasma. It will also be assumed here that ion drift in the unperturbed solution and ion collisions can be neglected. (A more general derivation and discussion which does not neglect these factors is given in Appendix 3.) With these assumptions the perturbation equations for (1.1-1.5) can be written:

$$\nabla^2 \phi = -\frac{e}{\epsilon_0}\left(n_p - n_e\right), \tag{1.7}$$

$$\frac{\partial n_p}{\partial t} = -N_0 \nabla \cdot \vec{u} , \tag{1.8}$$

$$\frac{e}{m_p}\left(-\nabla\phi + \vec{u}\times\vec{B}_0\right) = \frac{\partial \vec{u}}{\partial t} , \tag{1.9}$$

$$\text{and} \quad n_e = N_0\left[\exp\frac{e\phi}{kT} - 1\right].$$

This last equation is not yet in a linear form. If the perturbed potential energy is small compared with the thermal electron energy, then the exponential of this expression can be approximated by the first two terms of its power series, and

$$n_e = \frac{eN_o\phi}{kT} \quad . \tag{1.10}$$

Equations (1.7-1.10) represent the perturbation form of the equations (1.1-1.5). They can be combined to obtain a linear differential equation in the velocity $\vec{u}$, as will now be described. The electron density can be eliminated using (1.7) and (1.10).

$$\nabla^2\phi = -\frac{e}{\epsilon_o}\left(n_p - \frac{eN_o\phi}{kT}\right). \tag{1.11}$$

Differentiating this partially with respect to time and substituting $\frac{\partial n_p}{\partial t}$ from (1.8) into the result gives,

$$\frac{\partial}{\partial t}\left(\nabla^2\phi\right) = \frac{e}{\epsilon_o}\left(N_o\,\nabla\cdot\vec{u} + \frac{eN_o}{kT}\,\frac{\partial\phi}{\partial t}\right). \tag{1.12}$$

Taking the gradient of this expression and substituting $\nabla\phi$ from equation (1.9) gives

$$\nabla^2\left[\frac{\partial^2\vec{u}}{\partial t^2} - \frac{\partial\vec{u}}{\partial t}\times\vec{\omega}_c\right] = \frac{\omega_p^{\,2}\,m_p}{kT}\left[\frac{\partial^2\vec{u}}{\partial t^2} - \frac{\partial\vec{u}}{\partial t}\times\vec{\omega}_c\right]$$

$$-\omega_p^{\,2}\,\nabla\left(\nabla\cdot\vec{u}\right), \tag{1.13}$$

where $\vec{\omega}_c = \frac{e\vec{B}_o}{m_p}$, the cyclotron frequency vector, and

$\omega_p = \sqrt{\frac{e^2 N_o}{\epsilon_o m_p}}$, the plasma ion radian frequency.

1.3 The dispersion relation for a set of solutions

The differential equation (1.13) is certainly not simple, but since the noise spectrum is of particular interest, is is natural to investigate the frequency structure of solutions to (1.13), that is, to seek a set of solutions with the form,

$$\vec{u} = \left[u_1 e^{i(\omega t - \beta z)}, \; u_2 e^{i(\omega t - \beta z)}, \; u_3 e^{i(\omega t - \beta z)} \right] \quad (1.14)$$

where u_1, u_2, and u_3 are constants. Thus, we are looking for solutions of equation (1.13) in the form of waves propagated in the z-direction with a frequency ω and a propagation constant β. Without loss of generality the component of the cyclotron frequency vector in the x-direction can be taken equal to zero. Then,

$$\vec{\omega}_c = (0, \; \omega_c \sin\theta, \; \omega_c \cos\theta) , \quad (1.15)$$

where θ is the angle between the direction of propagation and the direction of the magnetic field.

Now substituting from (1.14) and (1.15) into (1.13) gives,

$$\left(\beta^2 + \frac{\omega_p^2 m_p}{kT} \right) \left[\omega^2 u_1 + i\omega \left(u_2 \omega_c \cos\theta - u_3 \omega_c \sin\theta \right) \right] = 0, \quad (1.16a)$$

$$\left(\beta^2 + \frac{\omega_p^2 m_p}{kT} \right) \left[\omega^2 u_2 - i\omega u_1 \omega_c \cos\theta \right] = 0, \text{ and} \quad (1.16b)$$

$$\left(\beta^2 + \frac{\omega_p^2 m_p}{kT} \right) \left[\omega^2 u_3 + i\omega u_1 \omega_c \sin\theta \right] - \omega_p^2 \beta^2 u_3 = 0 . \quad (1.16c)$$

Equations (1.16) are three linear, homogeneous equations in the three unknowns, u_1, u_2, and u_3. Therefore a solution exists if and only if the determinant of the coefficients vanishes. Thus,

$$\begin{vmatrix} \omega^2 & i\omega\omega_c\cos\theta & -i\omega\omega_c\sin\theta \\ -i\omega\omega_c\cos\theta & \omega^2 & 0 \\ i\omega\omega_c\sin\theta & 0 & \omega^2-\omega_0^2 \end{vmatrix} = 0$$

where

$$\omega_0^2 \equiv \frac{\omega_p^2}{1+\dfrac{\omega_p^2 m_p}{\beta^2 kT}} \tag{1.17}$$

has been introduced to simplify the notation. Expanding the determinant gives

$$\left(\omega^2-\omega_c^2\cos^2\theta\right)\left(\omega^2-\omega_0^2\right)-\omega^2\omega_c^2\sin^2\theta = 0, \tag{1.18a}$$

and solving this expression which is quadratic in the square of the frequency leads to

$$\omega^2 = \frac{\omega_c^2+\omega_0^2}{2} \pm \sqrt{\left(\frac{\omega_c^2+\omega_0^2}{2}\right)^2 - \omega_0^2\,\omega_c^2\cos^2\theta}\ . \tag{1.18b}$$

A graphical representation of these two dispersion relations is given in Figures 1.1 and 1.2. The two solutions for frequency complement each other: the one solution applies when the frequency exceeds the cyclotron frequency, the other being appropriate when the frequency is less than the cyclotron frequency.

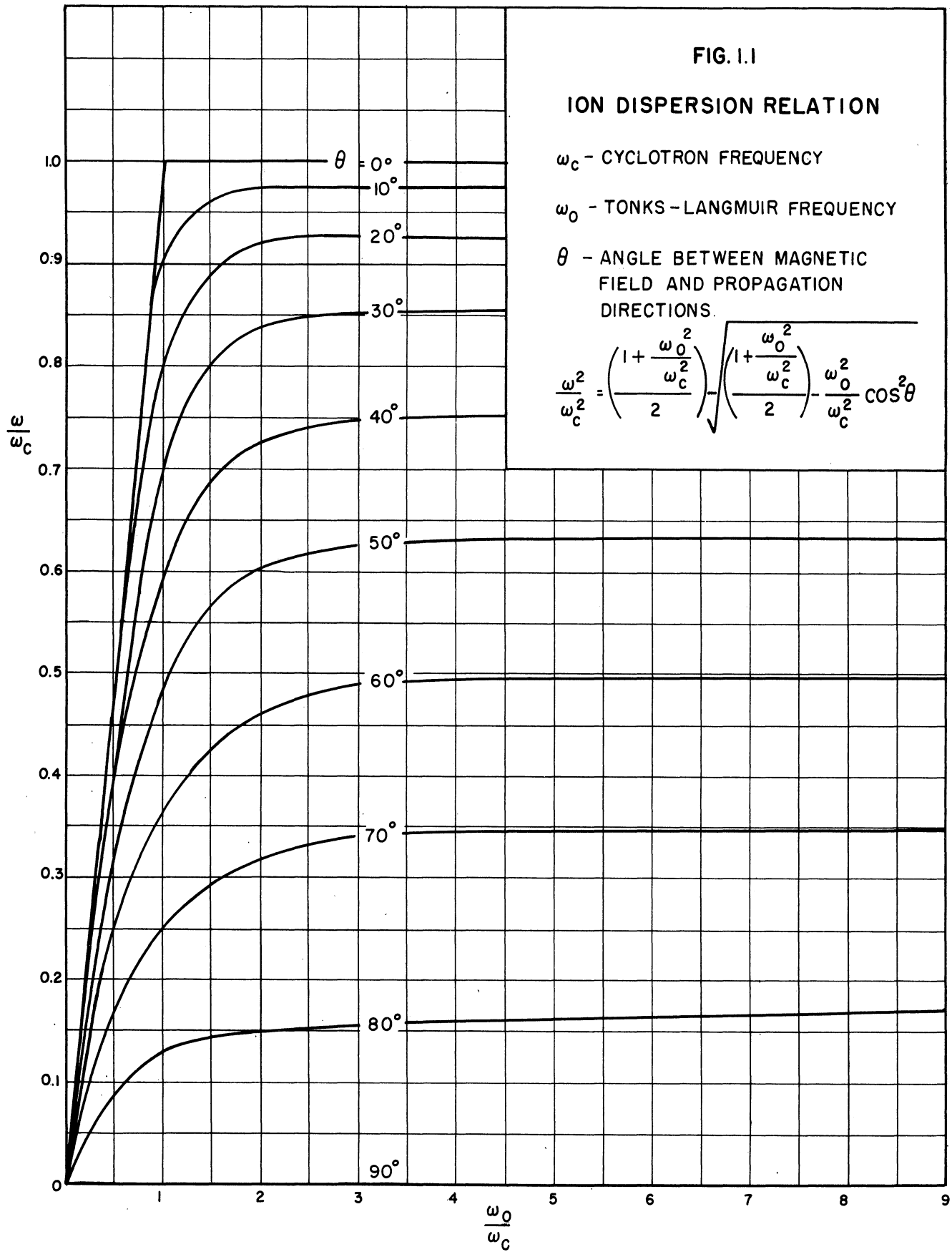
FIG. I.I
ION DISPERSION RELATION
ω_c - CYCLOTRON FREQUENCY
ω_0 - TONKS-LANGMUIR FREQUENCY
θ - ANGLE BETWEEN MAGNETIC FIELD AND PROPAGATION DIRECTIONS.
$\frac{\omega^2}{\omega_c^2} = \left(\frac{1+\frac{\omega_0^2}{\omega_c^2}}{2}\right) - \sqrt{\left(\frac{1+\frac{\omega_0^2}{\omega_c^2}}{2}\right) - \frac{\omega_0^2}{\omega_c^2}\cos^2\theta}$
θ = 0°
10°
20°
30°
40°
50°
60°
70°
80°
90°
$\frac{\omega}{\omega_c}$
$\frac{\omega_0}{\omega_c}$
0
0.1
0.2
0.3
0.4
0.5
0.6
0.7
0.8
0.9
1.0
1
2
3
4
5
6
7
8
9

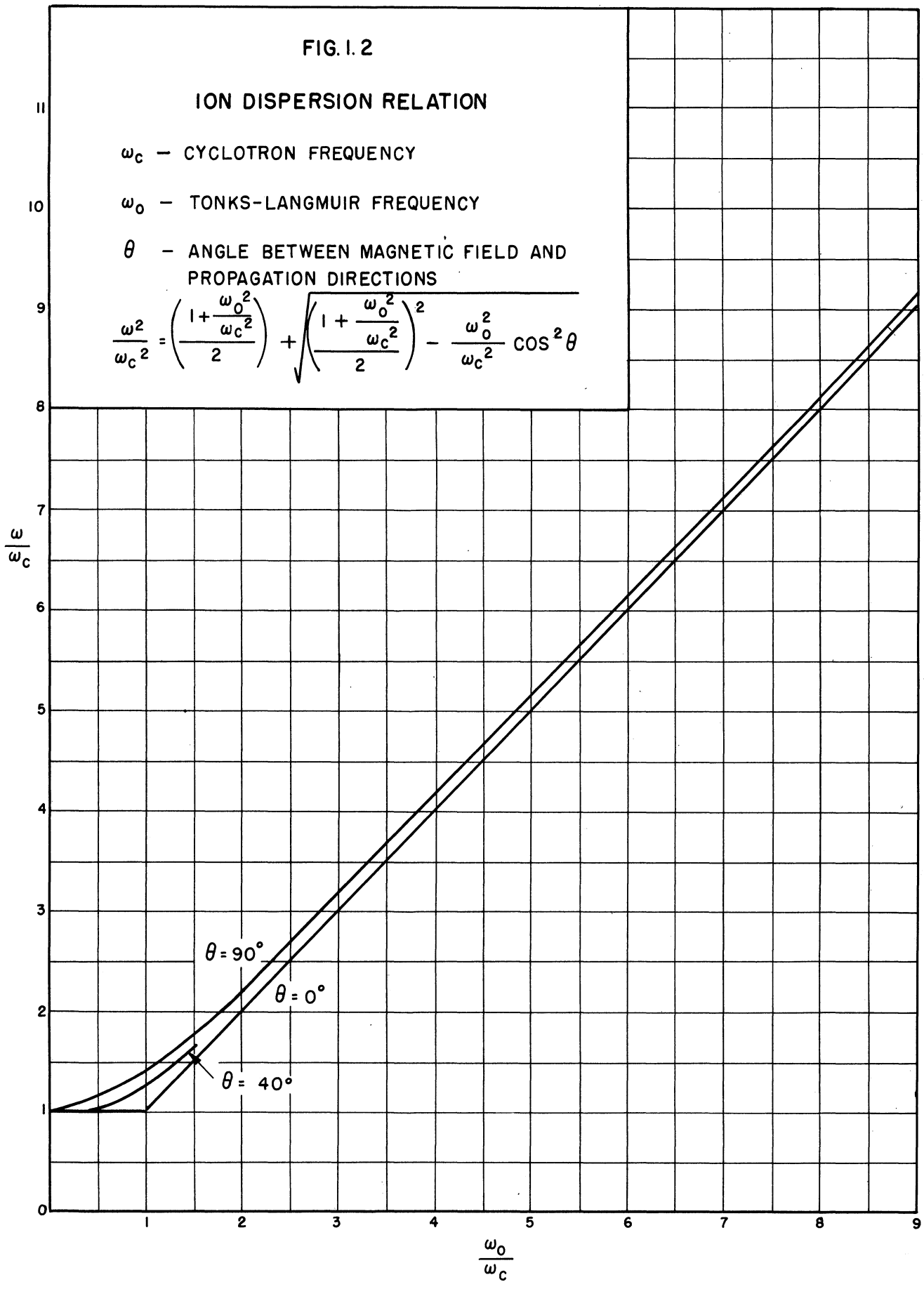
FIG. I. 2
ION DISPERSION RELATION
ω_c – CYCLOTRON FREQUENCY
ω_0 – TONKS-LANGMUIR FREQUENCY
θ – ANGLE BETWEEN MAGNETIC FIELD AND PROPAGATION DIRECTIONS
$\frac{\omega^2}{\omega_c^2} = \left(\frac{1+\frac{\omega_0^2}{\omega_c^2}}{2}\right) + \sqrt{\left(\frac{1+\frac{\omega_0^2}{\omega_c^2}}{2}\right)^2 - \frac{\omega_0^2}{\omega_c^2}\cos^2\theta}$
$\frac{\omega}{\omega_c}$
$\frac{\omega_0}{\omega_c}$
θ = 90°
θ = 0°
θ = 40°
0
1
2
3
4
5
6
7
8
9
10
11

Certain observations on the equations given in (1.18) are especially worthy of note.

a. $\omega_c = 0$. If the magnetic field vanishes, then the frequency reduces to that given by Tonks and Langmuir,[1]

$$\omega^2 = \omega_0^2 \equiv \frac{\omega_p^2}{1+\frac{\omega_p^2 m_p}{\beta^2 kT}} \quad . \tag{1.17}$$

This function is plotted in Figure 1.3.

b. $N_0 = 0$. If the density of charged particles approaches zero, the frequency is given by the cyclotron resonant frequency.

c. If the direction of propagation is parallel to the B_0 field, there are two solutions, $\omega = \omega_0$ and $\omega = \omega_c$. The ion motion for the first of these is entirely in the direction of the magnetic field (longitudinal propagation) and consequently independent of the magnetic field. In the second case the ion motion is transverse to the field.

d. If the propagation is normal to the magnetic field,

$$\omega^2 = \omega_0^2 + \omega_c^2 \quad .$$

e. For all possible real propagation constants there is a greatest frequency given by,

$$\omega_{max}^2 = \omega_p^2 + \omega_c^2 \quad . \tag{1.19}$$

f. The frequency as a function of ω_0 and ω_c is symmetric in ω_0 and ω_c, i.e.,

$$\omega(\omega_0, \omega_c) = \omega(\omega_c, \omega_0) \quad .$$

g. In Figure 1.1 the asymptotes are given by

$$\frac{\omega}{\omega_c} = \cos\theta,$$

in Figure 1.2 by

$$\frac{\omega^2}{\omega_c^2} = \sin^2\theta + \frac{\omega_0^2}{\omega_c^2} \quad .$$

---

[1] Reference 59.

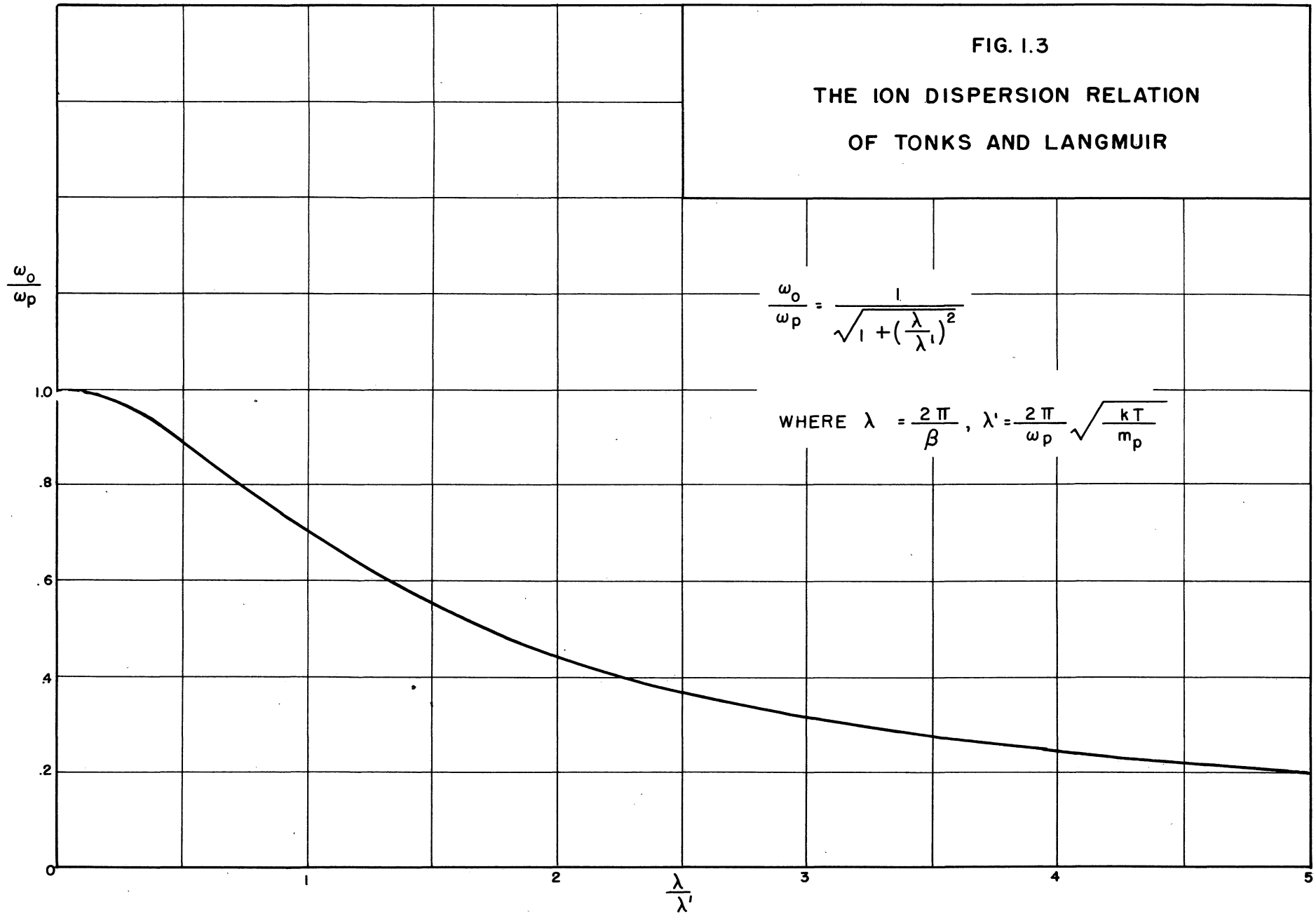
FIG. 1.3
THE ION DISPERSION RELATION
OF TONKS AND LANGMUIR
$\frac{\omega_0}{\omega_p} = \frac{1}{\sqrt{1+\left(\frac{\lambda}{\lambda'}\right)^2}}$
WHERE $\lambda = \frac{2\pi}{\beta}$, $\lambda' = \frac{2\pi}{\omega_p}\sqrt{\frac{kT}{m_p}}$
$\frac{\omega_0}{\omega_p}$
1.0
.8
.6
.4
.2
0
1
2
3
4
5
$\frac{\lambda}{\lambda'}$

1.4 The solutions of the perturbed equations

1.4.1 The ion velocity

It was pointed out in the last section that the differential equation in the velocity (1.13) can be satisfied by

$$\vec{u} = \left[u_1, u_2, u_3\right] e^{i(\omega t - \beta z)} \tag{1.14}$$

with u_1, u_2, and u_3 constant if and only if the dispersion relation (1.18) is satisfied. Using this dispersion relation the ion velocity, the ion trajectory, electron and ion densities, electric field, and so on can be determined. We proceed first to the velocity components given by equation (1.16). From (1.16c),

$$u_1 = -i \frac{\omega_0^2 - \omega^2}{\omega \omega_c \sin\theta} u_3 ,$$

or,

$$u_1 = i \frac{\omega \omega_c \sin\theta}{\omega^2 - \omega_c^2 \cos^2\theta} u_3 \tag{1.20}$$

by using the dispersion relation (1.18) to eliminate ω_0^2. From (1.16b),

$$u_2 = \frac{i \omega_c \cos\theta}{\omega} u_1 . \tag{1.21}$$

Since the equations (1.16) are linear and homogeneous the components u_1, u_2, and u_3 are only determined to a constant factor d which may depend on the frequency and other parameters such as the magnetic field. The role of d in the physical problem is one of scaling the solution which is arbitrary up

to a constant.[1] With the choice

$$u_3 = \frac{\omega^2 - \omega_c^2 \cos^2\theta}{\omega_c^2 \sin\theta}\, d$$

all other components are determined. From (1.20)

$$u_1 = i\,\frac{\omega}{\omega_c}\, d\,,$$

and putting this in (1.21) one obtains

$$u_2 = -d\,\cos\theta\,.$$

Thus,

$$\vec{u} = \left[i\,\frac{\omega}{\omega_c} d,\ -d\,\cos\theta,\ \frac{\omega^2 - \omega_c^2\cos^2\theta}{\omega_c^2 \sin\theta}\, d \right] e^{\,i(\omega t - \beta z)}\,. \qquad (1.22)$$

For simplicity of notation we now write $\omega_1 = \frac{\omega}{\omega_c}$, i.e., ω is normalized with respect to ω_c , and also let

$$\zeta = \omega t - \beta z\ . \qquad (1.23)$$

Apart from a phase change common to all the components, the velocity $\vec{u}$ can be expressed merely as its real part, and

$$\vec{u} = \left[u_x, u_y, u_z\right] = \left[-d\,\omega_1 \sin\zeta,\ -d\cos\theta\cos\zeta,\ \frac{\omega_1^2 - \cos^2\theta}{\sin\theta}\, d\,\cos\zeta \right]. \qquad (1.24a)$$

In this form the components of the ion velocity are given in terms of the variable ζ , and in the velocity space with u_x, u_y , and u_z as coordinates

$$\begin{aligned} u_x &= -d\,\omega_1 \sin\zeta\,, \\ u_y &= -d\cos\theta\,\cos\zeta\,, \\ \text{and} \\ u_z &= \frac{\omega_1^2 - \cos^2\theta}{\sin\theta}\, d\,\cos\zeta \end{aligned} \qquad (1.24b)$$

---

[1] It should be intuitively clear that if one has a solution with certain velocity components, electric field components, a potential, etc., that doubling these velocity components, field components, and the potential, etc. also gives a solution. This freedom in the solution is carried mathematically in the factor d.

parametrically define a curve. Indeed this curve is an ellipse with center at the origin, for $\frac{u_y}{u_z}$ = constant, and

$$\left(\frac{u_x}{d\omega}\right)^2 + \left(\frac{u_y}{d\cos\theta}\right)^2 = 1 .$$

A sketch for such a curve is given in Figure 1.4.

Since this curve of velocity is an ellipse, it is evident that both the velocity and the position of the ion are in the plane of this ellipse, and there is merit in choosing a new set of axes in that plane to study the particle behavior. It is clear from Figure 1.4 that u_x can be retained as a coordinate since it is parallel to an axis of the ellipse. The choice of a new axis $u_{y'}$ as shown in the figure with

$$\rho = \tan^{-1}\frac{u_z}{u_y} = \tan^{-1}\left(\frac{\cos^2\theta - \omega_1^2}{\cos\theta\ \sin\theta}\right) \qquad (1.25)$$

reduces the description of the velocity orbit to the ellipse

$$\left(\frac{u_x}{d\omega_1}\right)^2 + \left(\frac{u_{y'}\sin\rho}{d\cos\theta}\right)^2 = 1 . \qquad (1.26)$$

Equation (1.26) is one type of solution for the motion of the particle in velocity space. It is also possible to express the velocity components u_x and $u_{y'}$ as functions of time, but these solutions are clumsy and of lesser interest.

1.4.2 The ion path

We now turn to the problem of solving the system of equations (1.24b) to determine the path of the ion. These equations can be rewritten:

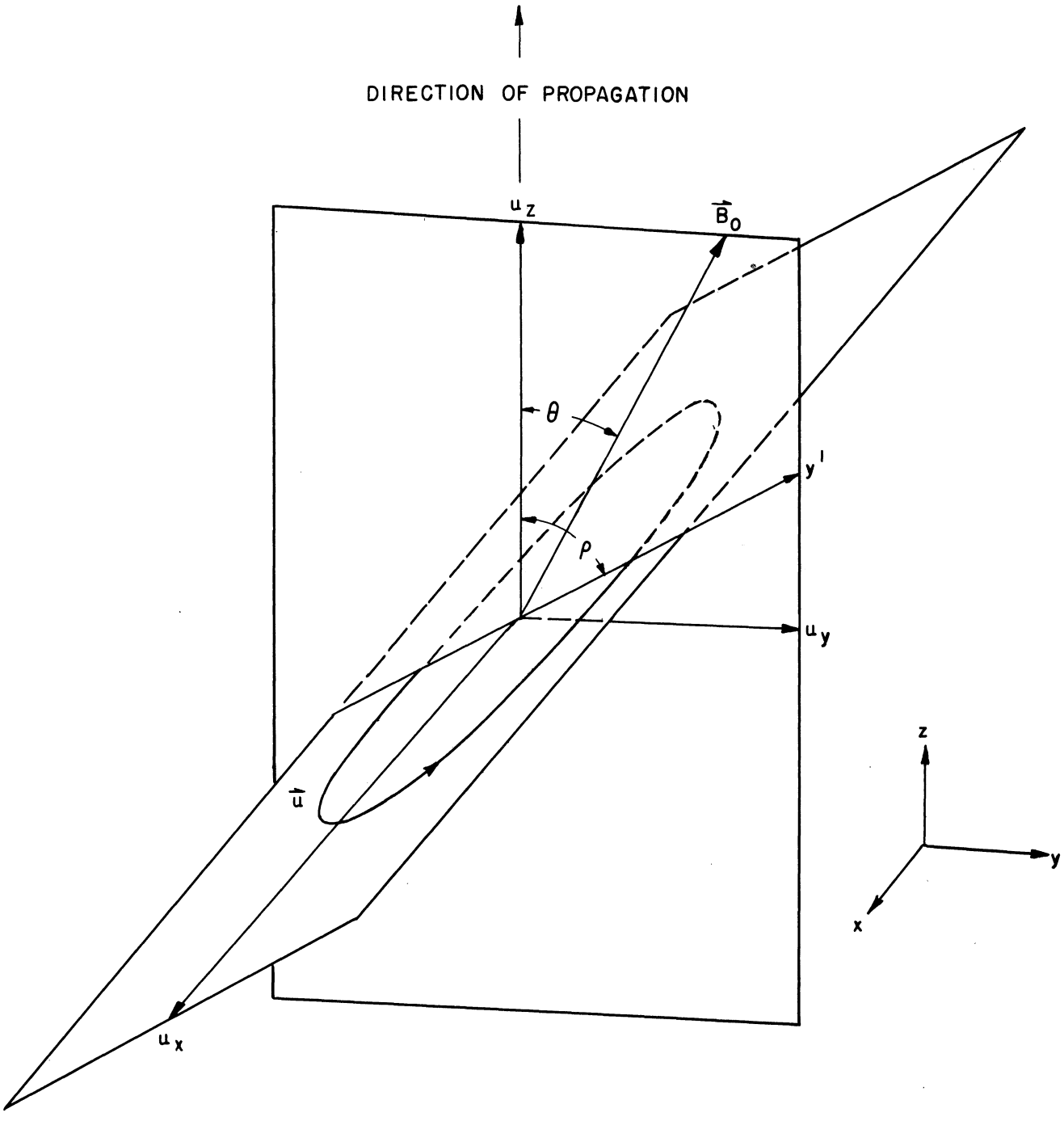

FIG. 1.4

FIGURE SHOWING THE PLANE OF PARTICLE MOTION AND A TYPICAL ORBIT FOR THE ION VELOCITY VECTOR

$$u_x \equiv \frac{dx}{dt} = -a \sin \zeta ,$$

$$u_y \equiv \frac{dy}{dt} = -b \cos \zeta , \qquad (1.24c)$$

$$\text{and} \quad u_y \equiv \frac{dz}{dt} = c \cos \zeta ,$$

where $$\zeta = \omega t - \beta z \ . \qquad (1.23)$$

-a, -b, and c are merely new symbols for the constant coefficients. From (1.23)

$$\frac{d\zeta}{dt} = \omega - \beta \frac{dz}{dt} = \omega - \beta c \cos \zeta , \qquad (1.27)$$

and dividing this into u_x in (1.24c) gives

$$\frac{dx}{d\zeta} = -\frac{a \sin \zeta}{\omega - \beta c \cos \zeta} \ .$$

Integrating this expression and choosing

$x = 0$ for $\zeta = \frac{\pi}{2}$, one obtains

$$x = -\frac{a}{\omega} \int_{\frac{\pi}{2}}^{\zeta} \frac{\sin p \, dp}{1 - \frac{\beta c}{\omega} \cos p} \qquad (1.28)$$

$$= -\frac{a}{\beta c} \ln \left(1 - \frac{\beta c}{\omega} \cos \zeta \right);$$

solving this for cos ζ gives

$$\cos \zeta = \frac{\omega}{\beta c} \left(1 - e^{-\frac{\beta c}{a} x} \right) \ . \qquad (1.29)$$

Now from (2.24c)

$$\frac{dy}{dx} = \frac{b \cos \zeta}{a \sin \zeta} = \frac{b \cos \zeta}{\pm a \sqrt{1 - \cos^2 \zeta}} ,$$

and substitution into this from (1.29) for cos ζ gives

$$\frac{dy}{dx} = \frac{b\omega}{a\beta c} \frac{\left(1 - e^{-\frac{\beta c}{a} x} \right)}{\pm \sqrt{1 - \left(\frac{\omega}{\beta c} \right)^2 \left(1 - e^{-\frac{\beta c}{a} x} \right)^2}} \ . \qquad (1.30)$$

The integration of this expression gives the ion path, for as argued in the last section the particle motion is in the x-y' plane and

$$y = y' \sin \rho \tag{1.31}$$

where ρ is a constant given by (1.25). Thus choosing $y' = 0$ where $x = 0$ one obtains

$$\left(\frac{a \sin \rho}{b}\right) y' = \pm \int_0^x \frac{\left(1 - e^{-\frac{\beta c}{a} p}\right) dp}{\sqrt{g^2 - \left(1 - e^{-\frac{\beta c}{a} p}\right)^2}} \tag{1.32a}$$

with $g = \dfrac{\beta c}{\omega}$. (1.33)

Under a change of variables this integral can be written in several different forms including:

$$\left(\frac{\beta c \sin \rho}{b}\right) y' = \pm \int_0^{\frac{\beta c x}{a}} \frac{\left(1 - e^{-p}\right) dp}{\sqrt{g^2 - \left(1 - e^{-p}\right)^2}} \tag{1.32b}$$

and

$$\left(\frac{\omega \sin \rho}{b}\right) y' = \pm \int_0^{\sin^{-1}\left(\frac{1 - e^{-\frac{\beta c}{a} x}}{g}\right)} \frac{\sin p \, dp}{1 - g \sin p} \, . \tag{1.32c}$$

In this last form the integration can be carried out (see Dwight, 436.01), but the expression is so awkward that it is more convenient to use an integral form directly in studying the particle path. From (1.32b) it is clear that the normalized y' variable $\left(\dfrac{\beta c \sin \rho}{b}\right) y'$ as a function of the normalized x variable $\left(\dfrac{\beta c}{a}\right) x$ depends only on the single

parameter g. Figure 1.5 shows some solutions for the ion path obtained by solving (1.32b) graphically. The apparent similarity between these curves and the trochoidal orbits that arise for isolated charged particles in crossed electric and magnetic fields should not be taken too seriously, for these orbits are not cycloidal, nor is there a static electric field in this case; also the drift velocity for an ion here is not normal to the magnetic field, and the frequency in this motion is the frequency of the wave, not the cyclotron frequency.[1]

1.4.3 The electric field

The perturbed velocities corresponding to a given frequency and choice of propagation direction are now known (equation(1.24b)); consequently the electric field can be obtained using equation (1.9). Expressing (1.9) as three scalar equations gives

$$\frac{e}{m_p}\xi_x = \frac{\partial u_x}{\partial t} - u_y \cos\theta + u_z \omega_c \sin\theta,$$

$$\frac{e}{m_p}\xi_y = \frac{\partial u_y}{\partial t} + u_x \omega_c \cos\theta, \qquad (1.33)$$

$$\text{and} \quad \frac{e}{m_p}\xi_z = \frac{\partial u_z}{\partial t} - u_x \omega_c \sin\theta.$$

Now substituting the velocity components from (1.24b) into these equations gives

---

[1] Figure 1.5 shows that the fluctuations provide a mobility in the direction y'.

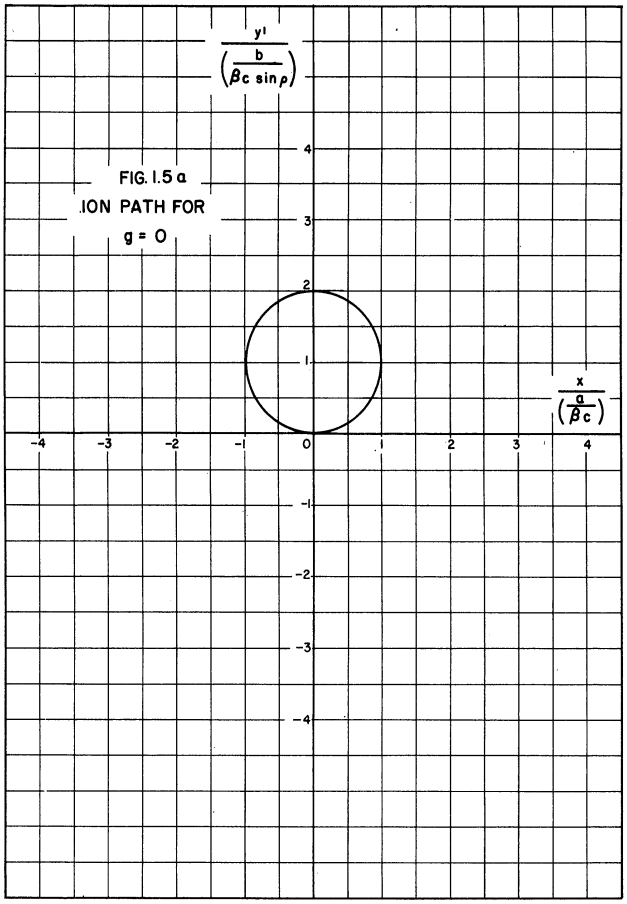

FIG. 1.5a
ION PATH FOR
g = 0

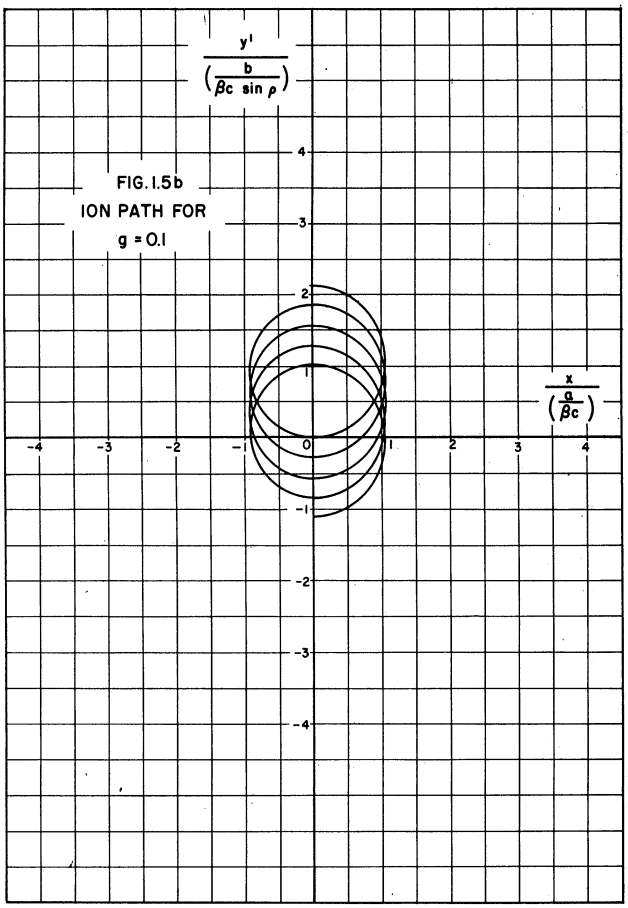

FIG. 1.5b
ION PATH FOR
g = 0.1

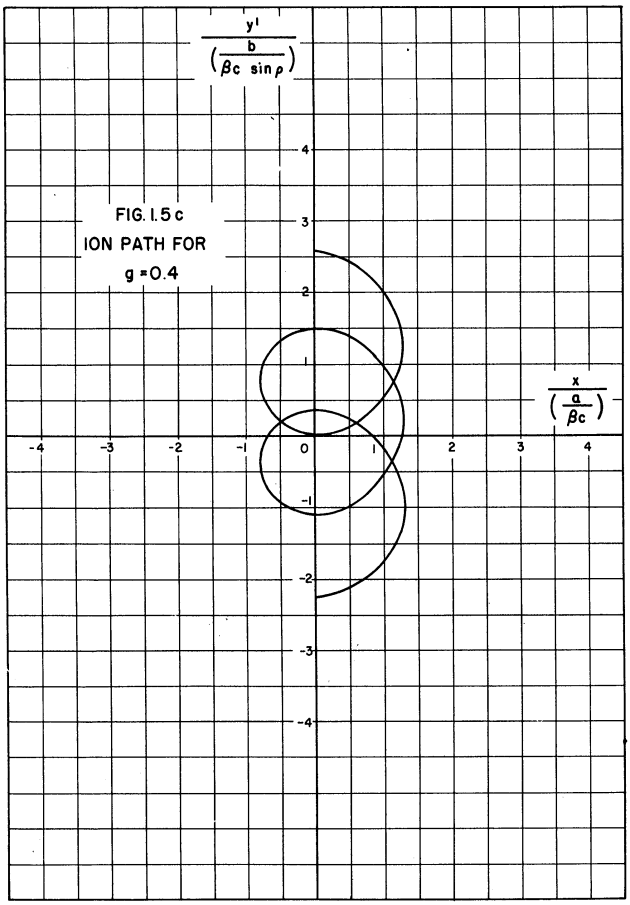

FIG. 1.5c
ION PATH FOR
g = 0.4

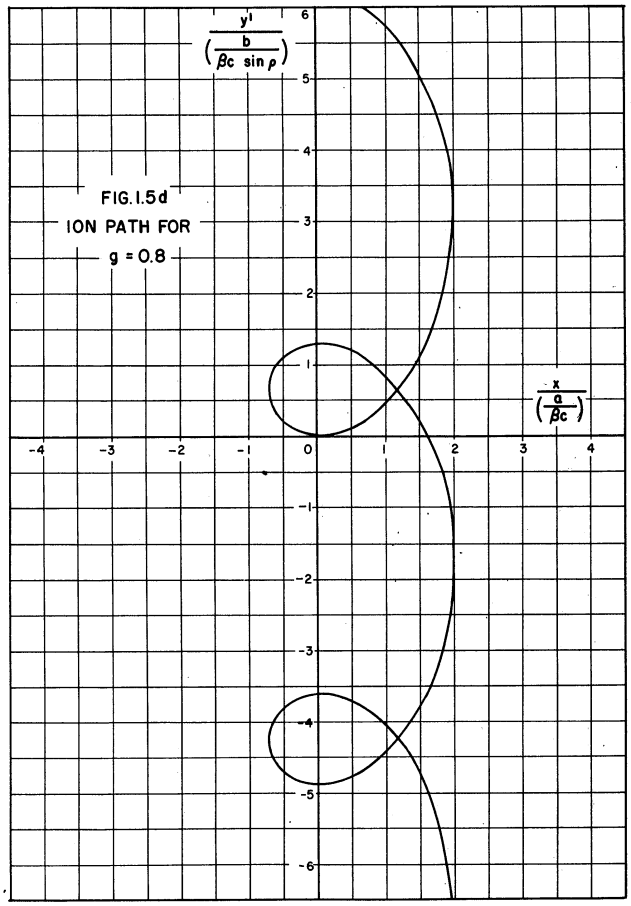

FIG. 1.5d
ION PATH FOR
g = 0.8

$$\frac{e}{\omega_c m_p}\xi_x = -d\omega_1^2\cos\zeta + d\cos^2\theta\cos\zeta + \left(\omega_1^2-\cos^2\theta\right) d\cos\zeta = 0\ ,$$

$$\frac{e}{\omega_c m_p}\xi_y = d\,\omega_1\cos\theta\sin\zeta - d\,\omega_1\cos\theta\sin\zeta = 0, \quad \text{and}$$

$$\begin{aligned}\frac{e}{\omega_c m_p}\xi_z &= -\omega_1\frac{\omega_1^2-\cos^2\theta}{\sin\theta}\, d\sin\zeta + d\,\omega_1\sin\theta\sin\zeta \\ &= \frac{d\omega_1}{\sin\theta}\left(-\omega_1^2+\cos^2\theta+\sin^2\theta\right)\sin\zeta \\ &= \frac{d\,\omega_1}{\sin\theta}\left(1-\omega_1^2\right)\sin\zeta\ .\end{aligned} \tag{1.34}$$

Thus, <u>the components of the electric field normal to the direction of propagation vanish.</u> The component of the electric field in the direction of propagation is given by (1.34).

1.4.4 The ion and electron densities

Integration of the electric field (1.34) gives the perturbed potential

$$\frac{e}{\omega_c m_p}\phi = \frac{-d\omega_1}{\beta\sin\theta}\left(1-\omega_1^2\right)\cos\zeta, \tag{1.35}$$

and then equation (1.10) provides the corresponding electron density at once,

$$n_e = \frac{eN_0\phi}{kT} = -\frac{N_0 m_p d\,\omega}{kT\beta\sin\theta}\left(1-\omega_1^2\right)\cos\zeta\ . \tag{1.36}$$

The ion density can similarly be obtained from (1.8) since the velocity is known.

$$n_p = \frac{N_0\beta\, d}{\omega\sin\theta}\left(\omega_1^2-\cos^2\theta\right)\cos\zeta\ . \tag{1.37}$$

Now it should be clear from the general approach given to the problem of ion oscillations that the electrons in seeking their thermal equilibrium tend to diminish the amplitude of the ion oscillations, and it is informative to inquire how successful they are in this role of damping the ion disturbances. We take as a measure of this damping the quantity $\left(1-\frac{n_e}{n_p}\right)$ since the perturbed potential will vanish when this expression does. Use of (1.36) and (1.37) gives

$$\left(1-\frac{n_e}{n_p}\right)=1-\frac{m_p\omega^2}{kT\beta^2}\,\frac{\left(1-\omega_1^2\right)}{\left(\cos^2\theta-\omega_1^2\right)}\,, \tag{1.38}$$

but solving the dispersion relation (1.18a) for ω_0^2 leads to

$$\omega_0^{\,2}=\frac{\omega^2\left(1-\omega_1^2\right)}{\left(\cos^2\theta-\omega_1^2\right)}\,. \tag{1.39}$$

Substitution for the right member of this expression which appears in (1.38) gives

$$\left(1-\frac{n_e}{n_p}\right)=1-\frac{m_p\omega_0^{\,2}}{kT\beta^2}\,.$$ Replacing

ω_0^2 by its value which is given in (1.17), one obtains

$$\left(1-\frac{n_e}{n_p}\right)=1-\frac{m_p}{kT\beta^2}\cdot\frac{\omega_p^2}{1+\dfrac{\omega_p^{\,2}m_p}{kT\beta^2}}\,,$$

or

$$\left(1-\frac{n_e}{n_p}\right)=\frac{1}{1+\dfrac{\omega_p^{\,2}m_p}{kT\beta^2}}=\frac{\omega_0^2}{\omega_p^2}\,. \tag{1.40}$$

This is an interesting expression. Note first of all that it is independent of the magnetic field and of the direction of propagation with respect to the magnetic field. Thus

although the electron and ion perturbed densities depend on these quantities, their ratio does not. Also, the electron and ion densities are in phase and the ion density must exceed that of the electrons. Assuming that the other factors on the right in (1.40) do not change, then an increase in electron temperature T requires a decrease in the ratio of electron to ion density. This might be anticipated since the potential peaks and potential troughs established by the ions cannot so readily capture and reject higher energy electrons.

1.4.5 The energy densities

This study of a set of particular solutions for the perturbed differential equations concludes with observations on the time average ion kinetic energy per unit volume and the average electric energy per unit volume. From the expressions for these quantities comes an important feature of the spectral density that has its parallel in the experimental data.

The electric energy density is given by

$$W_E = \frac{\epsilon_0}{2}\vec{\xi}^2 = \frac{\epsilon_0}{2}\left(\frac{m_p d\omega}{e \sin\theta}\right)^2 \left(1-\omega_1^2\right)^2 \sin^2\zeta,$$

using equation (1.34). The kinetic energy per unit volume for the ions is

$$W_M = \frac{1}{2} m_p N_0 \vec{u}^2 = \frac{1}{2} m_p N_0 \left(u_x^2 + u_y^2 + u_z^2\right)$$

$$= \frac{1}{2} m_p N_0 d^2 \left[\omega_1^2 \sin^2\zeta + \cos^2\theta \cos^2\zeta + \frac{\left(\omega_1^2 - \cos^2\theta\right)^2}{\sin^2\theta} \cos^2\zeta\right]$$

where the velocity relations of (1.24b) have been used. Taking the time average of these two expressions gives

$$\overline{W_E} = \frac{\epsilon_0}{4}\left(\frac{m_p d\omega}{e \sin\theta}\right)^2\left(1-\omega_1^{2'}\right)^2, \text{ and} \tag{1.41}$$

$$\overline{W_M} = \frac{1}{4} m_p N_0 d^2\left[\omega_1^2+\cos^2\theta+\frac{\left(\omega_1^2-\cos^2\theta\right)^2}{\sin^2\theta}\right]. \tag{1.42}$$

The ratio of these two quantities is worth studying since it is independent of the scaling factor d and gives a measure of the distribution of energy between the kinetic and electric forms. We have

$$R(\omega,\theta) \equiv \frac{\overline{W_E}}{\overline{W_M}} = \frac{\epsilon_0 m_p}{e^2 N_0}\cdot\frac{\omega^2\left(1-\omega_1^2\right)^2}{\sin^2\theta\left(\omega_1^2+\cos^2\theta\right)+\left(\omega_1^2-\cos^2\theta\right)^2}$$

$$= \frac{\omega_c^2}{\omega_p^2}\cdot\frac{\omega_1^2\left(1-\omega_1^2\right)^2}{\sin^2\theta\left(\omega_1^2+\cos^2\theta\right)+\left(\omega_1^2-\cos^2\theta\right)^2}. \tag{1.43}$$

This function is plotted in Figure 1.6 with θ as a parameter. The discontinuity in the curves is imposed by the dispersion relation which excludes certain frequencies for a given direction of propagation (see Figure 1.1). An interesting property of these curves is that they go to zero at the cyclotron frequency indicating that the electric energy density is zero at the ion cyclotron frequency for all directions of propagation.

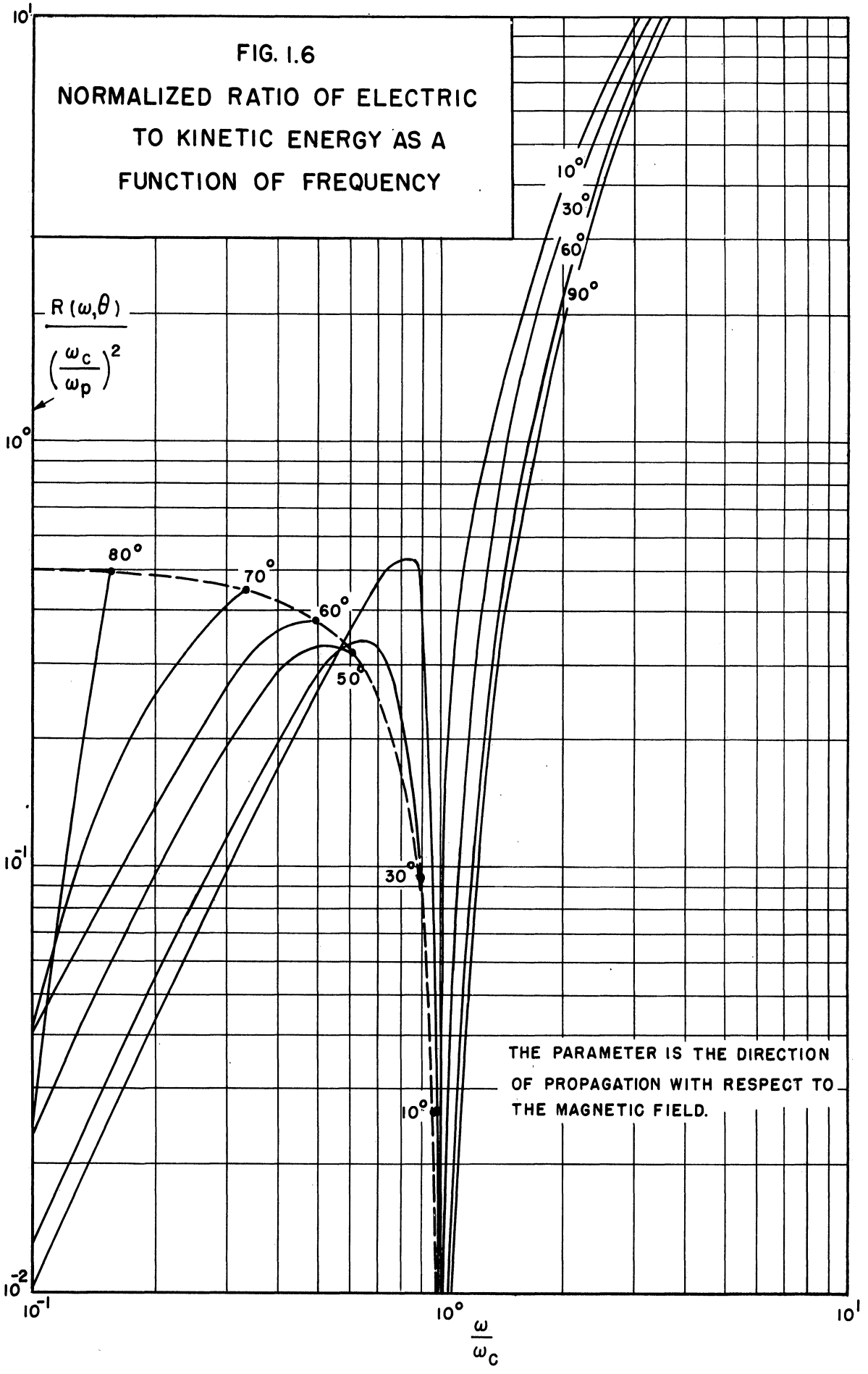
FIG. 1.6
NORMALIZED RATIO OF ELECTRIC TO KINETIC ENERGY AS A FUNCTION OF FREQUENCY
$\frac{R(\omega,\theta)}{\left(\frac{\omega_c}{\omega_p}\right)^2}$
10^1
10^0
10^{-1}
10^{-2}
10^{-1}
10^0
10^1
$\frac{\omega}{\omega_c}$
10°
30°
60°
90°
80°
70°
60°
50°
30°
10°
THE PARAMETER IS THE DIRECTION OF PROPAGATION WITH RESPECT TO THE MAGNETIC FIELD.

Chapter II

A THEORY OF ELECTRON FLUCTUATIONS

The theory developed in Chapter I was a study of ion fluctuations in a plasma. The electrons were taken into account by assuming that they had sufficient mobility to be in thermal equilibrium with the electric potential established by the fluctuations. This chapter examines the electron fluctuations, and although the restriction is not imposed in the early sections of the general theory, the influence of the ions will later be disposed by assuming that they are evenly distributed in the plasma and move with a constant velocity. This is tantamount to assuming that the ions were not there in the first place from the theoretical point of view. Taking a little liberty, the following statement is a consequence: investigators working with electron fluctuations in gas-discharge tubes, those studying ionospheric propagations, those investigating solar radiation, and those individuals examining propagation in electron-beam tubes are essentially solving the same mathematical problem. Perhaps it is not surprising that the first three of these groups are studying the same mathematical model, for in all cases propagation in a plasma is involved. The mathematics for electron plasma propagations is the same as that of electron beam propagations since the plasma ions are usually ignored under one assumption or another in examining electronic disturbances in a plasma. The idea is that the ions are relatively so heavy that their motion is not altered by rapid fluctuations of the electrons.

The theory of this chapter proceeds in a manner similar to that of Chapter I; a general system of differential equations is introduced, a perturbation form is given for these equations, and a set of component solutions for these perturbed equations is studied. This work is not carried out as completely as that of Chapter I since the theory on the electronic disturbances has been more thoroughly investigated in the literature. Those subjects already in the literature are developed only if they are pertinent in explaining the experimental studies of Chapters III and IV; in addition the low-frequency propagations normal to the magnetic field are studied in some detail, and a derivation is given for the dispersion relation of transverse propagation which includes the influence of electron temperature.

2.1 A set of self-consistent equations for electrically charged streams[1]

A set of differential equations are developed in this section for the "stream" vectors of interacting electrically charged streams.

Beginning with the Lorentz equation for the force on a charged particle,[2] one has

$$\upsilon \vec{v} + \frac{d\vec{v}}{dt} = \frac{e}{m} (\vec{E} + \vec{v} \times \vec{B}) , \qquad (2.1)$$

[1]It should be remarked that except for minor changes the general theory developed in the first two sections of this chapter is due to Gabor, References 23 and 24.

[2]Symbols that have been previously introduced and defined in the text are not defined again in the text. Appendix 2 gives a list of symbols.

and expanding the derivative gives[1]

$$\nu\vec{v}+\dot{\vec{v}}+(\vec{v}\cdot\nabla)\vec{v}=\frac{e}{m}(\vec{E}+\vec{v}\times\vec{B})\,. \qquad (2.2)$$

Equation (2.2) can be written,

$$\frac{m}{e}\left[\nu\vec{v}+\dot{\vec{v}}+(\vec{v}\cdot\nabla)\vec{v}-\vec{v}\times\vec{\omega}_c\right]=\vec{E}, \qquad (2.3)$$

where $\vec{\omega}_c=\frac{e\vec{B}}{m}$, the cyclotron frequency vector. This is the appropriate form for the Lorentz equation in stream theory, for if we imagine the medium to be made up of many interacting streams of charged particles, each stream having particles of the same mass, charge, and collision rate, then the left member of equation (2.3) depends only on the particular stream involved, whereas the right member is the field contributed by all of the streams. To indicate this, we write for the r'th stream,

$$\left(\frac{m}{e}\right)_r\left[\nu\vec{v}+\dot{\vec{v}}+(\vec{v}\cdot\nabla)\vec{v}-\vec{v}\times\vec{\omega}_c\right]_r=\vec{E}\,, \qquad (2.4)$$

where it is understood that the r applies to all of the components inside the bracket.

The next step is to express $\vec{E}$ in terms of a "stream vector." Using the familiar relations of electromagnetic field theory,

$$\vec{E}=-\nabla\Phi-\dot{\vec{A}}\,, \qquad (2.5)$$

$$\Box\vec{A}=-\mu_0\vec{J}\,, \qquad (2.6)$$

---

[1]Because of the complexity of the expressions in this chapter, a dot is used to indicate partial differentiation with respect to time.

and

$$\Box \Phi = - \frac{\rho}{\epsilon_0} \quad , \tag{2.7}$$

where $\vec{A}$ is the vector potential, $\vec{J}$ the current density, μ_0 the permeability of free space, and $\Box$ is the D'Alembertian operator $\left(\nabla^2 - \mu_0 \epsilon_0 \frac{\partial^2}{\partial t^2} \right)$. Also,

$$\Box \vec{E} = \frac{\nabla \rho}{\epsilon_0} + \mu_0 \dot{\vec{J}} \quad . \tag{2.8}$$

Now if the current density and space charge density of the r'th stream are denoted by $\vec{J}_r$ and ρ_r, continuity implies that

$$\nabla \cdot \vec{J}_r + \dot{\rho}_r = 0 \quad . \tag{2.9}$$

Therefore, an r'th stream vector $\vec{S}_r$ can be defined by

$$\vec{J}_r = \epsilon_0 \dot{\vec{S}}_r \text{ and } \rho_r = - \epsilon_0 \nabla \cdot \vec{S}_r \tag{2.10}$$

which is consistent with equation (2.9). Defining the total stream vector by

$$\vec{S} = \sum_{\text{STREAMS}} \vec{S}_r \quad , \tag{2.11}$$

the electric field can now be expressed in terms of $\vec{S}$, using (2.8) and (2.10).

$$\begin{aligned} \Box \vec{E} &= - \nabla \left(\nabla \cdot \vec{S} \right) + \mu_0 \epsilon_0 \ddot{\vec{S}} \\ &= - \left(\nabla \nabla \cdot - \frac{1}{c^2} \frac{\partial^2}{\partial t^2} \right) \vec{S} \quad . \end{aligned} \tag{2.12}$$

Taking the D'Alembertian of equation (2.4) and substituting from (2.12) on the right side gives,

$$\begin{aligned} &\left(\frac{m}{e} \right)_r \Box \left[v \vec{v} + \dot{\vec{v}} + (\vec{v} \cdot \nabla) \vec{v} - \vec{v} \times \vec{\omega}_c \right]_r \\ &= - \left(\nabla \nabla \cdot - \frac{1}{c^2} \frac{\partial^2}{\partial t^2} \right) \vec{S} \, . \end{aligned} \tag{2.13}$$

Using (2.10), the stream velocities in this expression can be written $\vec{v}_r = \frac{\vec{J}_r}{\rho_r} = -\frac{\dot{\vec{S}}_r}{\nabla\cdot\vec{S}_r}$, so that <u>equations (2.13) express the problem of M interacting streams in terms of M vector differential equation in the M stream vectors</u>.

2.2 A perturbation form of the stream equations

We now turn to a perturbation form for the equations of (2.13). Perturbing the streams gives,

$$\begin{aligned} \vec{S}_r &= \vec{S}_r^{\,\circ} + \vec{s}_r \,, \\ \vec{J}_r &= \rho_r^{\,\circ}\vec{v}_r^{\,\circ} + \vec{\imath}_r \,, \\ \text{and}\quad \rho_r &= \rho_r^{\circ} + n_r \end{aligned} \tag{2.14}$$

where $\vec{s}_r$, $\vec{\imath}_r$ and n_r represent the perturbation values, and the superscript zero indicates the unperturbed value of the quantity. From the definition of the stream vector given in equation (2.10), the currents and space charges of (2.14) can be written,

$$\begin{aligned} \vec{J}_r &= \rho_r^{\,\circ}\vec{v}_r^{\,\circ} + \epsilon_0\dot{\vec{s}}_r \\ \text{and}\quad \rho_r &= \rho_r^{\,\circ} - \epsilon_0\,\nabla\cdot\vec{s}_r \end{aligned} \tag{2.15}$$

Using these forms the velocity in the r'th stream can be approximated by,

$$\vec{v}_r = \frac{\vec{J}_r}{\rho_r} = \frac{\rho_r^{\,\circ}\vec{v}_r^{\,\circ} + \epsilon_0\dot{\vec{s}}_r}{\rho_r^{\,\circ} - \epsilon^{\circ}\nabla\cdot\vec{s}_r} = \left(\vec{v}_r^{\,\circ} + \frac{\epsilon_0}{\rho_r^{\circ}}\dot{\vec{s}}_r\right)\left(1 - \frac{\epsilon_0}{\rho_r^{\circ}}\nabla\cdot\vec{s}_r\right)^{-1}$$

$$= \left(\vec{v}_r^{\,\circ} + \frac{\epsilon_0}{\rho_r^{\circ}}\dot{\vec{s}}_r\right)\left(1 + \frac{\epsilon_0}{\rho_r^{\circ}}\nabla\cdot\vec{s}_r + \cdots\right), \quad \text{or} \tag{2.16}$$

$$\vec{v}_r \simeq \vec{v}_r^{\,\circ} + \frac{\epsilon_0}{\rho_r^{\circ}}\left(\dot{\vec{s}}_r + \vec{v}_r^{\,\circ}\,\nabla\cdot\vec{s}_r\right) .$$

This value for the velocity of the r'th stream can be substituted in the left member of equation (2.13), but before making the substitution, it is convenient to calculate some of the terms.

$$\dot{\vec{v}}_r \simeq \frac{\epsilon_0}{\rho_r^\circ}\left(\ddot{\vec{s}}_r + \vec{v}_r^\circ \nabla\cdot\dot{\vec{s}}_r\right). \tag{2.17}$$

Notice that $\dot{\vec{v}}_r^\circ$ and $\dot{\rho}_r^\circ$ are taken equal to zero here, since it is assumed that the undisturbed streams are steady. Also,

$$\begin{aligned}(\vec{v}_r\cdot\nabla)\vec{v}_r &= (\vec{v}_r^\circ\cdot\nabla)\vec{v}_r^\circ + (\vec{v}_r^\circ\cdot\nabla)\left[\frac{\epsilon_0}{\rho_r^\circ}\left(\dot{\vec{s}}_r + \vec{v}_r^\circ\nabla\cdot\vec{s}_r\right)\right] \\ &+ \frac{\epsilon_0}{\rho_r^\circ}\left[\left(\dot{\vec{s}}_r + \vec{v}_r^\circ\nabla\cdot\vec{s}_r\right)\cdot\nabla\right]\vec{v}_r^\circ ,\end{aligned} \tag{2.18}$$

and

$$s = \sum_{\text{STREAMS}} \vec{s}_r \,. \tag{2.19}$$

Then putting these forms in equation (2.13) and using the fact that the unperturbed basis streams satisfy the differential equation leads to

$$\begin{aligned}&\left(\frac{m}{e}\right)_r \square\left\{\frac{\epsilon_0}{\rho^\circ}\left(v\dot{s} + v\vec{v}^\circ\nabla\cdot\vec{s} + \ddot{\vec{s}} + \vec{v}^\circ\nabla\cdot\dot{\vec{s}}\right) + (\vec{v}^\circ\cdot\nabla)\left[\frac{\epsilon_0}{\rho^\circ}\left(\dot{\vec{s}} + \vec{v}^\circ\nabla\cdot\vec{s}\right)\right]\right. \\ &\left. + \frac{\epsilon_0}{\rho^\circ}\left[\left(\dot{\vec{s}} + \vec{v}^\circ\nabla\cdot\vec{s}\right)\cdot\nabla\right]\vec{v}^\circ - \frac{\epsilon^\circ}{\rho^\circ}\left(\dot{\vec{s}} + \vec{v}^\circ\nabla\cdot\vec{s}\right)\times\vec{\omega}_c\right\}_r \\ &= -\left(\nabla\nabla\cdot - \frac{1}{c^2}\frac{\partial^2}{\partial t^2}\right)\vec{s}\,.\end{aligned} \tag{2.20}$$

<u>These are the fundamental perturbation equations of interacting streams</u>. Imposing the assumption that each undisturbed stream has a constant velocity $\vec{v}_r^\circ$ and a constant space charge density ρ_r°, equations (2.20) reduce to the form,

$$\begin{aligned}&\frac{1}{\omega_r^2}\square\left\{v\dot{\vec{s}} + v\vec{v}^\circ\nabla\cdot\vec{s} + \ddot{\vec{s}} + \vec{v}^\circ\nabla\cdot\dot{\vec{s}} + (\vec{v}^\circ\cdot\nabla)\left(\dot{\vec{s}} + \vec{v}^\circ\nabla\cdot\vec{s}\right)\right. \\ &\left. - \left(\dot{\vec{s}} + \vec{v}^\circ\nabla\cdot\vec{s}\right)\times\vec{\omega}_c\right\}_r = -\left(\nabla\nabla\cdot - \frac{1}{c^2}\frac{\partial^2}{\partial t^2}\right)\vec{s}\,,\end{aligned} \tag{2.21}$$

where $\omega_r = \sqrt{\left(\frac{e\rho^\circ}{m\epsilon_0}\right)_r}$ is the characteristic frequency of the r'th stream. If there is only one stream then the characteristic frequency is the more familiar plasma frequency of the stream, and in this case we write $\omega_r = \omega_p$. Using (2.12), the corresponding perturbed electric field can be written,

$$\vec{\xi} = \frac{1}{\omega_r^2}\left\{v\dot{\vec{s}} + v\vec{v}^\circ \nabla\cdot\vec{s} + \ddot{\vec{s}} + \vec{v}^\circ \nabla\cdot\dot{\vec{s}} + \left(\vec{v}^\circ\cdot\nabla\right)\left(\dot{\vec{s}} + \vec{v}^\circ\nabla\cdot\vec{s}\right) - \left(\dot{\vec{s}} + \vec{v}^\circ \nabla\cdot\vec{s}\right)\times\vec{\omega}_c\right\}_r , \tag{2.22}$$

for any stream r. Consequently, the solution of (2.21) leads at once to the value of the perturbed electric field. Similarly such other quantities as the space-charge density and particle motion are derivable once the stream vector is known.

2.3 The perturbation equations for particular solutions

Equations (2.21) are a set of linear homogeneous differential equations in the perturbed stream vectors, and consequently solutions can be sought corresponding to waves propagated through the ionized gas. The resulting perturbation relation is derived in this section. The argument and procedure is much like that of Chapter I.

Assume the perturbation stream vectors of (2.21) are given by,

$$\vec{s}_r = \underline{\vec{s}}_r\, e^{i\left(\omega t - \beta_1 x - \beta_2 y - \beta_3 z\right)} = \underline{\vec{s}}_r\, e^{i\left(\omega t - \vec{\beta}\cdot\vec{x}\right)} , \tag{2.23}$$

where the components of $\underline{\vec{s}}_r$ are complex quantities, but do not depend on the space coordinates or time. Likewise the frequency ω and the propagation constant $\vec{\beta}$ are taken constant.

For this choice of stream vectors,

$$\begin{aligned}
&\Box \vec{s}_r = -\left(\beta^2 - \frac{\omega^2}{c^2}\right)\vec{s}_r \,, \\
&\nabla\cdot\vec{s}_r = -i\vec{\beta}\cdot\vec{s}_r \,, \\
&\ddot{\vec{s}}_r = -\omega^2\vec{s}_r \,, \\
&\nabla\cdot\dot{\vec{s}}_r = \omega\vec{\beta}\cdot\vec{s}_r \,, \\
&\left(\vec{v}^{\circ}\cdot\nabla\right)\vec{s}_r = -i\left(\vec{v}^{\circ}\cdot\vec{\beta}\right)\vec{s}_r, \text{ and } \nabla\,\nabla\cdot\vec{s} = -\vec{\beta}\left(\vec{\beta}\cdot\vec{s}\right) .
\end{aligned} \tag{2.24}$$

Substituting these values into equations (2.21) gives,

$$\begin{aligned}
&\left(\omega^2 - c^2\beta^2\right)\Big\{\left(\omega - iv - \vec{v}^{\circ}\cdot\vec{\beta}\right)\omega\vec{s} + i\omega\vec{s}\times\vec{\omega}_c \\
&+\left(\vec{\beta}\cdot\vec{s}\right)\left[\vec{v}^{\circ}\left(-\omega + iv + \vec{v}^{\circ}\cdot\vec{\beta}\right) - i\vec{v}^{\circ}\times\vec{\omega}_c\right]\Big\}_r \\
&= \omega_r^2\left[\omega^2\vec{s} - c^2\left(\vec{\beta}\cdot\vec{s}\right)\vec{\beta}\right] .
\end{aligned} \tag{2.25}$$

This vector equation is the general form of the perturbation equations for the particular solutions of interest in this study. However, it is often more useful to have these equations in terms of scalar relations. For convenience and without loss of generality, the propagation is assumed in the z -direction and the magnetic field is taken in the yz - plane. Thus,

$$\begin{aligned}
&\vec{\beta} = (0,\, 0,\, \beta) \quad \text{and} \\
&\vec{\omega}_c = (0,\, \omega_c \sin\theta,\, \omega_c \cos\theta)
\end{aligned} \tag{2.26}$$

where θ is the angle between the propagation direction and the direction of the magnetic field. Then the component equations of (2.25) can be written,

$$\begin{aligned}
&\left(\omega^2 - c^2\beta^2\right)\Big\{\left(\omega - iv - v_3^{\circ}\beta\right)\omega s_1 + i\omega\omega_c\left(s_2\cos\theta - s_3\sin\theta\right) \\
&+\beta s_3\left[v_1^{\circ}\left(-\omega + iv + v_3^{\circ}\beta\right) - i\omega_c\left(v_2^{\circ}\cos\theta - v_3^{\circ}\sin\theta\right)\right]\Big\}_r \\
&= \omega_r^2\omega^2 s_1 \,,
\end{aligned} \tag{2.27a}$$

$$\begin{aligned}
&\left(\omega^2 - c^2\beta^2\right)\Big\{\left(\omega - iv - v_3^{\circ}\beta\right)\omega s_2 - i\omega\omega_c s_1\cos\theta \\
&+\beta s_3\left[v_2^{\circ}\left(-\omega + iv + v_3^{\circ}\beta\right) + i\omega_c v_1^{\circ}\cos\theta\right]\Big\}_r \\
&= \omega_r^2\omega^2 s_2 \,, \text{ and}
\end{aligned} \tag{2.27b}$$

$$\{(\omega - i\upsilon - v_3^\circ\beta)\omega s_3 + i\omega\omega_c s_1 \sin\theta + \beta s_3[v_3^\circ(-\omega + i\upsilon + v_3^\circ\beta) - i v_1^\circ \omega_c \sin\theta]\}_r = \omega_r^2 s_3 . \qquad (2.27c)$$

The subscripts 1, 2, and 3 have been used here to denote components in the x, y, and z directions respectively.

2.4 The role of temperature in the dispersion relation

The derivation of a dispersion relation for electron fluctuation that embraces the role of temperature is a difficult task. However, two special cases can be obtained from the system of equations given in (2.25) which include temperature; these are derived below. The first is a one-dimensional approximate form due to Bohm and Gross;[1] the other is the general case for transverse propagation.

2.4.1 A one-dimensional model

The one-dimensional model of Bohm and Gross will now be derived. Referring to equations (2.25), one allows for perturbations and propagation only in the direction of the magnetic field, and it is assumed that any velocities in the undisturbed streams are in that same direction. Then neglecting collisions, equations (2.25) reduce to

$$\{(\omega - v^\circ\beta)\omega s - v^\circ\beta s(\omega - v^\circ\beta)\}_r = \omega_r^2 s ,$$

or

$$\{(\omega - v^\circ\beta)^2 s\}_r = \omega_r^2 s .$$

---

[1] Reference 13.

This can be written

$$\mathcal{S}_r = \frac{\omega_r^2}{(\omega - v_r^\circ \beta)^2}\,\mathcal{S} \,. \qquad (2.28)$$

There are as many linear homogeneous equations here as there are unknowns, and therefore the determinant of the coefficients must vanish if there is to be a solution. Assuming M streams and using the notation

$$a_r = \frac{\omega_r^2}{(\omega - v_r^\circ \beta)^2} \,, \qquad (2.29)$$

this determinant is given by

$$\begin{vmatrix} a_1 - 1 & a_1 & a_1 & \cdots & a_1 \\ a_2 & a_2 - 1 & a_2 & \cdots & a_2 \\ \vdots & & & & \vdots \\ a_M & a_M & \cdots & a_M & a_M - 1 \end{vmatrix} = 0 \,.$$

Subtracting the first column from each of the succeeding columns gives

$$\begin{vmatrix} a_1 - 1 & 1 & 1 & \cdots & 1 \\ a_2 & -1 & & & \\ \vdots & & -1 & & \mathbf{0} \\ & & & \ddots & \\ a_M & & \mathbf{0} & & -1 \end{vmatrix} = 0 \,,$$

and adding each row to the first leads to

$$\begin{vmatrix} \sum_{i=1}^{M} a_i - 1 & 0 & 0 & \cdots & 0 \\ a_2 & -1 & & & \\ \vdots & & -1 & & \mathbf{0} \\ & & & \ddots & \\ a_M & & \mathbf{0} & & -1 \end{vmatrix} = 0 \,.$$

Expanding, $\sum_{i=1}^{M} a_i = 1$, or substituting from (2.29) for a_i, one obtains

$$\sum_{1}^{M} \frac{\omega_r^2}{(\omega - v_r^\circ \beta)^2} = 1 \ . \tag{2.30}$$

Now $\omega_r^2 = \frac{e^2 N_r}{\epsilon_0 m}$ where N_r is the number of particles per unit volume in the r'th stream, so that by defining a particle density $f(v_r^\circ)$ in coordinate and velocity space by

$$N_r = f(v_r^\circ)(v_r^\circ - v_{r-1}^\circ) \ , \tag{2.31}$$

equation (2.30) can be written

$$\frac{e^2}{\epsilon_0 m} \sum_{1}^{M} \frac{f(v_r^\circ)}{(\omega - v_r^\circ \beta)^2} (v_r^\circ - v_{r-1}^\circ) = 1 \ .$$

Formally passing to the limit, this sum becomes the integral,

$$\frac{e^2}{\epsilon_0 m} \int_{-\infty}^{\infty} \frac{f(v)}{(\omega - \beta v)^2} dv = 1 \ . \tag{2.32}$$

This expression is the dispersion relation for the Bohm and Gross model.[1]

An approximate solution of (2.32) will now be derived. Assume that the phase velocity $(\frac{\omega}{\beta})$ is large compared to the particle velocities permitted by the distribution function $f(v)$. Then the denominator of the integrand can be approximated by

$$\frac{1}{(\omega - \beta v)^2} \simeq \frac{1}{\omega^2} \left[1 + 2 \frac{\beta v}{\omega} + 3 \left(\frac{\beta v}{\omega} \right)^2 \right] \ .$$

Putting this approximation in (2.32) gives

$$\frac{\omega_p^2}{\omega^2} \left[1 + 2 \frac{\beta \bar{v}}{\omega} + 3 \left(\frac{\beta}{\omega} \right)^2 \overline{v^2} \right] = 1 \ . \tag{2.33}$$

---

[1] Reference 13.

where the bar over the quantity indicates the mean. In particular if there is no average drift $(\bar{v}=0)$ and the distribution of velocities is Maxwell-Boltzmann, then (2.33) becomes

$$\frac{\omega_p^2}{\omega^2}\left[1+3\frac{\beta^2}{\omega^2}\frac{kT}{m}\right]=1 \quad .$$

By the original assumption, the thermal term in this expression is small compared to unity, and consequently the first two terms of an approximation give,

$$\omega^2 = \omega_p^2 + 3\frac{\beta^2 kT}{m} \quad . \qquad (2.34)$$

This is the result given by Bohm and Gross. It should be noted that if the temperature is zero, the frequency is merely the familiar plasma electron frequency; the effect of temperature is to broaden the spectrum.

2.4.2 The influence of temperature on transverse propagation

The case just discussed has serious shortcomings. It is restricted to longitudinal propagation, i.e. the perturbation and propagation are in the same direction. More serious is the necessary assumption that the thermal motion is limited to one direction. Also the lack of influence of any magnetic field is inherent when only one-dimensional perturbations are tolerated.

The case discussed in this section is somewhat more satisfying. It embraces the influence of the magnetic field,

and a general distribution of thermal velocities is tolerated. However, it is also a rather special case since it is assumed that the propagation and the perturbation are transverse.

Returning again to equation (2.25), neglecting the effects of collisions, and assuming transverse propagation, $\vec{\beta} \cdot \vec{\mathcal{S}}_r = 0$, one has

$$\left(\omega^2 - c^2\beta^2\right)\left\{\left(\omega - \vec{v}^\circ \cdot \vec{\beta}\right)\omega \mathcal{S}_1 + i\omega\omega_c \mathcal{S}_2\right\}_r = \omega_r^2 \omega^2 \mathcal{S}_1 \quad , \tag{2.35a}$$

$$\left(\omega^2 - c^2\beta^2\right)\left\{\left(\omega - \vec{v}^\circ \cdot \vec{\beta}\right)\omega \mathcal{S}_2 - i\omega\omega_c \mathcal{S}_1\right\}_r = \omega_r^2 \omega^2 \mathcal{S}_2 \quad , \tag{2.35b}$$

and $$\left(\omega^2 - c^2\beta^2\right)\left\{\left(\omega - \vec{v}^\circ \cdot \vec{\beta}\right)\omega \mathcal{S}_3\right\}_r = \omega_r^2 \omega^2 \mathcal{S}_3 \tag{2.35c}$$

where $\vec{\omega}_c$ is now taken in the z -direction for convenience. Clearly (2.35c) is independent of (2.35a) and (2.35b); it can be written:

$$\mathcal{S}_{3r} = \frac{\omega}{\left(\omega^2 - c^2\beta^2\right)} \cdot \frac{\omega_r^2}{\left(\omega - \vec{v}_r^\circ \cdot \vec{\beta}\right)} \mathcal{S}_3 . \tag{2.36}$$

Now (2.25a) and (2.35b) can be combined and reduced to a form similar to (2.36), for multiplying (2.35b) by $\pm i$ and adding the result to (2.35a) gives

$$\left(\omega - c^2\beta^2\right)\left\{\left(\omega - \vec{v}^\circ \cdot \vec{\beta}\right)\omega\left(\mathcal{S}_1 \pm i\mathcal{S}_2\right) \pm \omega\omega_c\left(\mathcal{S}_1 \pm i\mathcal{S}_2\right)\right\}_r = \omega_r^2\omega^2\left(\mathcal{S}_1 \pm i\mathcal{S}_2\right) .$$

This can be written

$$\left(\mathcal{S}_1 \pm i\mathcal{S}_2\right)_r = \frac{\omega}{\left(\omega^2 - c^2\beta^2\right)} \cdot \frac{\omega_r^2}{\left(\omega - \vec{v}_r^\circ \cdot \vec{\beta} \pm \omega_c\right)}\left(\mathcal{S}_1 \pm i\mathcal{S}_2\right) . \tag{2.37}$$

The solution of (2.36) and the two solutions of (2.37) include all possible waves that are launched transversely. It is clear that the propagation direction is normal to the

direction of the magnetic field in the case of (2.36) and parallel to the field in (2.37). It also should be noted that the solution of (2.36) can be obtained from the solution of (2.37) by merely setting $\omega_c = 0$ in the solution of (2.37).

The three expressions (2.36) and (2.37) are of the same form as equation (2.28), and the dispersion relation can be obtained in the same way. Corresponding to (2.36), the dispersion relation is

$$\frac{\omega}{(\omega^2 - c^2\beta^2)} \frac{e^2}{\epsilon_0 m} \int_{-\infty}^{\infty} \frac{f(v)}{(\omega - v\beta)} dv = 1 \qquad (2.38)$$

where v is the component of velocity in the direction of propagation and $f(v)$ is the distribution of particles in this velocity per unit volume.

Corresponding to (2.37), one has

$$\frac{\omega}{(\omega^2 - c^2\beta^2)} \cdot \frac{e^2}{\epsilon_0 m} \int_{-\infty}^{\infty} \frac{f(v)}{(\omega - v\beta \pm \omega_c)} dv = 1. \qquad (2.39)$$

The next step is to evaluate the integral in these dispersion relations.

Suppose that the distribution function is Maxwell-Boltzmann so that

$$f(v) = N_0 \sqrt{\frac{m}{2\pi kT}} \, e^{-\frac{m}{2kT}(v-\bar{v})^2} \qquad (2.40)$$

where N_0 is the density of the charged particles in all the streams. Then (2.39) can be written

$$\frac{\omega}{(\omega^2 - c^2\beta^2)} \cdot \frac{e^2 N_0}{\epsilon_0 m} \cdot \sqrt{\frac{m}{2\pi kT}} \cdot \int_{-\infty}^{\infty} \frac{e^{-\frac{m}{2kT}(v-\bar{v})^2}}{(\omega - v\beta \pm \omega_c)} dv = 1.$$

Making the change of variable

$\eta = \sqrt{\frac{m}{2kT\beta^2}}\,(\omega - v\beta \pm \omega_c)$, and temporarily using the notation $b = \sqrt{\frac{m}{2kT\beta^2}}\,(\omega - v\beta \pm \omega)$, this becomes (2.41)

$$\frac{\omega\omega_p^2}{(\omega^2 - c^2\beta^2)}\sqrt{\frac{m}{2\pi kT\beta^2}}\int_{-\infty}^{\infty}\frac{e^{-(\eta-b)^2}}{\eta}\,d\eta = 1 \,. \tag{2.42}$$

The integral in this expression does not exist in the Riemann sense, but properly interpreted in the Cauchy sense, it is a well behaved function of b. This integral is defined and evaluated in Appendix 4; here the same result is obtained by a formal method. Writing

$$g(b) = \int_{-\infty}^{\infty}\frac{e^{-(\eta-b)^2}}{\eta}\,d\eta \,, \quad \text{one has}$$

$$g(b)e^{b^2} = \int_{-\infty}^{\infty}\frac{e^{-\eta^2+2b\eta}}{\eta}\,d\eta \,.$$

Differentiating this expression with respect to b gives

$$\frac{d}{db}\left[g(b)e^{b^2}\right] = 2\int_{-\infty}^{\infty} e^{-\eta^2+2b\eta}\,d\eta$$

$$= 2e^{b^2}\int_{-\infty}^{\infty} e^{-(\eta-b)^2}\,d\eta = 2\sqrt{\pi}\;e^{b^2} \,.$$

Now integrating on b leads to

$$g(b) = 2\sqrt{\pi}\;e^{-b^2}\int_0^b e^{\eta^2}\,d\eta \,. \tag{2.43}$$

The constant of integration is zero since g(o) must vanish. $\frac{g(b)}{2\sqrt{\pi}}$ has been tabulated;[1] a plot of the function together

[1]Reference 31.

with an approximation for large arguments is shown in Figure 2.1. The approximation is of particular interest because if it is used instead of the integral in the dispersion relation the result is the more familiar expression valid when the temperature can be ignored, i.e. when T = 0 is a good approximation. From Figure 2.1 it appears that the approximation is good for arguments greater than five or ten. Here some evidence will be given to this point of view by showing that the integral and its approximation have the same limiting values and their ratio approaches unity.

$\frac{1}{2b}$ certainly has the limiting value zero so that it is only necessary to show that

$$\lim_{b\to\infty} \frac{e^{-b^2}\int_0^b e^{\eta^2}d\eta}{\frac{1}{2b}} = 1 \quad . \tag{2.44}$$

Using L'Hopital's rule, one obtains

$$\lim_{b\to\infty} 2\frac{\int_0^b e^{\eta^2}d\eta}{b^{-1}e^{b^2}} = \lim_{b\to\infty} 2\frac{e^{b^2}}{e^{b^2}\left(2-b^{-2}\right)} = 1 \ ,$$

confirming (2.44).

Returning now to the dispersion relation (2.42) and substituting in the value obtained for the integral gives

$$\frac{\omega\omega_p^2}{\omega^2-c^2\beta^2}\sqrt{\frac{m}{2\pi kT\beta^2}}\cdot 2\sqrt{\pi}\ e^{-b^2}\int_0^b e^{\eta^2}d\eta = 1.$$

Replacing b by its value from (2.41) and using $U_T = \sqrt{\frac{2kT}{m}}$, the most probable thermal speed, this equation can be written,

$$\frac{2\omega\omega_p^2}{\left(\omega^2-c^2\beta^2\right)}\cdot\frac{1}{\beta U_T}\cdot e^{-\left(\frac{\omega-\overline{\nu}\beta\pm\omega_c}{\beta U_T}\right)^2}\int_0^{\left(\frac{\omega-\overline{\nu}\beta\pm\omega_c}{\beta U_T}\right)} e^{\eta^2}d\eta = 1 \ . \tag{2.45}$$

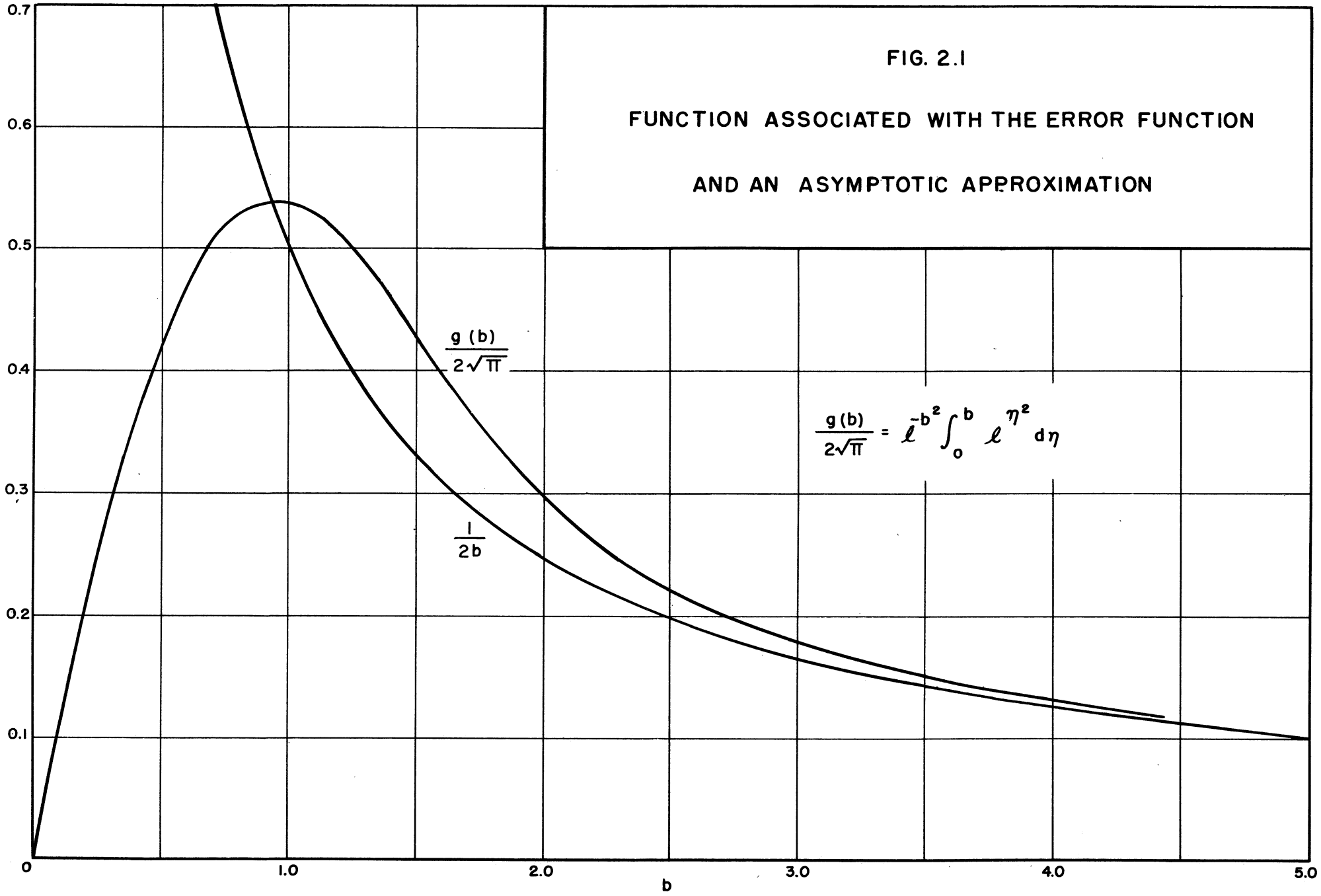
FIG. 2.1
FUNCTION ASSOCIATED WITH THE ERROR FUNCTION
AND AN ASYMPTOTIC APPROXIMATION
$\frac{g(b)}{2\sqrt{\pi}} = e^{-b^2}\int_0^b e^{\eta^2}\,d\eta$
$\frac{g(b)}{2\sqrt{\pi}}$
$\frac{1}{2b}$
0.7
0.6
0.5
0.4
0.3
0.2
0.1
0
1.0
2.0
3.0
4.0
5.0
b

This is the dispersion relation for transverse propagation in an ionized gas. It is more general than the usual expression presented in the literature since it includes the effect of a magnetic field, temperature, and drift. The two cases given in (2.45) apply when the propagation is in the direction of the magnetic field. The dispersion relation for transverse propagation normal to the magnetic field can be obtained from this expression by setting the magnetic field equal to zero. No other directions of transverse propagation are possible.

The expression (2.45) is quite complicated and difficult to interpret. Using the asymptotic approximation for the integral the dispersion relation is

$$\frac{\omega \omega_p^2}{\omega^2 - c^2\beta^2} = \left(\omega - \bar{v}\beta \pm \omega_c \right) . \qquad (2.46)$$

This equation is independent of temperature and represents a considerable simplification in other respects; it is worth noting just when it can be used. From Figure 2.1 it appears that the approximation is justified for

$$\left| b \right| = \left| \frac{\omega - \bar{v}\beta \pm \omega_c}{\beta U_T} \right| > 5 . \qquad (2.47)$$

Restricting the consideration to that of strong magnetic fields one sees that the approximation (2.46) is always good for the dispersion relation with the positive sign, but the approximation breaks down near the cyclotron frequency when the negative sign is chosen. The temperature must be taken into account under these circumstances. Figure 2.2 is

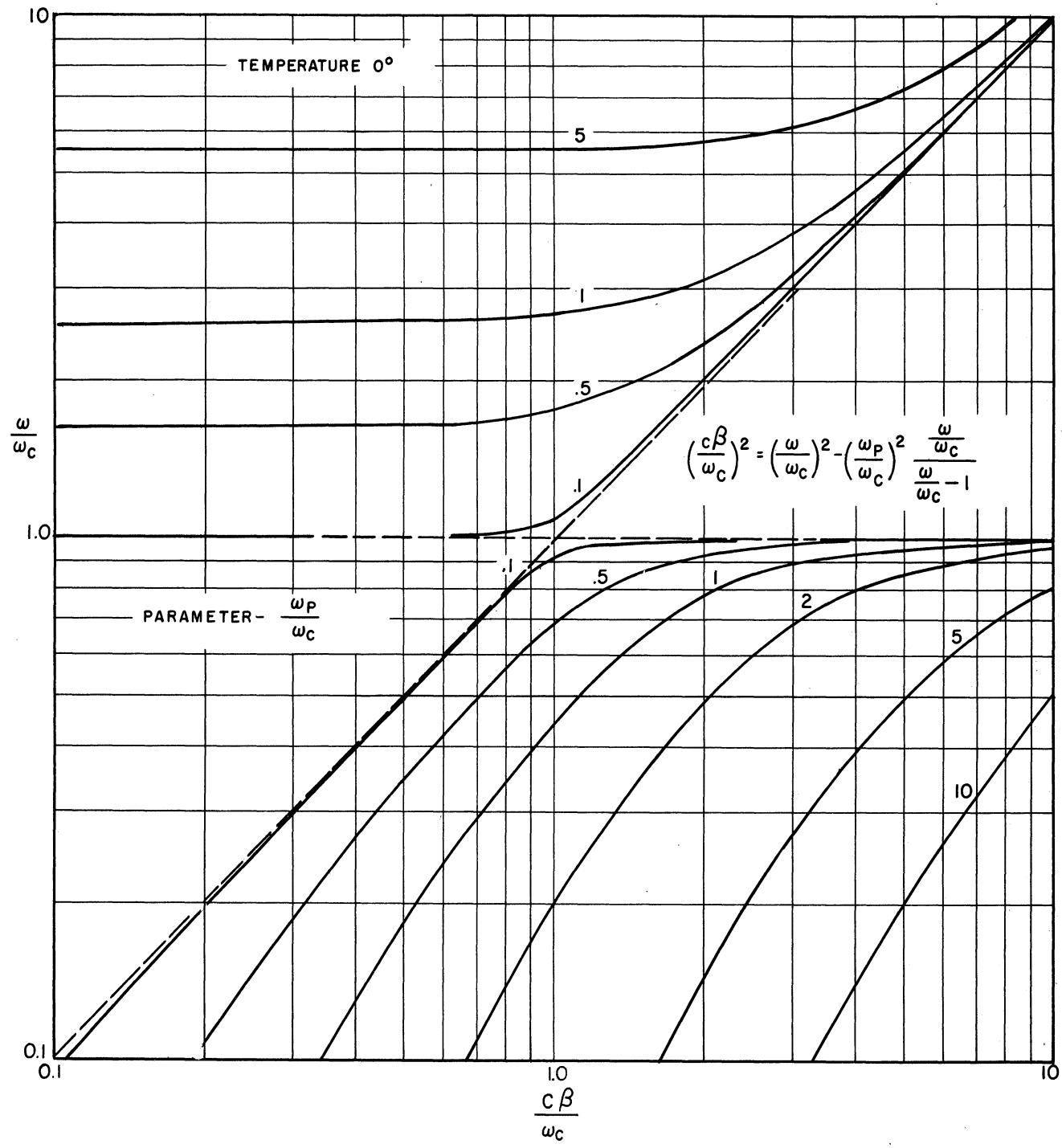

FIG. 2.2 A DISPERSION RELATION FOR TRANSVERSE PROPAGATION

a family of curves representing the dispersion relation (2.46) assuming the drift velocity is zero and taking the negative sign. The modification that the temperature introduces into these curves near the cyclotron frequency is shown in Figure 2.3. These curves were obtained directly from the general dispersion relation (2.45) after neglecting the drift velocity $\overline{v}$. It is clear that neglecting the effect of temperature introduces a radical error into the dispersion relation for frequencies near the cyclotron frequency.

2.5 The magneto-ionic dispersion relation

A derivation of the familiar dispersion relation for the ionosphere is given in this section. It is introduced here because the Bailey bands for wave amplification are determined from this dispersion relation, and these bands play an important role in the interpretation of the experimental data in the next two chapters.

The general equations of (2.27) are now specialized to the case of a single stream, and the velocity of drift, $\overrightarrow{v^\circ}$, is neglected.[1] Rewriting the equations (2.27) for this case gives

$$(\omega^2-c^2\beta^2)\left[(\omega-i\nu)\omega\Delta_1+i\omega\omega_c(\Delta_2\cos\theta-\Delta_3\sin\theta)\right]=\omega_p^2\omega^2\Delta_1 \quad , \quad (2.48)$$

$$(\omega^2-c^2\beta^2)\left[(\omega-i\nu)\omega\Delta_2-i\omega\omega_c\Delta_1\cos\theta\right]=\omega_p^2\omega^2\Delta_2 \quad , \quad (2.49)$$

[1]The extention to include drift velocity can readily be made, but the result is not pertinent in this development.

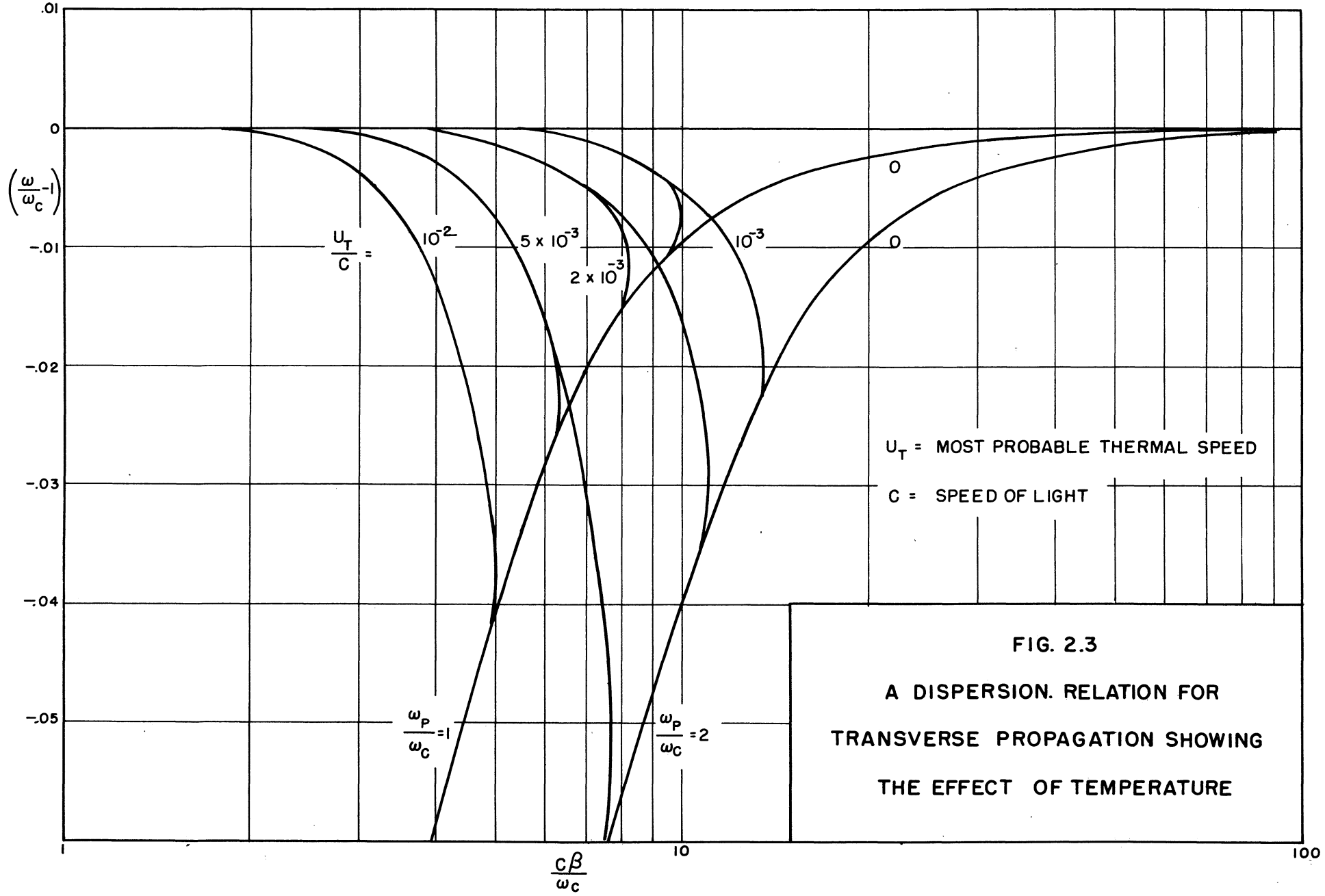

FIG. 2.3

A DISPERSION. RELATION FOR TRANSVERSE PROPAGATION SHOWING THE EFFECT OF TEMPERATURE

and

$$(\omega - i\nu)\omega A_3 + i\omega\omega_c A_1 \sin\theta = \omega_p^2 A_3 \quad . \tag{2.50}$$

Here there are three linear homogeneous equations in the three components of the perturbed stream vector. Consequently, a solution exists if and only if the determinant of the coefficients vanishes. Thus

$$\begin{vmatrix} \dfrac{\omega^2\omega_p^2}{\omega^2 - c^2\beta^2} - \omega(\omega - i\nu) & -i\omega\omega_c\cos\theta & i\omega\omega_c\sin\theta \\ i\omega\omega_c\cos\theta & \dfrac{\omega^2\omega_p^2}{\omega^2 - c^2\beta^2} - \omega(\omega - i\nu) & 0 \\ -i\omega\omega_c\sin\theta & 0 & \omega_p^2 - \omega(\omega - i\nu) \end{vmatrix} = 0 \ ,$$

and expanding in terms of the first row one obtains

$$\left[\frac{\omega^2\omega_p^2}{\omega^2 - c^2\beta^2} - \omega(\omega - i\nu)\right]^2 \left[\omega_p^2 - \omega(\omega - i\nu)\right] - \omega^2\omega_c^2\cos^2\theta\left[\omega_p^2 - \omega(\omega - i\nu)\right]$$

$$- \omega^2\omega_c^2\sin^2\theta\left[\frac{\omega^2\omega_p^2}{\omega^2 - c^2\beta^2} - \omega(\omega - i\nu)\right] = 0 \ .$$

This expression is quadratic in $\dfrac{\omega^2\omega_p^2}{\omega^2 - c^2\beta^2}$; solving for this quantity gives

$$\frac{\omega^2\omega_p^2}{\omega^2 - c^2\beta^2} = \omega(\omega - i\nu) + \frac{1}{2}\frac{\omega^2\omega_c^2\sin^2\theta}{\omega_p^2 - \omega(\omega - i\nu)} \pm \sqrt{\left[\frac{1}{2}\frac{\omega^2\omega_c^2\sin^2\theta}{\omega_p^2 - \omega(\omega - i\nu)}\right]^2 + \omega^2\omega_c^2\cos^2\theta}$$

Now the propagation constant can be obtained by inverting and transposing in this expression; also normalizing all frequencies and $(c\beta)$ in terms of the plasma electron frequency ω_p one has

$$c^2\beta^2=\omega^2-\left\{\frac{\omega-i\upsilon}{\omega}+\frac{1}{2}\frac{\omega_c^2\sin^2\theta}{1-\omega(\omega-i\upsilon)}\pm\sqrt{\left[\frac{1}{2}\frac{\omega_c^2\sin^2\theta}{1-\omega(\omega-i\upsilon)}\right]+\frac{\omega_c^2}{\omega^2}\cos^2\theta}\right\}^{-1} \qquad (2.52)$$

This is the important magneto-ionic dispersion equation used extensively during the thirties to examine the propagation properties of the ionosphere.[1]

2.6 The amplification bands of Bailey[2]

Bailey has pointed out that if the magneto-ionic dispersion relation is plotted with the propagation constant β as a function of frequency ω, neglecting collisions υ, then there are certain intercepts on the frequency axis and certain vertical asymptotes. These are given by the frequencies

$$\pm 0,\ \pm\omega_p,\ \pm\omega_1,\ \pm\omega_2,\ \pm\omega_3,\ \text{AND}\ \pm\omega_4,$$

where

$$\omega_1,\ \omega_2 = \frac{1}{2}\left[\sqrt{\omega_c^2+4\omega_p^2}\pm\omega_c\right]$$

and

$$\omega_3,\ \omega_4 = \left[\frac{1}{2}\left(\omega_c^2+\omega_p^2\right)\pm\frac{1}{2}\sqrt{\left(\omega_c^2+\omega_p^2\right)^2-4\omega_p^2\omega_c^2\cos^2\theta}\right]^{\frac{1}{2}}.$$

Bailey states that these frequencies are the edges of frequency bands within which the propagation constant is pure imaginary, and therefore waves cannot propagate in these bands through the medium. However,

"When an electron drift velocity $\vec{v}$ exists the corresponding (ω,β) curve has some branches which are

---

[1] References 1, 2, and 30.

[2] Reference 8.

similar to the ones just considered but distorted in a skew manner so that they become unsymmetrical about the ω-axis. The principal consequence is that in general we now obtain bands in which β is a complex number $(\alpha \pm ib)$.

"These bands approximate to the bands considered above in the magneto-ionic theory. We thus see that the effect of electron drift is to create wave amplification and consequent electromagnetic noise in frequency bands in which otherwise waves cannot propagate."[1]

In this way Bailey concluded that there would be three frequency bands in which one could expect fluctuations. These bands were approximately the frequency intervals $(0, \omega_2)$, (ω_p, ω_4), AND (ω_1, ω_3).

2.7 The low-frequency propagation normal to the magnetic field

Chapter IV is an experimental study of the low-frequency propagation normal to the magnetic field. Anticipating that chapter, a brief theoretical study on such fluctuations is presented in this section. The objective is threefold: (1) to show that the group velocity of propagation is approximately equal to the electron drift velocity in the direction of propagation, (2) to show that there is amplification in this propagation and determine the dependence of this amplification on the plasma parameters, and (3) to show that the preferred direction of this propagation is parallel to the electron drift.

Returning to equation (2.25), and writing that expression for a single stream in which the cyclotron frequency is so

---

[1] Reference 8, p. 431. Some of Bailey's symbols have been altered in the quotation to bring them into agreement with the rest of this paper.

high that other terms in the equation on the left are negligible compared to those containing ω_c gives

$$(\omega^2-c^2\beta^2)\left[i\omega\vec{s}\times\vec{\omega}_c - i(\vec{\beta}\cdot\vec{s})\vec{v}^\circ\times\vec{\omega}_c\right] = \omega_p^2\left[\omega^2\vec{s}-c^2(\vec{\beta}\cdot\vec{s})\vec{\beta}\right] . \quad (2.53)$$

Following the previous convention of assuming propagation in the z-direction one has

$$\vec{\beta} = (0, 0, \beta) ,$$

and taking the magnetic field normal to that direction leads to

$$\vec{\omega}_c = (0, \omega_c, 0) .$$

Under these assumptions the vector equation (2.53) expands into two scalar equations:

$$(\omega^2-c^2\beta^2)\left[-i\omega s_3\omega_c + i\beta s_3 v_3^\circ\omega_c\right] = \omega_p^2\omega^2 s_1 , \quad (2.54a)$$

and if $(\omega^2-c^2\beta^2) \neq 0$,

$$\left[i\omega s_1\omega_c - i\beta s_3 v_1^\circ\omega_c\right] = \omega_p^2 s_3 \quad (2.54b)$$

As before the determinant of the coefficients must vanish, and

$$\begin{vmatrix} \dfrac{\omega_p^2\omega^2}{\omega^2-c^2\beta^2} & i\omega_c(\omega-\beta v_3^\circ) \\ -i\omega_c\omega & \omega_p^2+i\omega_c\beta v_1^\circ \end{vmatrix} = 0 ,$$

Expanding this expression and dividing out ω gives

$$\omega_p^2\omega(\omega_p^2+i\omega_c\beta v_1^\circ) - \omega_c^2(\omega^2-c^2\beta^2)(\omega-\beta v_3^\circ) = 0$$

Now assuming the phase velocity $(\omega/\beta) << c$, the velocity of light, this equation approximates,

$$\omega_p^2 \omega(\omega_p^2 + i\omega_c \beta v_1^\circ) + \omega_c^2 c^2 \beta^2 (\omega - \beta v_3^\circ) = 0 \ . \qquad (2.55)$$

This relation is the result of several approximations, and other simplifications will be made in the development of this section. These approximations are made assuming the following values as representative of the quantities in this experimental study

$$\begin{aligned} \omega &\sim 2\pi \cdot 10^5 && \text{radians per second} \\ \omega_p &\sim 2\pi \cdot 3 \cdot 10^9 && \text{radians per second} \\ \omega_c &\sim 2\pi \cdot 10^{10} && \text{radians per second} \\ |\beta \vec{v}^\circ| &\sim 2\pi \cdot 10^5 && \text{per second} \\ c\beta &\sim 2\pi \cdot 10^{10} && \text{per second.} \end{aligned} \qquad (2.56)$$

2.7.1 The velocity of propagation

Equation (2.55) can be simplified further by noting that the term involving v_1°, the velocity normal to the direction of propagation, is much smaller than the other terms present. Thus (2.55) can be approximated by

$$\omega_p^4 \omega + \omega_c^2 c^2 \beta^2 (\omega - \beta v_3^\circ) = 0 \qquad (2.57)$$

This equation is linear in the frequency of the disturbance; solving gives

$$\omega = \frac{\omega_c^2 c^2 \beta^3 v_3^\circ}{\omega_p^4 + \omega_c^2 c^2 \beta^2} = \beta v_3^\circ \frac{1}{1 + \dfrac{\omega_p^4}{\omega_c^2 c^2 \beta^2}}$$

Differentiating this equation with respect to the propagation constant gives the group velocity,

$$v_g = \frac{d\omega}{d\beta} = v_3^\circ \frac{\left(1 + 3\,\frac{\omega_p^4}{\omega_c^2 c^2 \beta^2}\right)}{\left(1 + \frac{\omega_p^4}{\omega_c^2 c^2 \beta^2}\right)^2} \qquad (2.58)$$

For the representative values of (2.56), $\frac{\omega_p^4}{\omega_c^2 c^2 \beta^2} < 1$, and the group velocity is approximately equal to the component of electron drift velocity in the direction of propagation.

2.7.2 The amplification with propagation

These low-frequency waves that propagate normally to the magnetic field at about the electron drift velocity can amplify as they propagate. This is clear from equation (2.57) which is cubic in the propagation constant and can be written:

$$\beta^3 - \left(\frac{\omega}{v_3^\circ}\right)\beta^2 - \frac{\omega_p^4 \omega}{\omega_c^2 c^2 v_3^\circ} = 0 \quad . \qquad (2.59)$$

Descartes' rule of signs implies one positive root and one complex conjugate pair of roots for this expression. Evidently the complex solution with the positive imaginary part represents a wave amplifying as it propagates. An important consideration is the amount of this amplification and its dependence on the velocity of electron drift and other properties of the medium; we turn now to an examination of that gain.

Equation (2.59) is a cubic and the three solutions can be written out explicitly in terms of the coefficients in (2.59). Writing $(\beta_1 + i\,\beta_2)$ as the solution for the amplifying wave, β_2 is given by

$$\frac{\beta_2}{\left(\frac{\omega_p^2}{\omega_c C}\right)} = \frac{3}{2\sqrt{X}} \left[\sqrt{3\sqrt{1+\frac{X}{2}+\sqrt{X\left(1+\frac{X}{4}\right)}}} - \sqrt{3\sqrt{1+\frac{X}{2}-\sqrt{X\left(1+\frac{X}{4}\right)}}} \right], \tag{2.60}$$

where $X = \frac{27\omega_p^4 \left(v_3^\circ\right)^2}{\omega_c^2 C^2 \omega^2}$. In this form β_2 is normalized with respect to its maximum value. Figure (2.4) is a graphical representation of this function. From the figure it is evident that the gain remains nearly constant for a wide range of frequencies and values for the electron drift parallel to the direction of propagation.

The maximum value of gain can be estimated using the representative values of (2.56).

$$\text{Maximum gain} = 20 \log_{10} \left(e^{\omega_p^2/\omega_c C} \right) \tag{2.61}$$

$$= \frac{20}{2.3} \frac{\omega_p^2}{\omega_c C} \sim 2 \text{ db per cm}.$$

2.7.3 The direction of propagation

The study of the last section was carried through assuming that the term involving velocity transverse to the direction of propagation, v_1°, could be ignored in the dispersion relation (2.55) since it is much smaller than the other terms. In this section that velocity is taken into account by a perturbation method. The result indicates that any such velocity transverse to the direction of propagation introduces attenuation and consequently, the preferred direction of low-frequency propagation normal to the magnetic field is parallel to the electron drift.

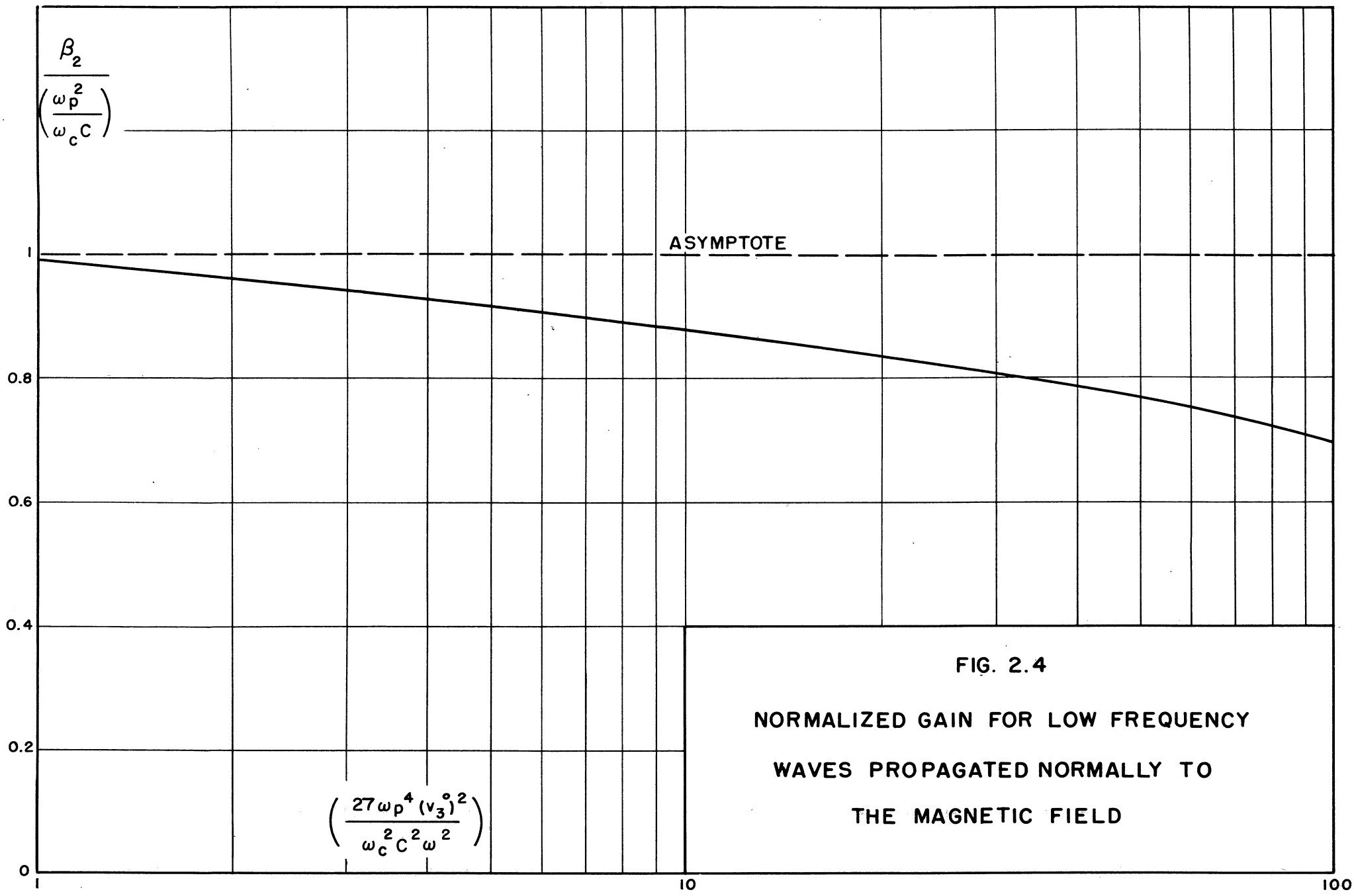

FIG. 2.4

NORMALIZED GAIN FOR LOW FREQUENCY WAVES PROPAGATED NORMALLY TO THE MAGNETIC FIELD

Equation (2.55) is a cubic in the propagation constant β ; it can be written,

$$\left(\omega_c^2 c^2 v_3^\circ\right)\beta^3 - \left(\omega_c^2 c^2 \omega\right)\beta^2 - \left(i\omega_p^2 \omega\omega_c v_1^\circ\right)\beta - \omega_p^4 \omega = 0 . \qquad (2.62)$$

This is just the same as the cubic (2.59) except that the term involving the transverse velocity has been added. Now this added term is presumed small compared to the others. Suppose that ignoring it the solution is β_0 ; we seek a solution $\beta_0 + \epsilon$ which includes this term with the understanding that $\epsilon << \beta_0$. Putting $\beta_0 + \epsilon$ into equation (2.62), using the fact that β_0 satisfies this equation if the higher order term is ignored, and keeping only first order terms in ϵ gives

$$\left(\omega_c^2 c^2 v_3^\circ\right)3\beta_0^2\epsilon - \left(\omega_c^2 c^2 \omega\right)2\beta_0\epsilon - i\omega_p^2 \omega\omega_c v_1^\circ \beta_0 = 0 .$$

Dividing out ω_c β_0 and solving for ϵ leads to

$$\epsilon = i\frac{\omega_p^2 \omega v_1^\circ}{3c^2\beta_0 \omega_c v_3^\circ - 2\omega_c c^2 \omega} . \qquad (2.63)$$

Now it is not difficult to show that the real part of β_0 is negative for the amplifying wave discussed in the last section. Consequently ϵ introduces a negative imaginary part into that solution. This corresponds to attenuation, and one can conclude that the maximum amplification of these low-frequency waves occurs when the propagation is parallel to the electron drift velocity.

Chapter III

AN EXPERIMENTAL STUDY OF THE POWER SPECTRUM, TECHNIQUE AND RESULTS

3.1 Gas diode and experimental apparatus

Several electrode structures were considered as a preliminary step in the experimental study of the power spectrum of a glow discharge in a magnetic field, but all of the spectral data of this report were obtained using the electrode geometry of Figure 3.1. The cylindrical anode shown in the figure is made of copper, the cathode discs of aluminum. A section of the anode is made of copper screen instead of plate copper so that the discharge can be observed visually. This electrode geometry is particularly useful for low-pressure work in the presence of a magnetic field, the cathode structure being similar to that incorporated into the Philips ionization gauge.

The construction of the probe shown in Figure 3.1 will be discussed later in the section on instrumentation. However, it is worth remarking early in this chapter that most of the spectral data were taken with an electrostatic probe like that indicated in the figure. In all cases this probe was located midway between the mycalex insulating plates and 1.5 inches from the anode.

Figures 3.2 and 3.3 are photographs of some of the experimental apparatus. Figure 3.3 includes a front view of the aluminum chamber that houses the gas diode. During

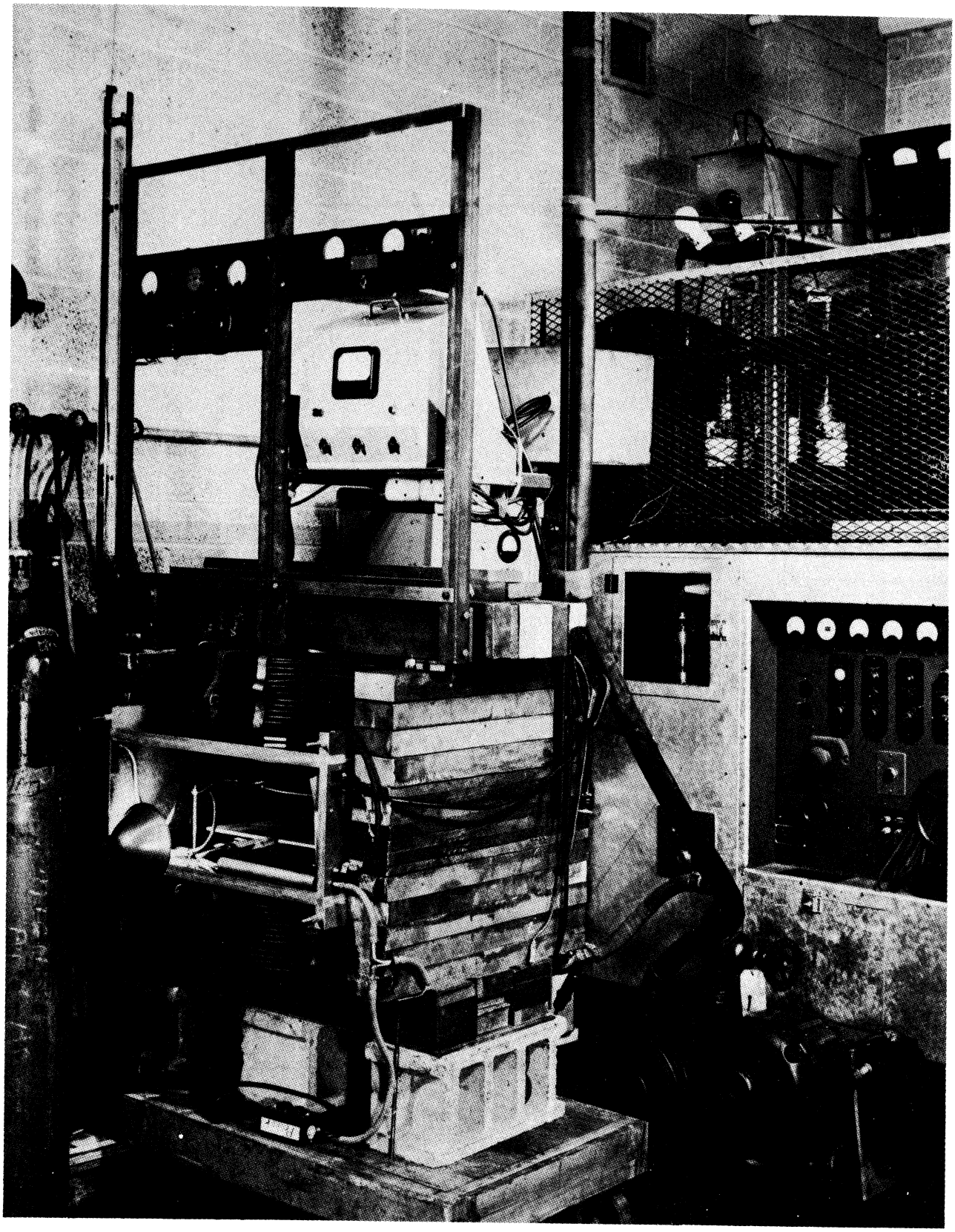

FIG. 3.2

GENERAL VIEW OF EXPERIMENTAL APPARATUS

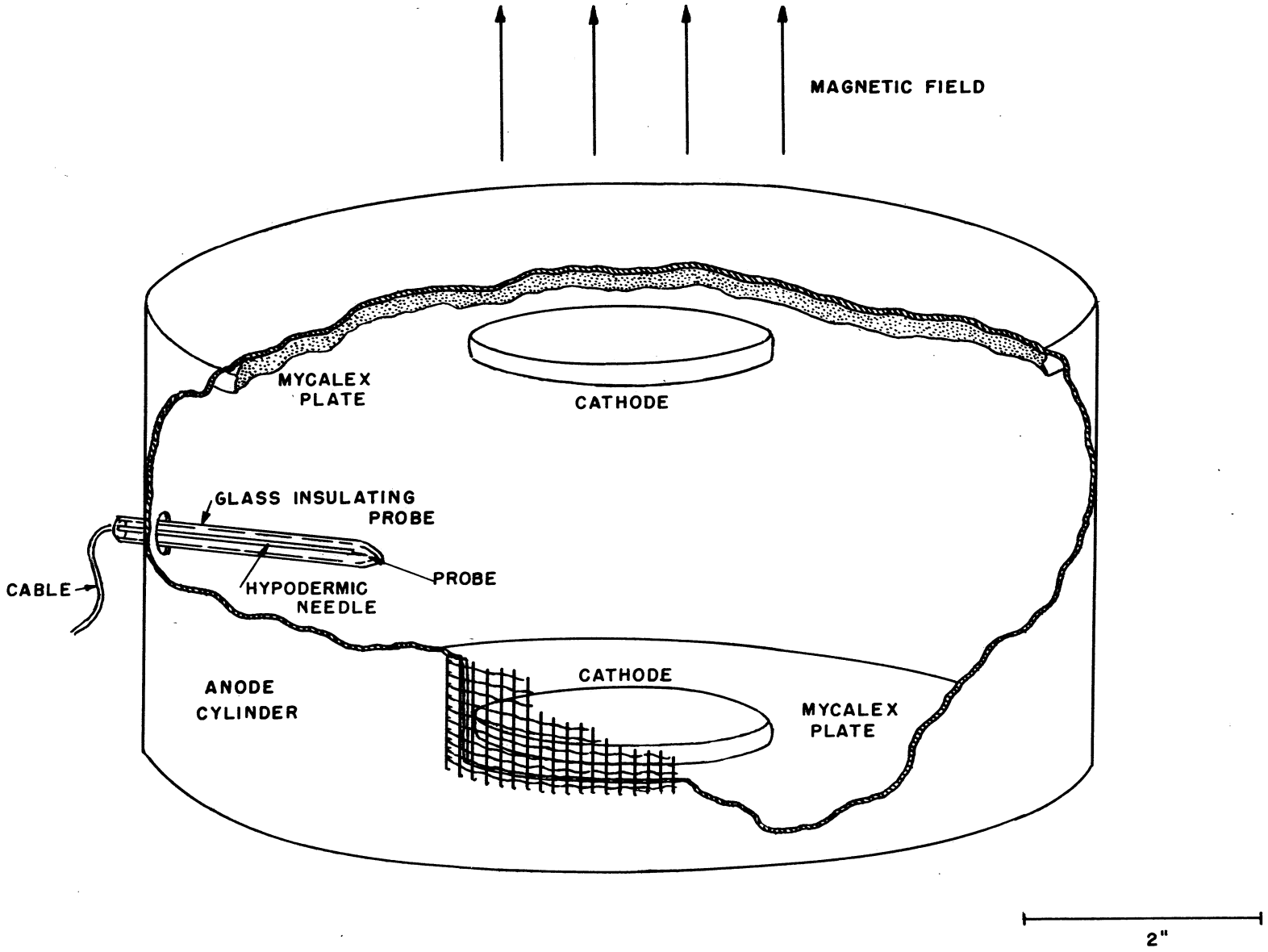

FIG. 3. 1 ELECTRODE STRUCTURE USED IN THE EXPERIMENTS, SHOWING PROBE IN PLACE.

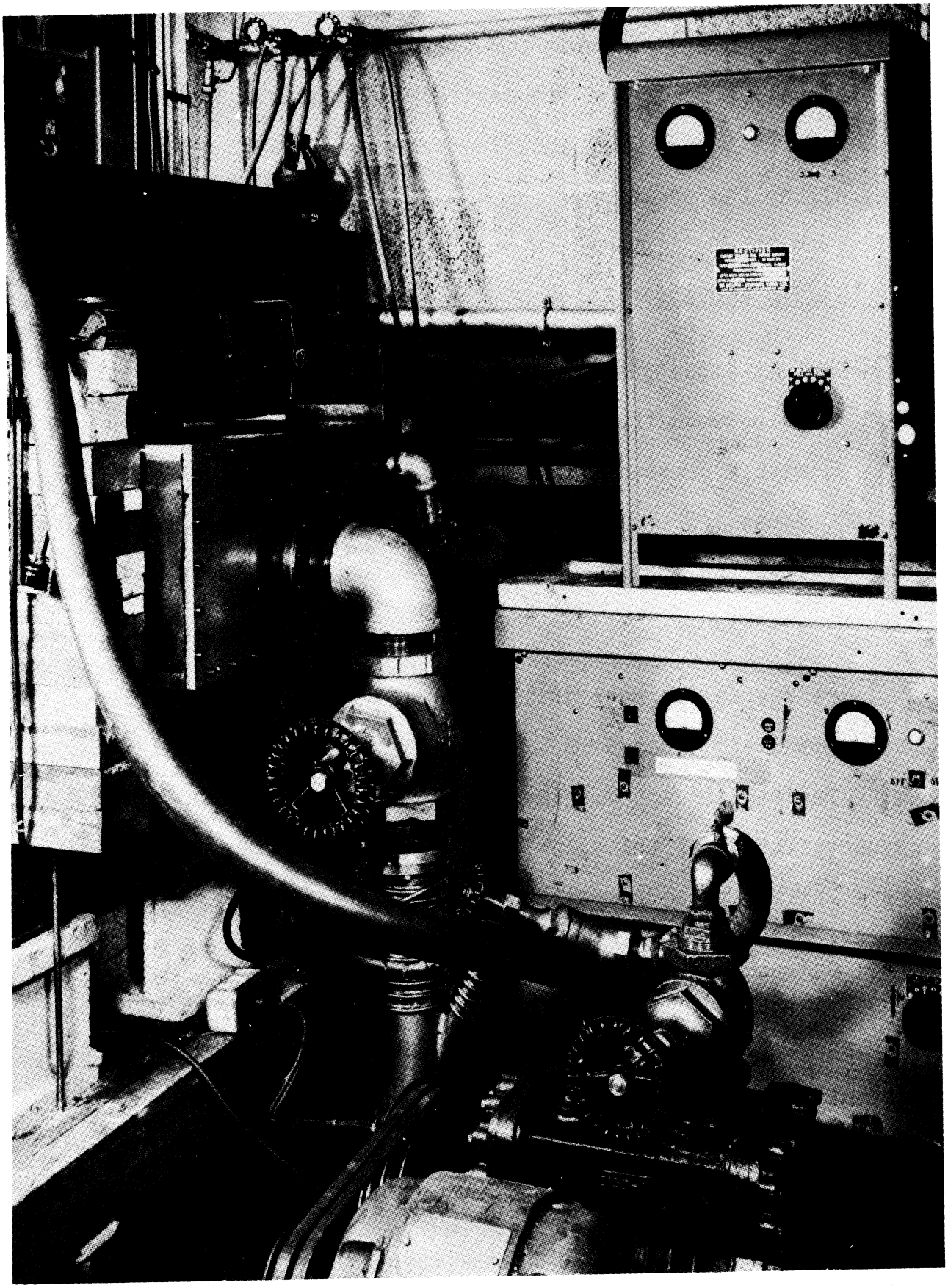

FIG. 3.3

REAR VIEW OF MAGNET AND BOX SHOWING
VACUUM PUMPS AND MAGNET POWER SUPPLIES

operation this whole chamber is evacuated; the chamber is continuously pumped, and the desired gas continuously enters. This assures a pure gas, and also provides an easy method of controlling the pressure.

3.2 Static characteristics of the discharge

The gas diode just described is typically operated with 1500 volts between the terminals. The current is about 0.5 amperes with a pressure of 10 microns and a magnetic field of 3500 gauss. The discharge appears as a uniform, transparent glow filling the whole volume of the diode under these circumstances.

The static characteristics for this type of discharge are extensively treated in a report by Early, Smith, and Lu.[1] The significant distinction between the volt-ampere characteristics of this glow discharge and the more familiar one at higher pressures with no magnetic field is that the magnetic field and the lower pressure tend to increase both the resistance and the incremental resistance of the characteristics. Thus the characteristics appear much like a conventional high-vacuum diode.

3.3 Instrumentation

The method used to obtain the spectral data can be understood by referring to Figure 3.4, which is a block diagram of the circuit arrangement.

---

[1] Reference 22.

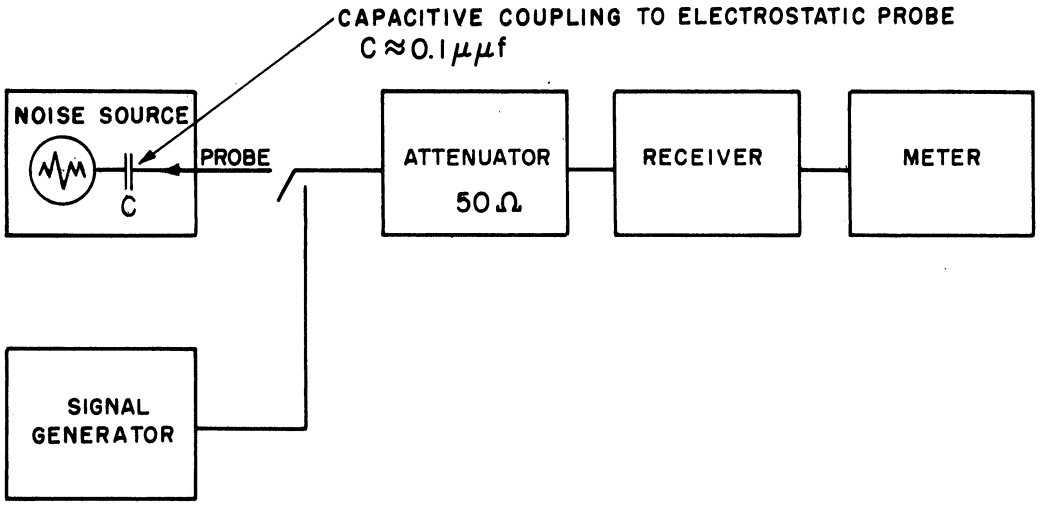

FIGURE 3.4

BLOCK DIAGRAM OF INSTRUMENTATION CIRCUIT.

A probe in the gas discharge, indicated here as a noise source, picks up the fluctuation in the discharge and feeds it into an attenuator. The role of the attenuator is a decoupling one: to insure that all frequency components in the fluctuations are presented the same loading. To maintain this constant loading even at very high frequencies, the electrostatic probe is so constructed that it is essentially a short section of coaxial transmission line using a hypodermic needle for an outer conductor, tungsten wire for an inner conductor, and a ceramic tube for a spacer. The probe dimensions are chosen to give a characteristic impedance of fifty ohms so that the probe conveniently connects to an R. G. coaxial cable that goes to the attenuator. A glass envelope shielded the probe so that all the current flowing in the probe is due to induction. From the attenuator the signal is fed to a receiver; the output of the receiver is metered so that the noise input in the pass band of the receiver

can readily be determined by using a signal generator as shown in Figure 3.4. An attempt is made to avoid errors by calibrating each point separately; that is, the output of the signal generator is adjusted to give the same meter deflection as the noise source produces at the same frequency. Using this method, the power spectrum at a given frequency is the output of the signal generator at that frequency divided by the noise bandwidth of the receiver.[1]

There are three significant errors in the method of instrumentation. (1) A 10 db fixed attenuator was used. Under the most extreme variation of the receiver input impedance from zero to infinity the input to the attenuator would vary from 44 to 67 ohms. For microwave frequencies the variation in resistance at the probe might be even greater because of the standing wave on the coaxial line. (2) Any nonlinearity in the amplification of the receiver before the second detector leads to error. It was presumed that the superheterodyne receivers used were linear as long as the metered output was below that value which indicated overload with a sine wave input. (3) The argument developed in Appendix 5 indicates that the meter following the linear amplification must be square-law. The meters in this study were connected to measure the filtered output of the second detector. For low power input this is square-law; for high power more nearly linear. The error introduced by this

---

[1] A proof of this statement is included in Appendix 5.

feature is outlined in Appendix 5. It is estimated there that the error in the square root of the power spectrum does not exceed 11% from this cause.

3.4 Presentation of data

There are a great many parameters that enter the experimental study of the power spectrum. They include the type of gas, gas pressure, magnetic field strength, discharge current, type of probe, position and orientation of the probe, and many others. Much of the data that have been taken in this study represent a survey of the influence of these factors on the spectrum. These data are coarse; the points are too far apart to indicate the detailed structure of the spectrum. On the other hand data have been obtained in an investigation of the spectrum near the ion cyclotron frequency in which the fine structure of the spectrum was examined with care. These data were taken using hydrogen and helium since these lighter gases have the higher ion cyclotron frequency for a given magnetic field. The rather sharp dip in the spectrum at the cyclotron frequency provides one of the few methods of comparing the theory and experiments.

3.4.1 The ion cyclotron frequency data

The emphasis in this section is on the power spectrum of hydrogen and helium near the ion cyclotron frequency. Consider Figure 3.5a; a curve is presented there for the square root of the power spectrum of hydrogen with the particular magnetic field, current, and pressure indicated.

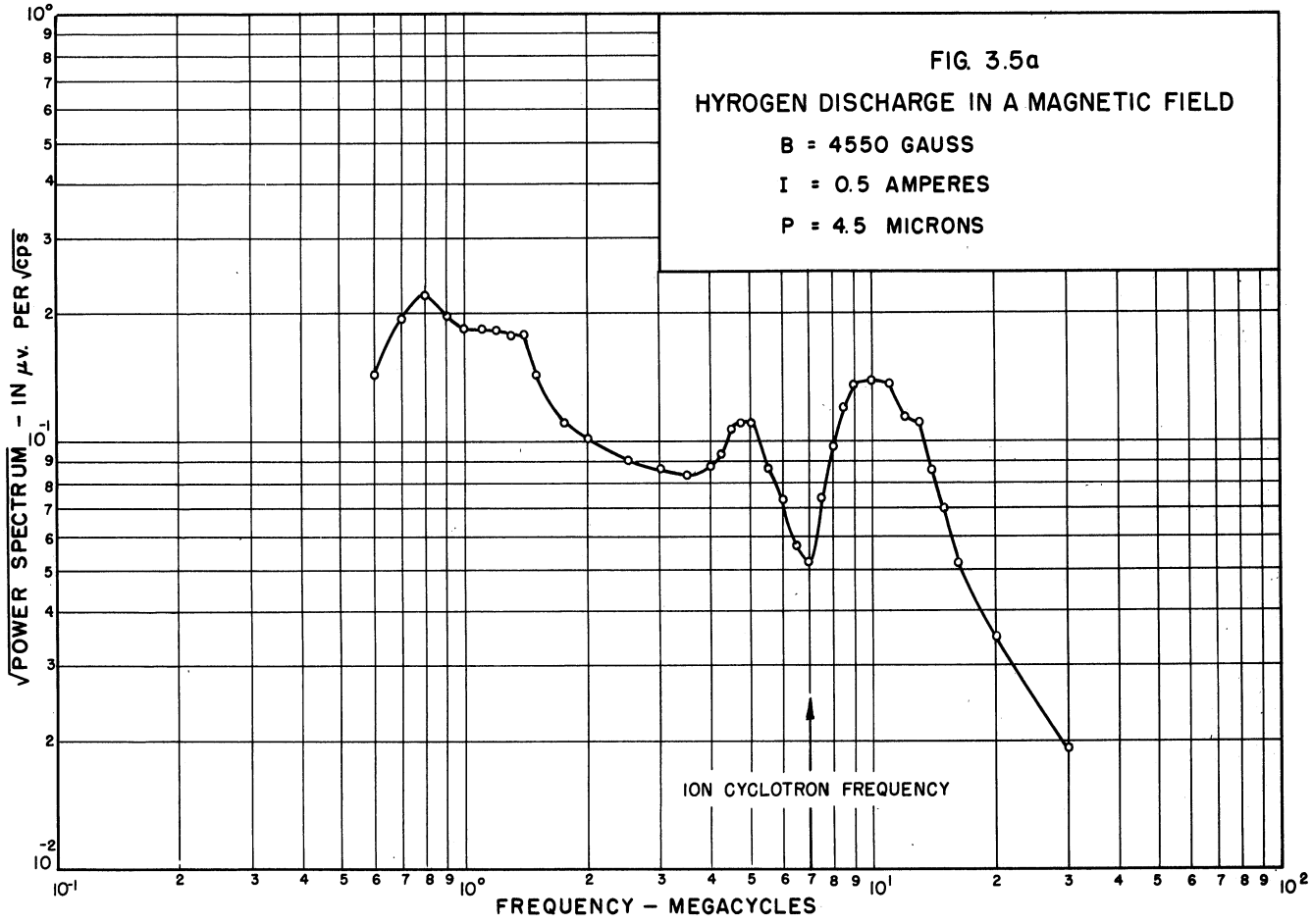
FIG. 3.5a
HYROGEN DISCHARGE IN A MAGNETIC FIELD
B = 4550 GAUSS
I = 0.5 AMPERES
P = 4.5 MICRONS
ION CYCLOTRON FREQUENCY
√POWER SPECTRUM - IN μv. PER √cps
FREQUENCY - MEGACYCLES

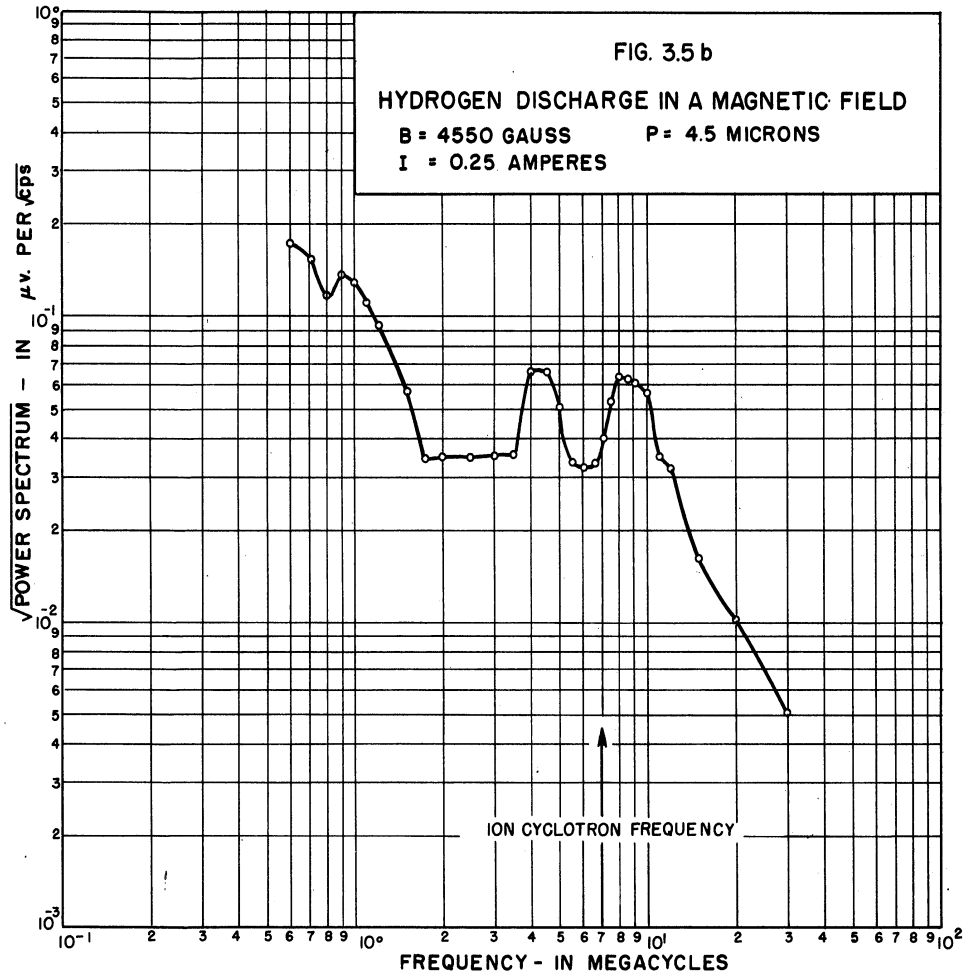
FIG. 3.5 b
HYDROGEN DISCHARGE IN A MAGNETIC FIELD
B = 4550 GAUSS P = 4.5 MICRONS
I = 0.25 AMPERES
ION CYCLOTRON FREQUENCY
√POWER SPECTRUM - IN μv. PER √cps
FREQUENCY - IN MEGACYCLES

The striking feature about this curve is the sharp dip at the ion cyclotron frequency and the rises in the curve above and below that frequency. This is reminiscent of Figure 1.6 in the theoretical study of the ion fluctuations. A discussion of this similarity in the theory and experiment is included in Chapter V where a general comparison of the theoretical and experimental work is presented. Two other features of Figure 3.5a are worthy of note. (1) Near the frequency of 800 kilocycles per second there appears to be a broad resonance. It is likely that this resonance is to be identified with ions oscillating in a potential minimum as discussed by Ballantine and later Cobine.[1] (2) The power spectrum seems to decrease markedly near 15 megacycles per second.

These features discussed in connection with Figure 3.5a are common to all of the data that have been taken near the ion cyclotron frequency. Figure 3.5b shows much the same behavior; the direct current is half that of Figure 3.5a and the amplitude is correspondingly depressed, but near the cyclotron frequency the behavior is much the same. It is important to note that the cyclotron frequency is computed assuming an ionized atom; if ionized molecules are present in the gas, their effect is certainly much less pronounced in the spectrum. Figure 3.6 shows the effect of a change in

[1] References 10, 16, 17, and 18.

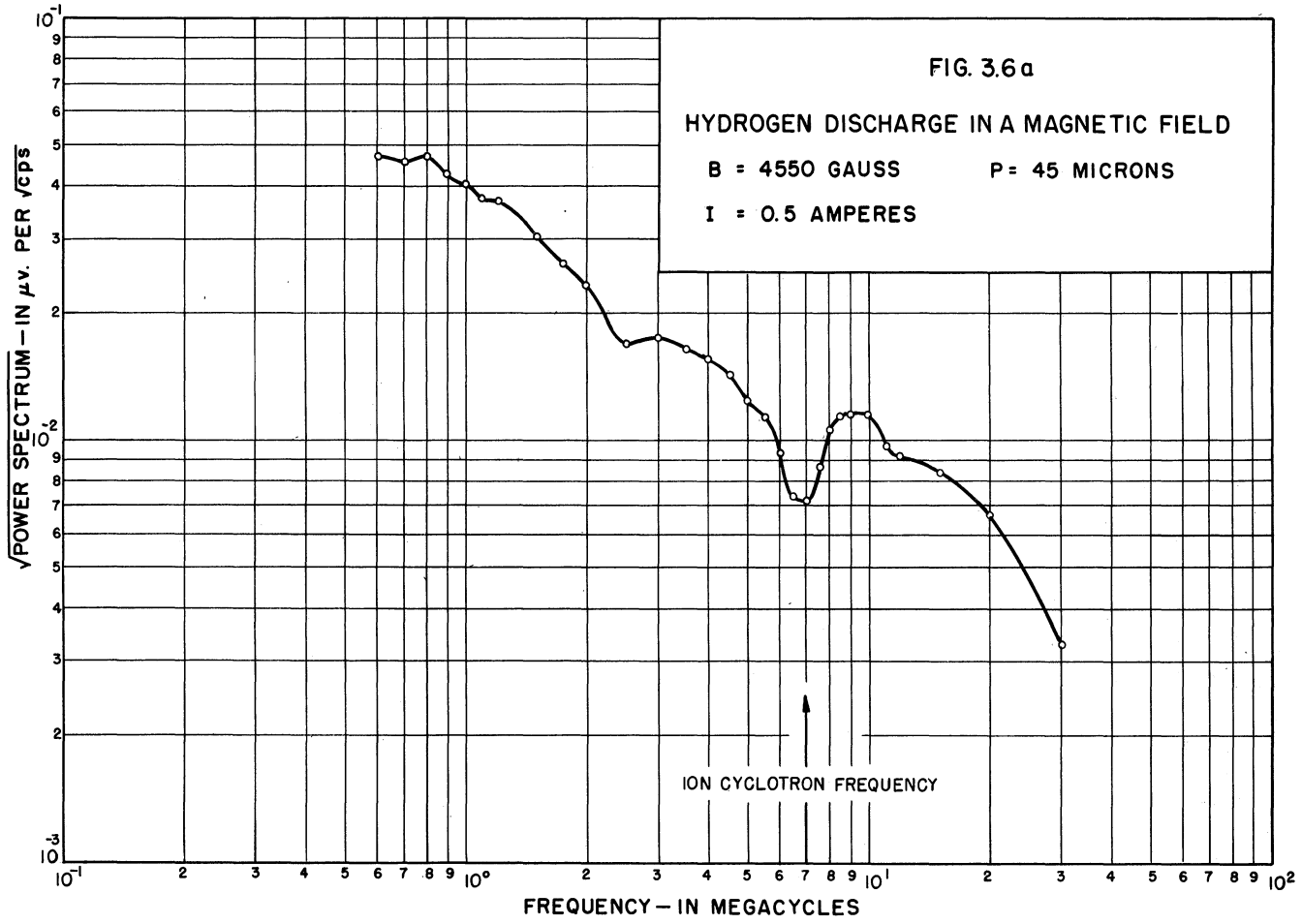
FIG. 3.6a
HYDROGEN DISCHARGE IN A MAGNETIC FIELD
B = 4550 GAUSS
P = 45 MICRONS
I = 0.5 AMPERES
ION CYCLOTRON FREQUENCY
√POWER SPECTRUM — IN μv. PER √cps
FREQUENCY — IN MEGACYCLES

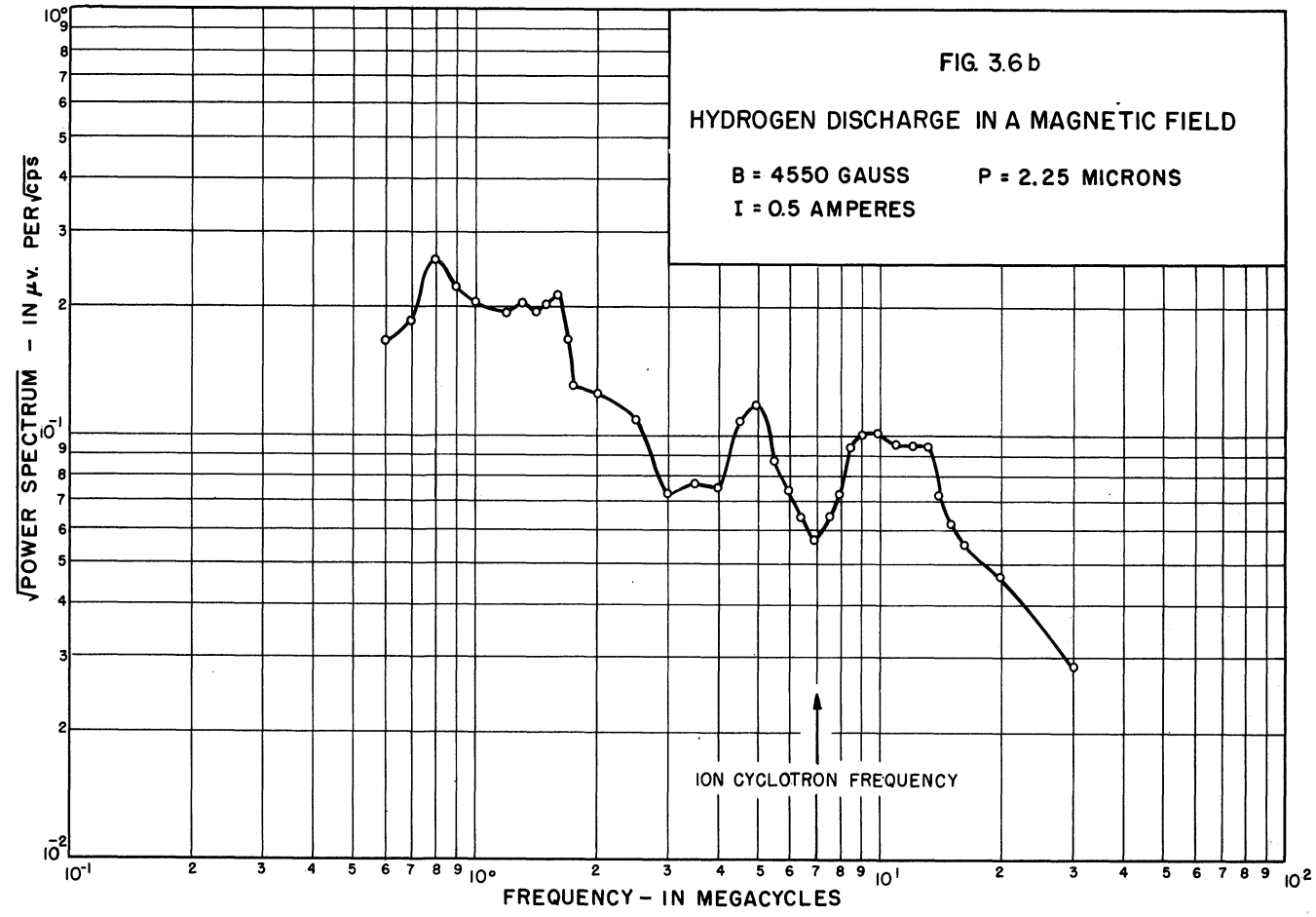
FIG. 3.6b
HYDROGEN DISCHARGE IN A MAGNETIC FIELD
B = 4550 GAUSS
P = 2.25 MICRONS
I = 0.5 AMPERES
ION CYCLOTRON FREQUENCY
√POWER SPECTRUM — IN μv. PER √cps
FREQUENCY — IN MEGACYCLES

pressure, and in 3.7 other values of magnetic field have been chosen. Figure 3.8 shows similar curves for helium.

The cyclotron dip associated with these curves seems to be less pronounced for gases of higher atomic weight, and for increases in pressure and decreases in magnetic field. Perhaps this is not surprising, for all these changes tend to increase the ion collision frequency relative to the cyclotron frequency, and such an increase would likely dampen any pronounced effect at the cyclotron frequency. Probably this is the reason Cobine in his extensive studies did not report any peculiar behavior of the spectrum at the ion cyclotron frequency.[1] Most of his work was with heavier gases than hydrogen and helium, and his pressures were higher and his fields lower than those considered here.

3.4.2 Reproducibility of data

The figures of the last section reflect the accuracy that can be attained if considerable care is taken in gathering the data. However these results are somewhat deceptive, for although successive points of these curves are in good agreement, if the electrode structure is taken apart, reassembled and the same data taken, the agreement is not nearly as satisfactory. This is shown in Figure 3.9 where the results of taking the same data on successive days after dismantling and reassembling the equipment are plotted.

---

[1]References 16 and 18.

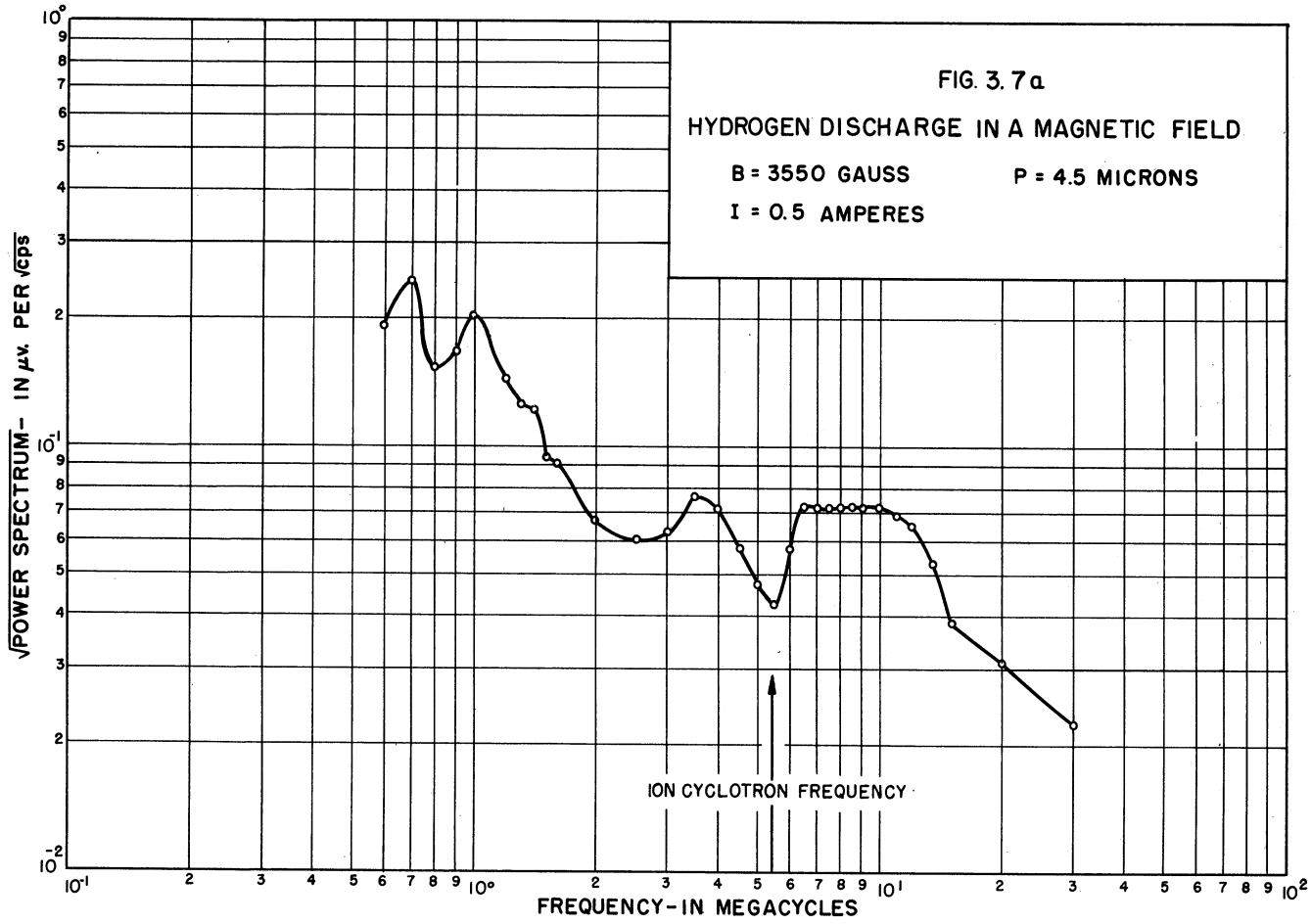
FIG. 3.7a
HYDROGEN DISCHARGE IN A MAGNETIC FIELD
B = 3550 GAUSS
P = 4.5 MICRONS
I = 0.5 AMPERES
ION CYCLOTRON FREQUENCY
√POWER SPECTRUM - IN μv. PER √cps
FREQUENCY - IN MEGACYCLES

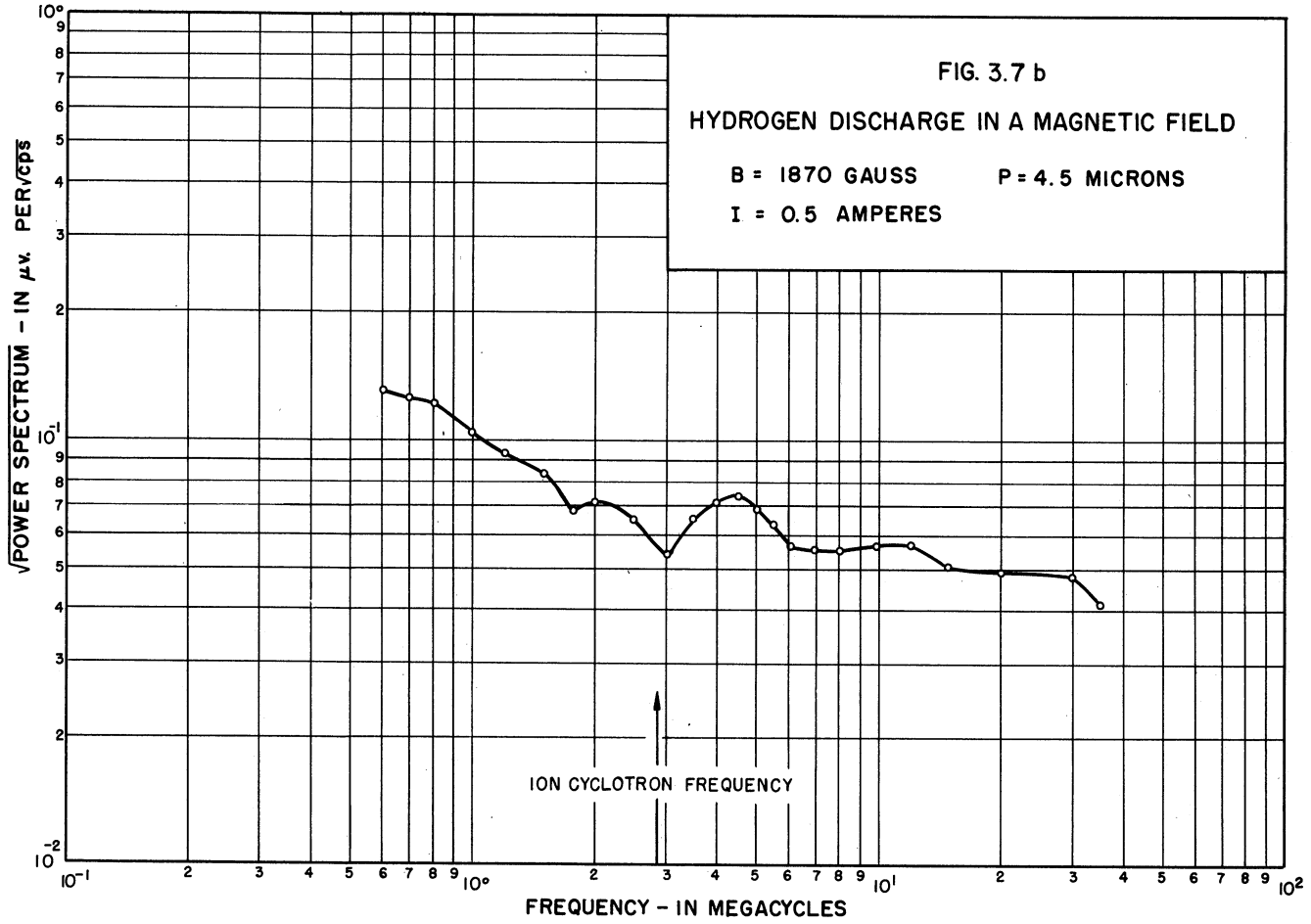
FIG. 3.7 b
HYDROGEN DISCHARGE IN A MAGNETIC FIELD
B = 1870 GAUSS
P = 4.5 MICRONS
I = 0.5 AMPERES
ION CYCLOTRON FREQUENCY
√POWER SPECTRUM - IN μv. PER √cps
FREQUENCY - IN MEGACYCLES

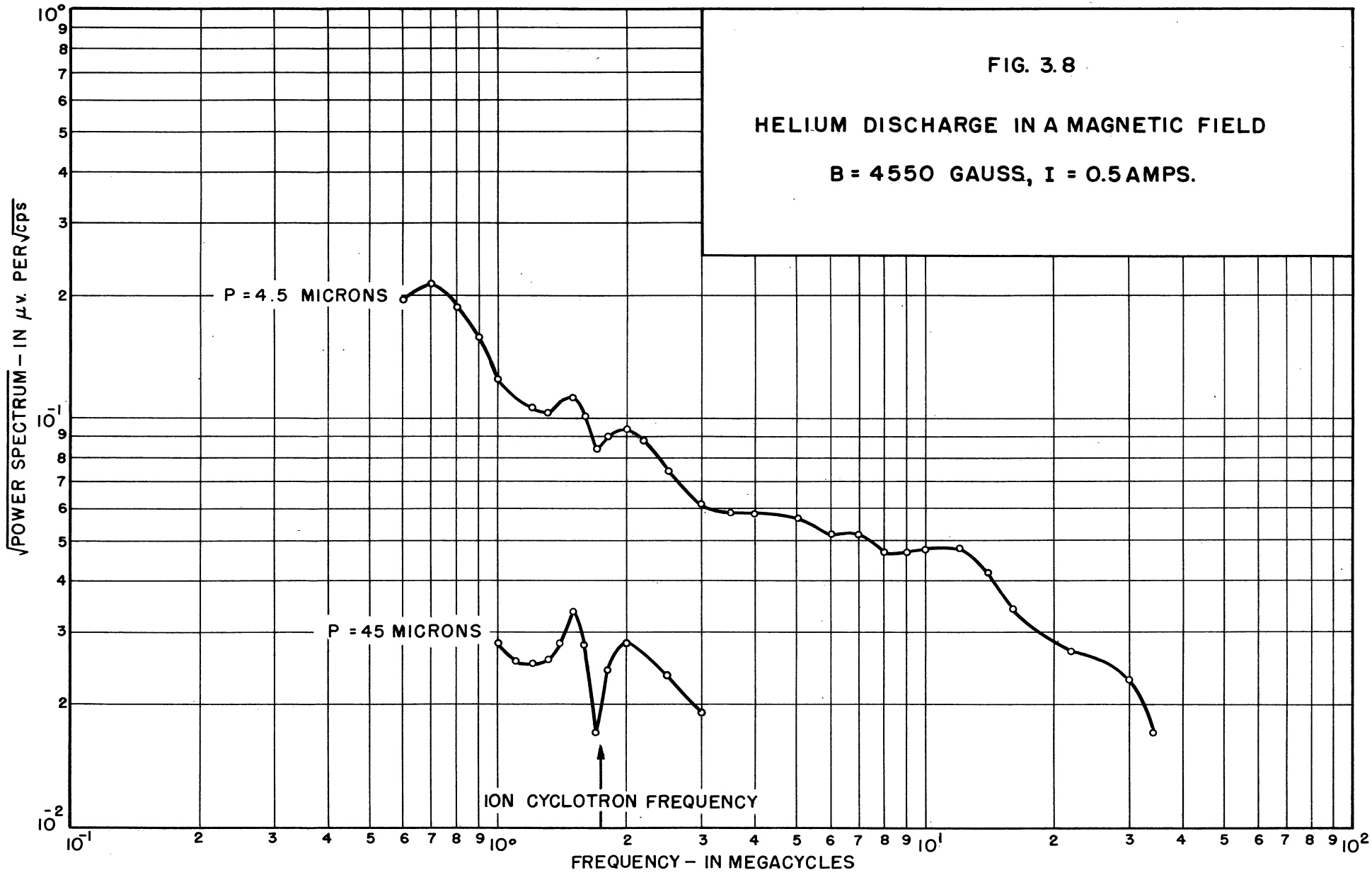
FIG. 3.8
HELIUM DISCHARGE IN A MAGNETIC FIELD
B = 4550 GAUSS, I = 0.5 AMPS.
P = 4.5 MICRONS
P = 45 MICRONS
ION CYCLOTRON FREQUENCY
√POWER SPECTRUM – IN μv. PER √cps
FREQUENCY – IN MEGACYCLES

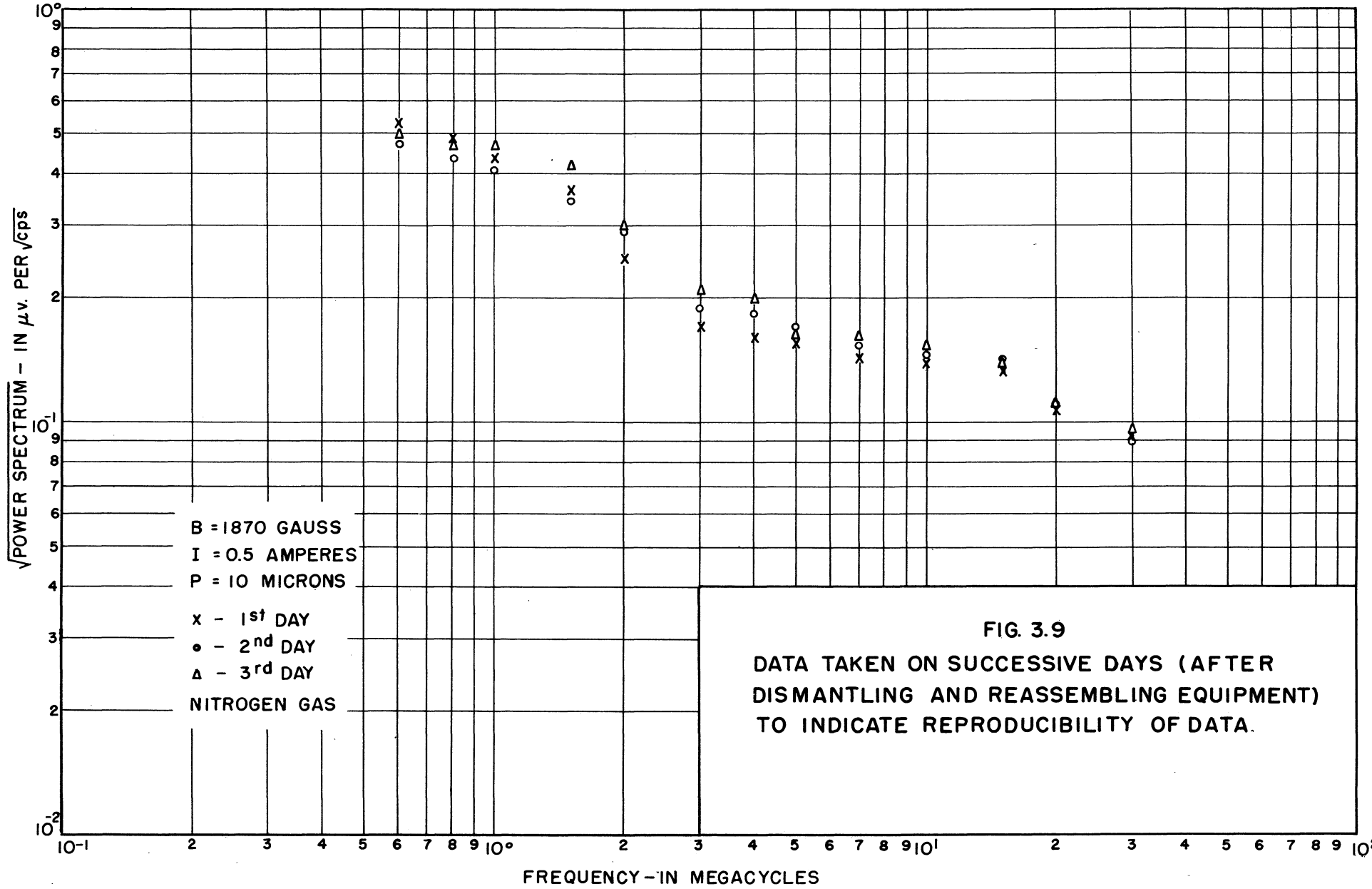

FIG. 3.9

DATA TAKEN ON SUCCESSIVE DAYS (AFTER DISMANTLING AND REASSEMBLING EQUIPMENT) TO INDICATE REPRODUCIBILITY OF DATA.

The average difference for these points is about 7%; this figure of 7% is a rough measure of the reproducibility of data in the low frequency range.

3.4.3 The power spectrum of a nitrogen discharge

Most of the survey data on the spectral distribution of the fluctuations were taken with nitrogen gas. The influence of gas pressure, magnetic field, type of probe, and probe location have been considered. Figure 3.10 presents some of these data for a wide frequency range. The ion cyclotron frequency for nitrogen gas is below half a megacycle per second and the characteristic dip does not appear. These curves show the relative behavior of the spectrum with frequency and pressure. The absolute calibration on the ordinate is not too significant since it depends on the probe size, but some idea of what the numerical value of the ordinate implies is given by noting that the thermal noise from a linear resistance of fifty ohms connected at the input to the probe would plot as a horizontal line in Figure 3.10 with an intercept at 4.5×10^{-4}. This value is far below the data represented in the Figure.[1]

The curves of Figure 3.10 show a very broad spectrum, high in intensity compared with thermal noise. The curves fall away to a minimum near 200 megacycles per second and increase above this value. In Chapter V the regions below

[1] This value for the thermal spectrum of a linear resistance is calculated assuming room temperature, 300° K.

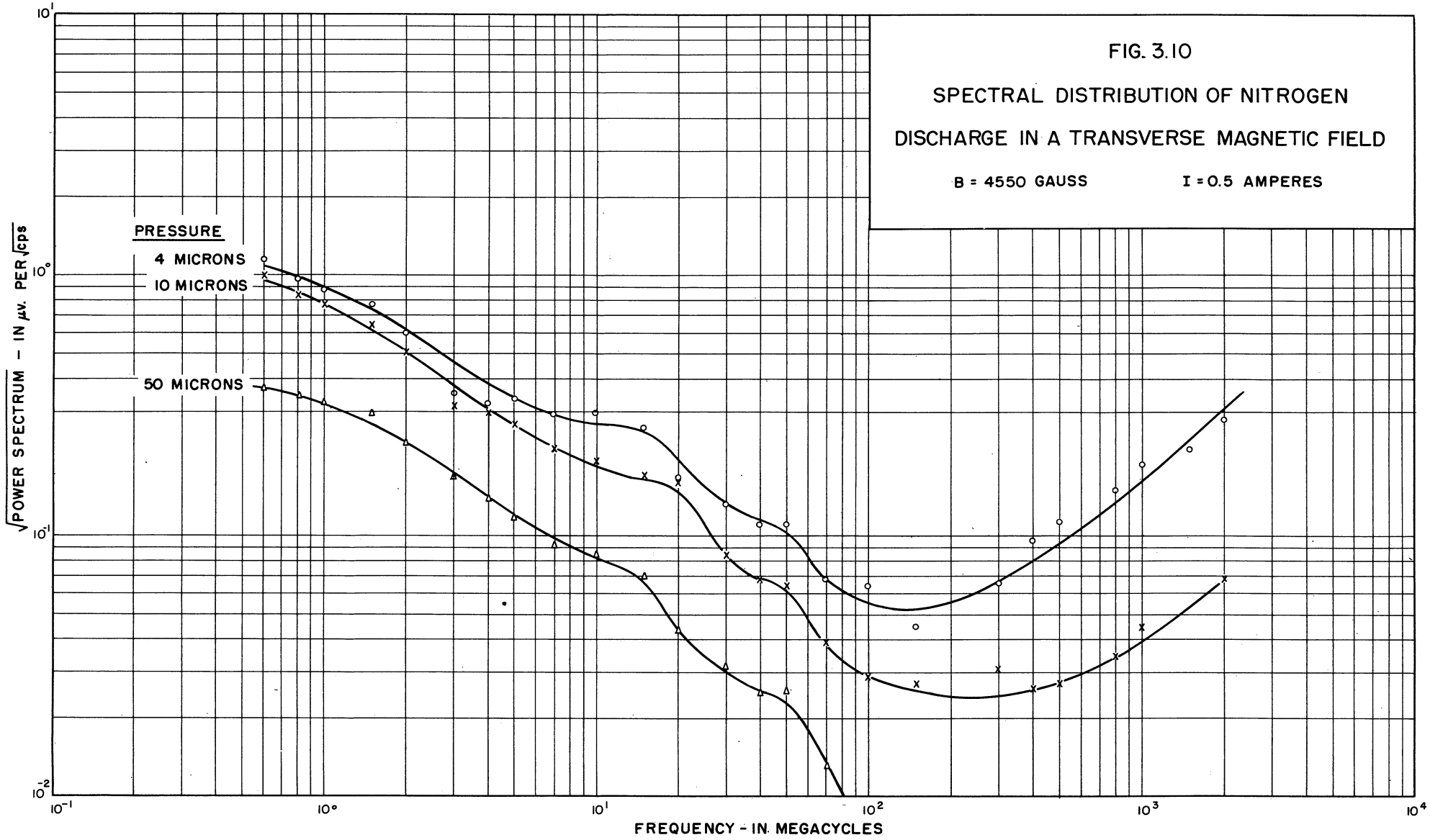
FIG. 3.10
SPECTRAL DISTRIBUTION OF NITROGEN
DISCHARGE IN A TRANSVERSE MAGNETIC FIELD
B = 4550 GAUSS
I = 0.5 AMPERES
PRESSURE
4 MICRONS
10 MICRONS
50 MICRONS
√POWER SPECTRUM - IN μv. PER √cps
FREQUENCY - IN MEGACYCLES
10¹
10°
10⁻¹
10⁻²
10⁻¹
10°
10¹
10²
10³
10⁴

and above this minimum are identified with the amplification bands of Bailey.[1] The rolling character in these curves that is most prominent near 30 megacycles per second is believed to be due to the slight mismatch on the line and probably has nothing to do with the fluctuations.

Figures 3.11 and 3.12 give similar curves for different choices of the magnetic field. Evidently for such high fields the value of the field has little influence, although the low-frequency spectrum tends to increase slightly with an increase in the field. The influence of pressure is more prominent. An increase in pressure seems to lead to a decrease in the power spectrum at all frequencies. This result was checked over a wider range of pressure for particular frequencies. The result is shown in Figure 3.13. The lowest pressures of these curves represent the lowest values of pressure at which the discharge could be sustained for the fixed power input. These curves indicate that over a wide pressure range a decrease in pressure implies an increase in the spectrum. In all the studies of hydrogen, helium, argon, and nitrogen, this same result has been observed. Different probes, magnetic fields, or other parameters do not seem to alter this statement, and it is apparently true that <u>if other things are unaltered an increase in the spectrum accompanies a decrease in pressure</u>. Perhaps such a general conclusion is to be anticipated because the damping on the

[1] Reference 8.

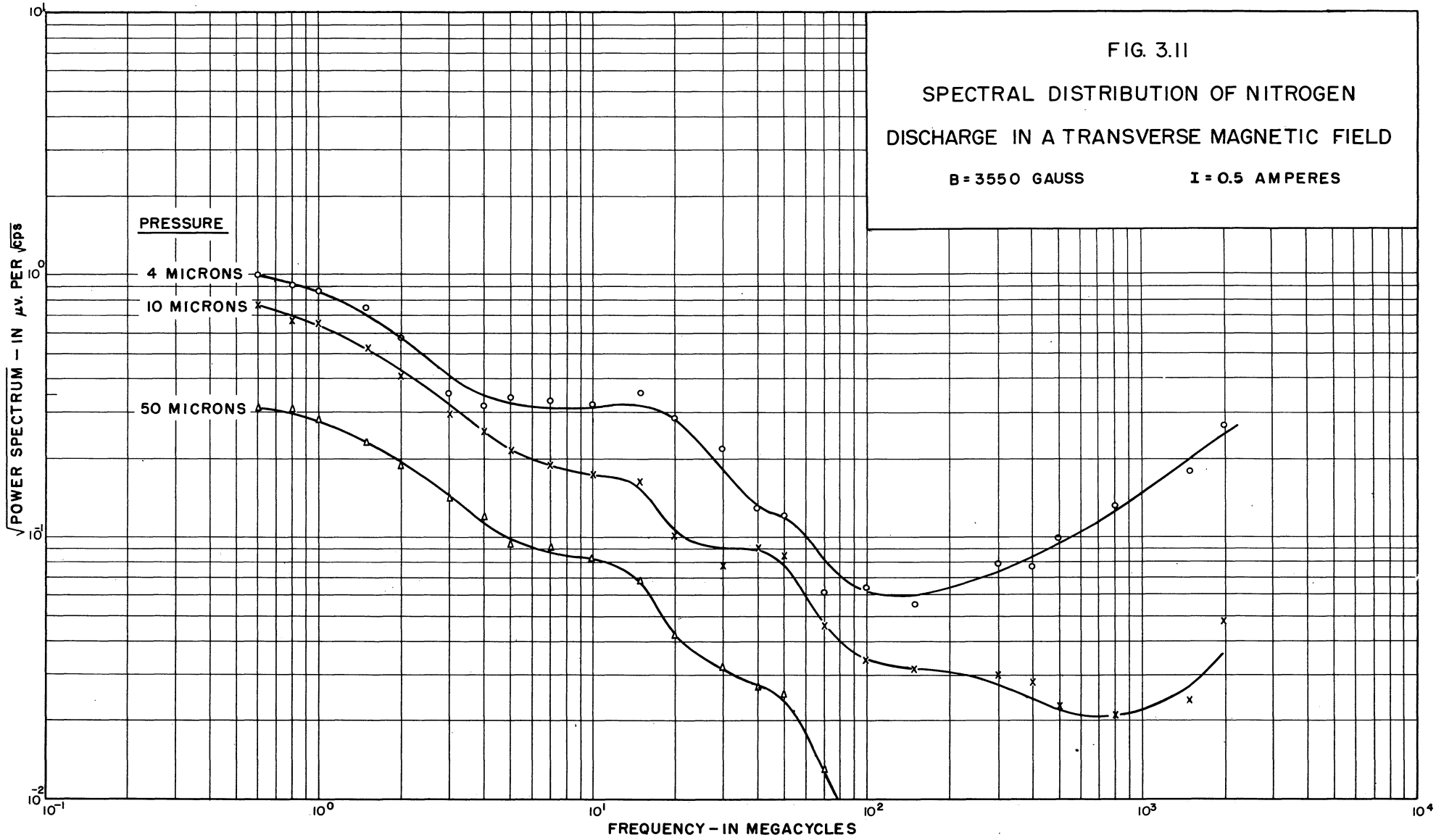
FIG. 3.11
SPECTRAL DISTRIBUTION OF NITROGEN
DISCHARGE IN A TRANSVERSE MAGNETIC FIELD
B = 3550 GAUSS
I = 0.5 AMPERES
PRESSURE
4 MICRONS
10 MICRONS
50 MICRONS
√POWER SPECTRUM – IN μv. PER √cps
FREQUENCY – IN MEGACYCLES
10¹
10⁰
10⁻¹
10⁻²
10⁻¹
10⁰
10¹
10²
10³
10⁴

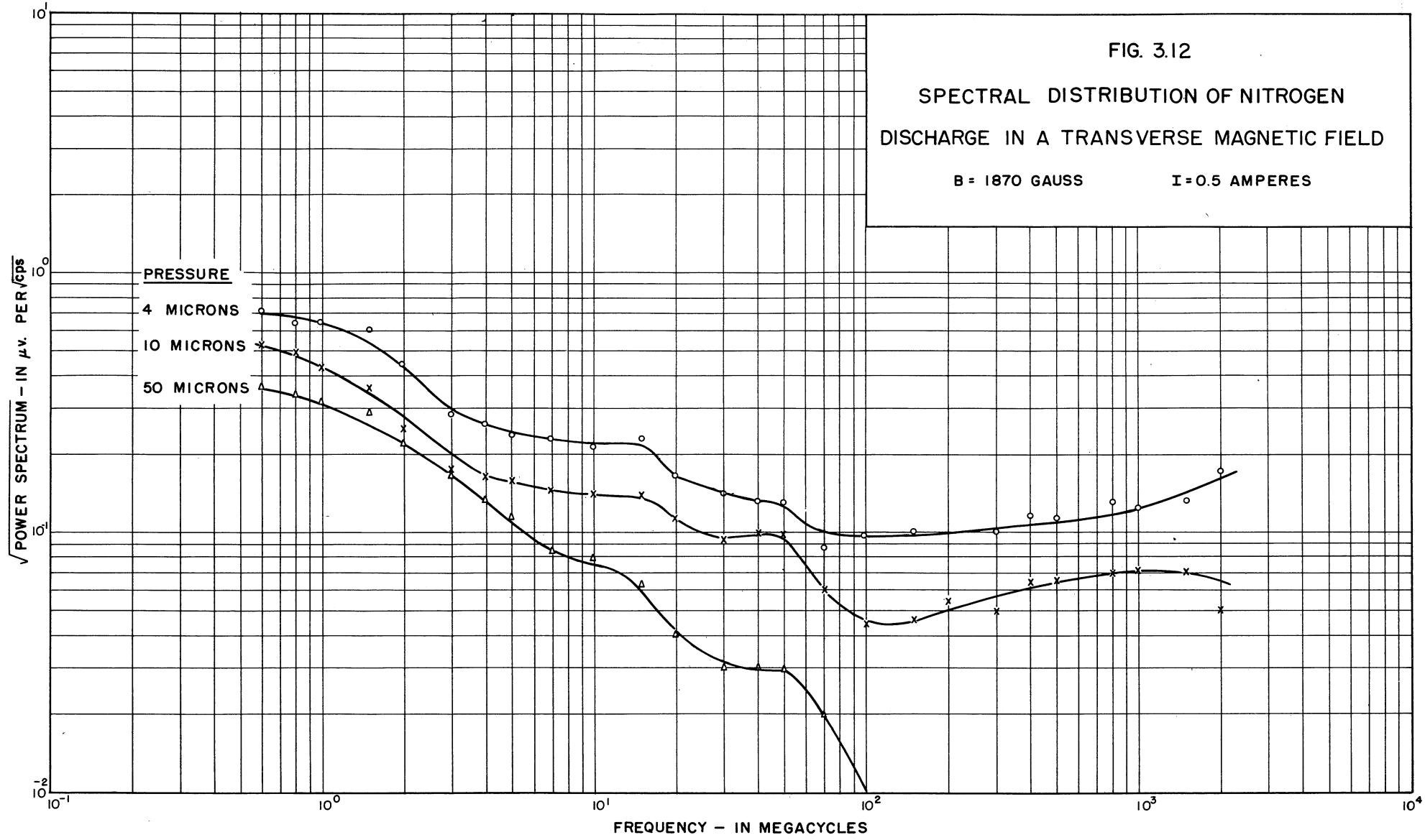
FIG. 3.12
SPECTRAL DISTRIBUTION OF NITROGEN
DISCHARGE IN A TRANSVERSE MAGNETIC FIELD
B = 1870 GAUSS
I = 0.5 AMPERES
PRESSURE
4 MICRONS
10 MICRONS
50 MICRONS
√POWER SPECTRUM – IN μv. PER √cps
FREQUENCY – IN MEGACYCLES
10^1
10^0
10^-1
10^-2
10^-1
10^0
10^1
10^2
10^3
10^4

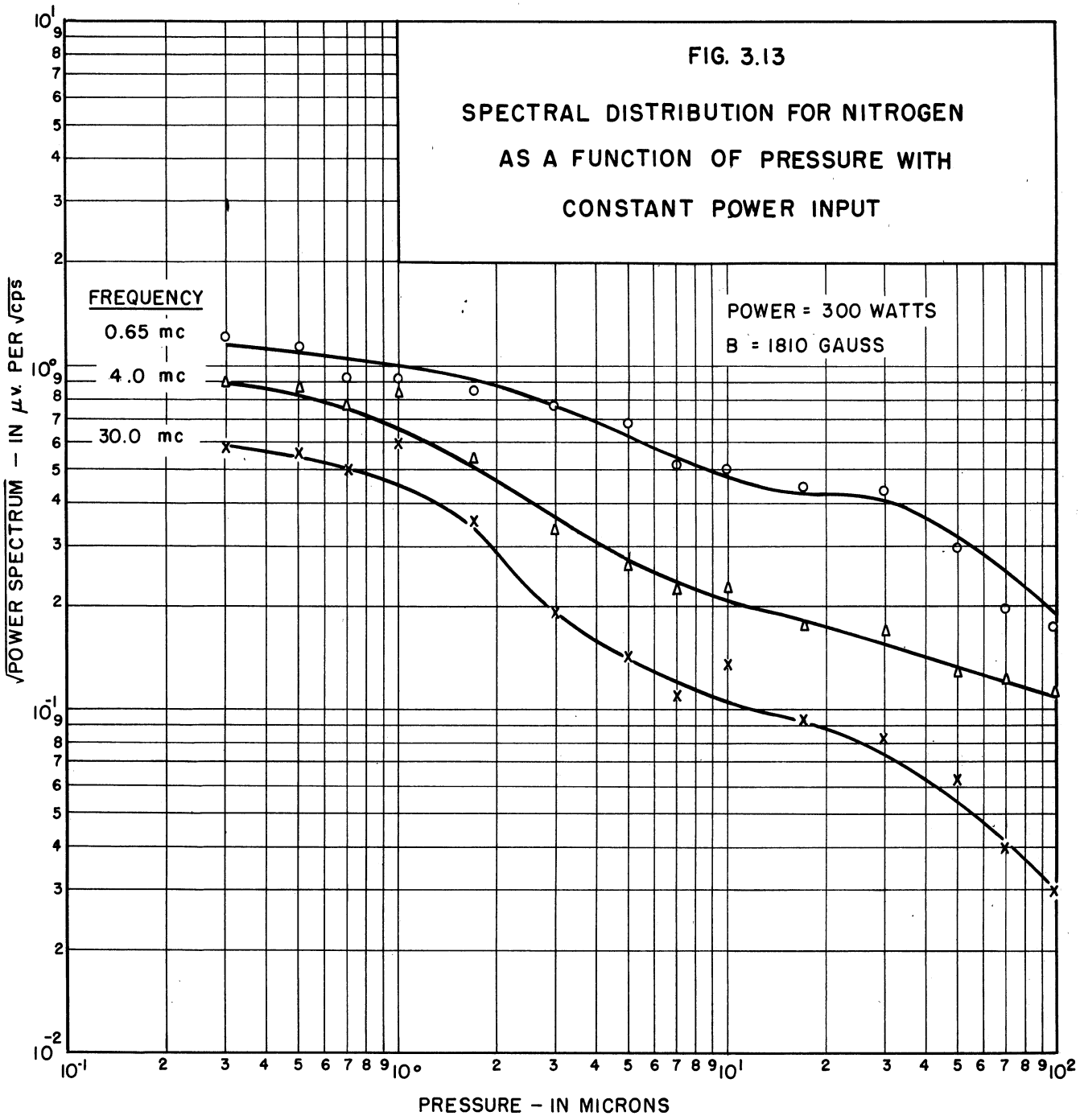
FIG. 3.13
SPECTRAL DISTRIBUTION FOR NITROGEN AS A FUNCTION OF PRESSURE WITH CONSTANT POWER INPUT
FREQUENCY
0.65 mc
4.0 mc
30.0 mc
POWER = 300 WATTS
B = 1810 GAUSS
√POWER SPECTRUM – IN μv. PER √cps
PRESSURE – IN MICRONS

fluctuations is due to the rate of collisions of the charged particles, and a reduction in pressure reduces the collision rate.

3.4.4 Data with a loop probe

Some of the survey data for the low-frequency end of the spectrum have been obtained using a two-turn loop probe. This probe was constructed in a manner similar to the electrostatic probe already discussed except that the termination was a two-turn loop of tungsten wire covered with a high temperature cement so that the wire was not directly exposed to the discharge. This type of probe seems to be of limited usefulness since it is necessarily more bulky than the electrostatic probe, and the inductive reactance of the two turns places an upper frequency limit on its application; the two-turn, quarter-inch diameter loop of this study was satisfactory to about 50 megacycles per second. However, by orienting the plane of loop in the direction of the magnetic field and normal to that direction, information about the fluctuations could be obtained that was not revealed by the electrostatic probe.

In many respects the data obtained using the loop probe was similar to that of the electrostatic probe. For example the spectrum obtained with the loop probe was relatively insensitive to the magnetic field and increased with a decrease in the gas pressure in much the same manner as the spectrum obtained when using the electrostatic probe. Figure 3.14 gives a new

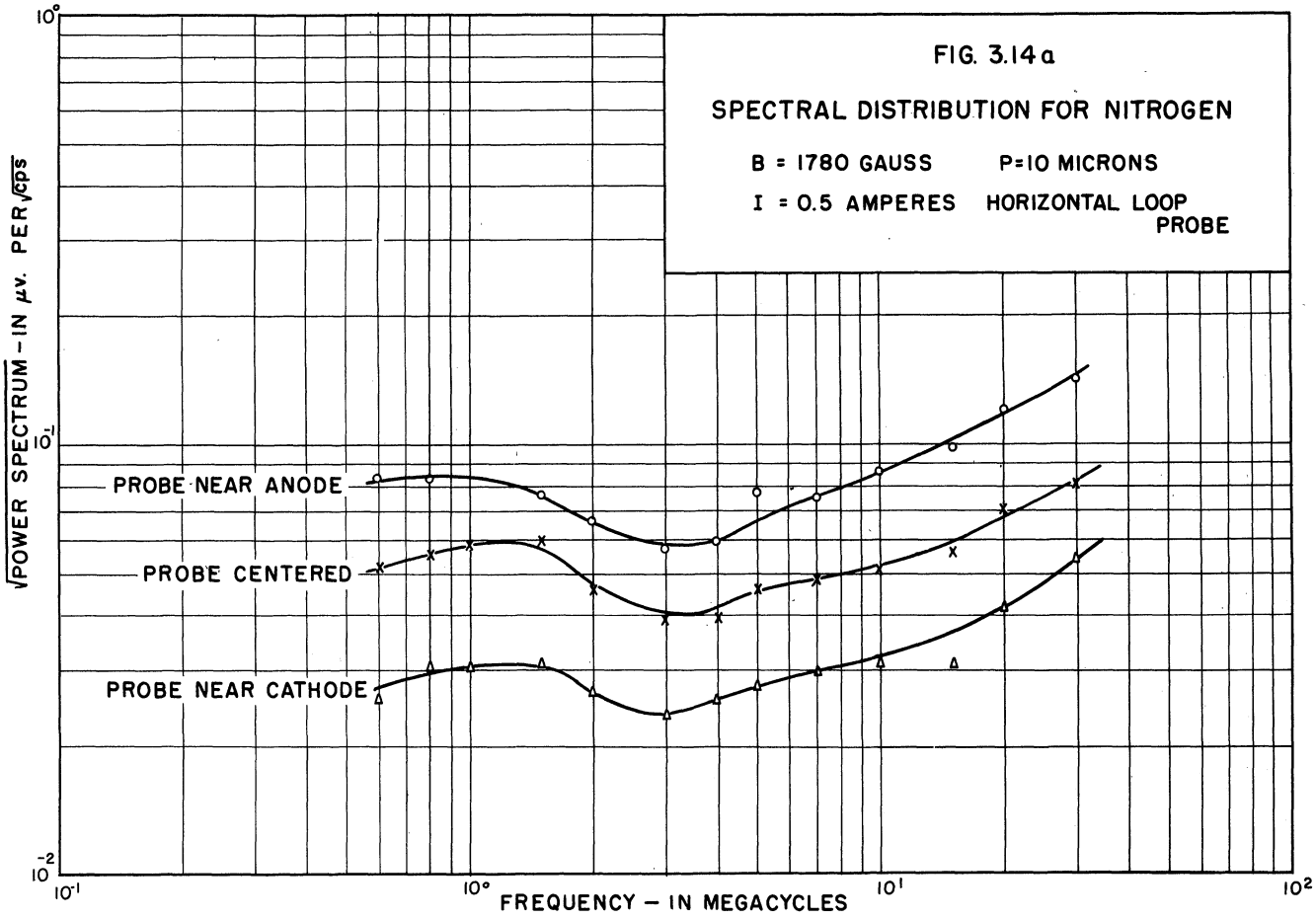
FIG. 3.14 a
SPECTRAL DISTRIBUTION FOR NITROGEN
B = 1780 GAUSS P=10 MICRONS
I = 0.5 AMPERES HORIZONTAL LOOP PROBE
PROBE NEAR ANODE
PROBE CENTERED
PROBE NEAR CATHODE
√POWER SPECTRUM – IN μv. PER √cps
FREQUENCY – IN MEGACYCLES

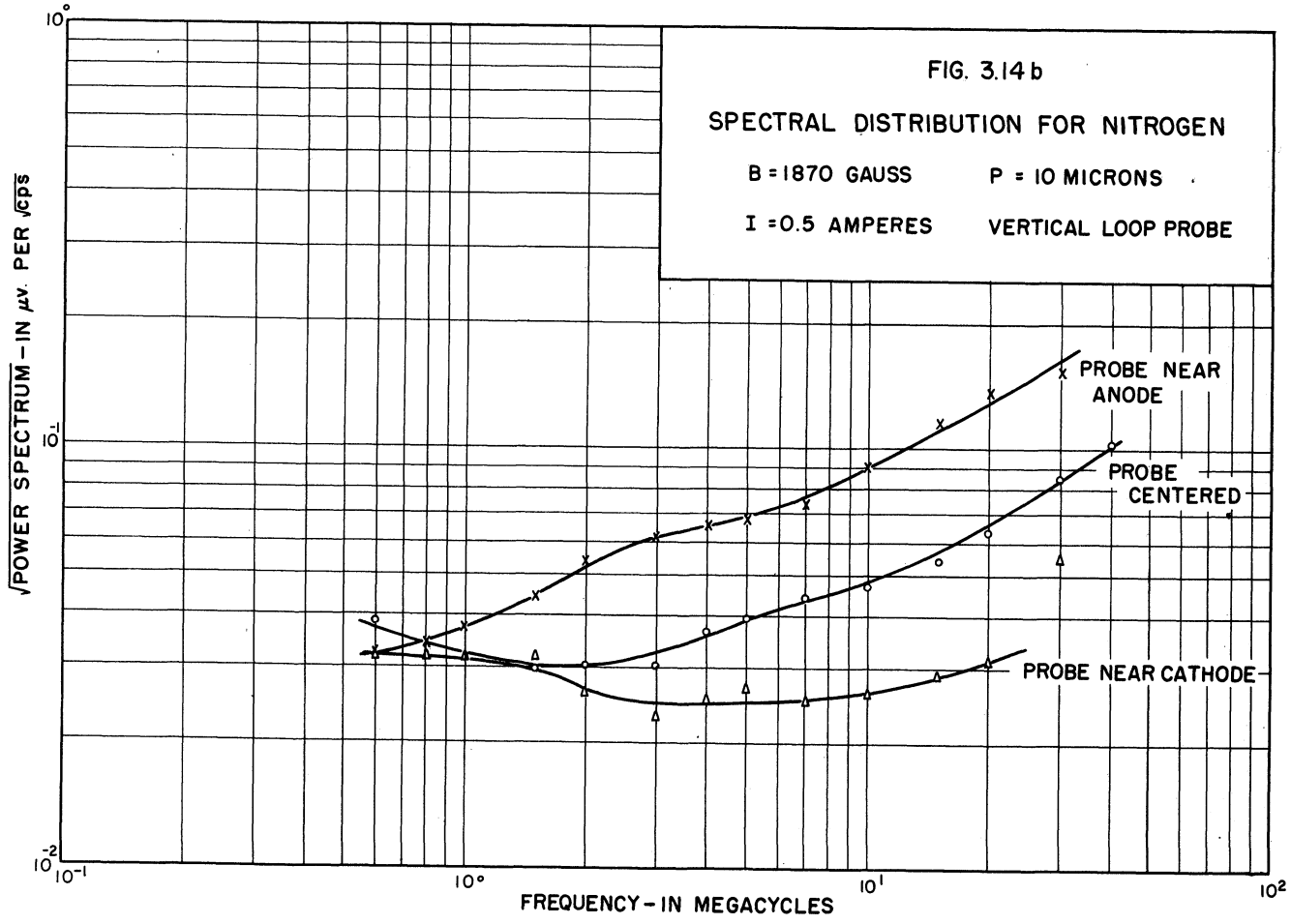
FIG. 3.14 b
SPECTRAL DISTRIBUTION FOR NITROGEN
B = 1870 GAUSS P = 10 MICRONS
I = 0.5 AMPERES VERTICAL LOOP PROBE
PROBE NEAR ANODE
PROBE CENTERED
PROBE NEAR CATHODE
√POWER SPECTRUM – IN μv. PER √cps
FREQUENCY – IN MEGACYCLES

result; it shows the influence of the location of the loop probe on the character of the spectrum. The probes in the three cases are located 0.5, 1.5, and 2.5 inches from the anode. The general tendency seems to be for an increase in the amplitude of the spectrum with the loop nearer to the anode. This has important implications, for it is argued in Chapters IV and V that much of this spectrum has its origin in waves that propagate from cathode to anode, increasing in amplitude as they move. The higher intensity of the spectrum near the anode is explained in this way.

Figure 3.15 presents a comparison of data taken with the probe in different orientations. An interesting feature in these curves is the change that seems to take place at about four megacycles per second. Above this frequency the horizontal and vertical orientation seem to give a similar spectrum. Below this frequency the horizontal probe seems to have a contribution that the vertical orientation does not provide.

There is a general tendency for the amplitude of the spectrum at low frequencies to increase with frequency when a loop probe is used and decrease with frequency when an electrostatic probe is used. This is not surprising for one can expect the ratio of the absolute values of the electric field and the magnetic field in the plasma to be approximately independent of frequency. Assuming that the voltage on the electrostatic probe is proportional to the electric field and that on the loop probe proportional to the time derivative of the magnetic field, the square root of the power spectra with the two probes will differ by a factor proportional to frequency. This is approximately the result obtained.

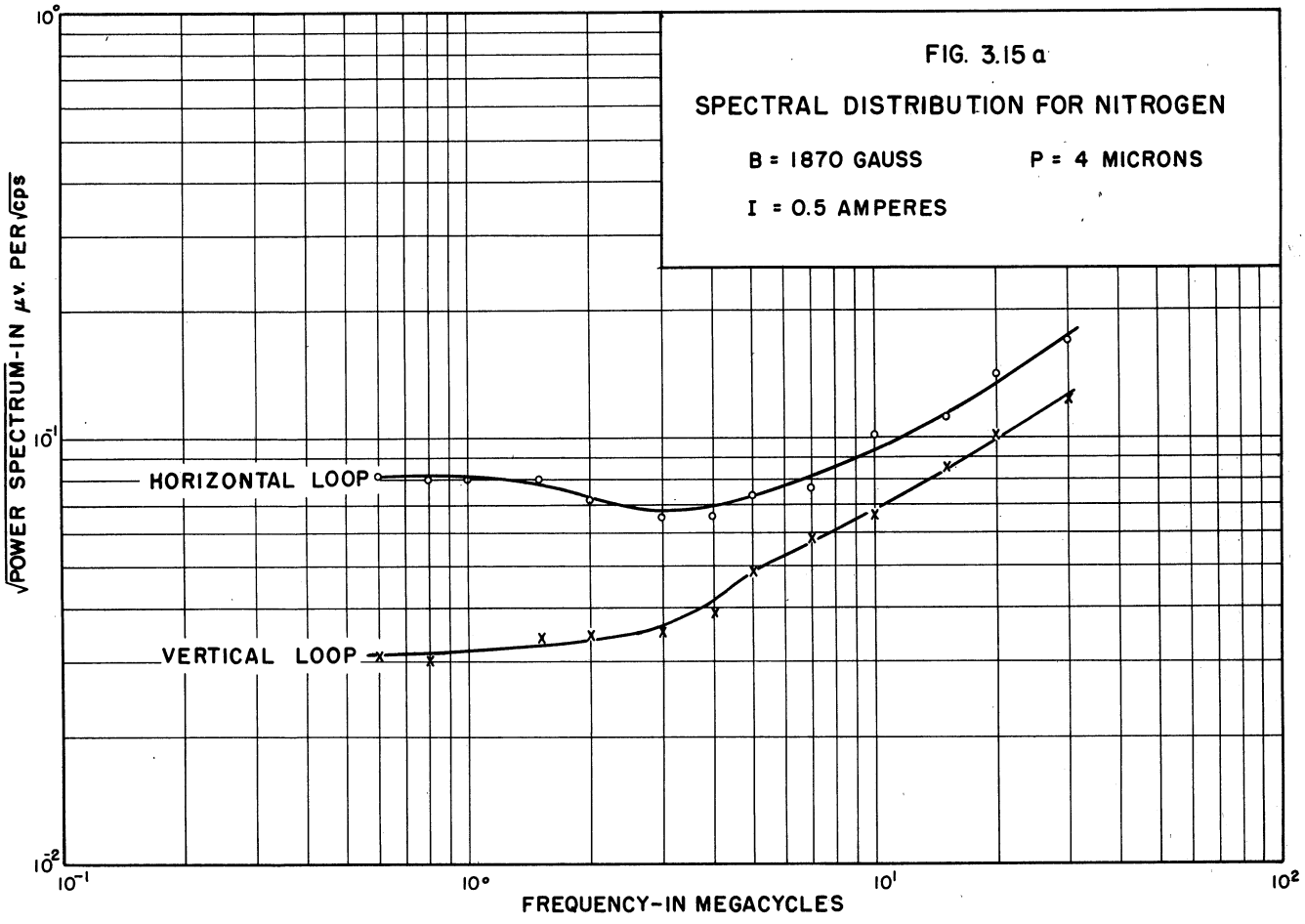
FIG. 3.15 a
SPECTRAL DISTRIBUTION FOR NITROGEN
B = 1870 GAUSS
P = 4 MICRONS
I = 0.5 AMPERES
HORIZONTAL LOOP
VERTICAL LOOP
√POWER SPECTRUM-IN μv. PER √cps
FREQUENCY-IN MEGACYCLES

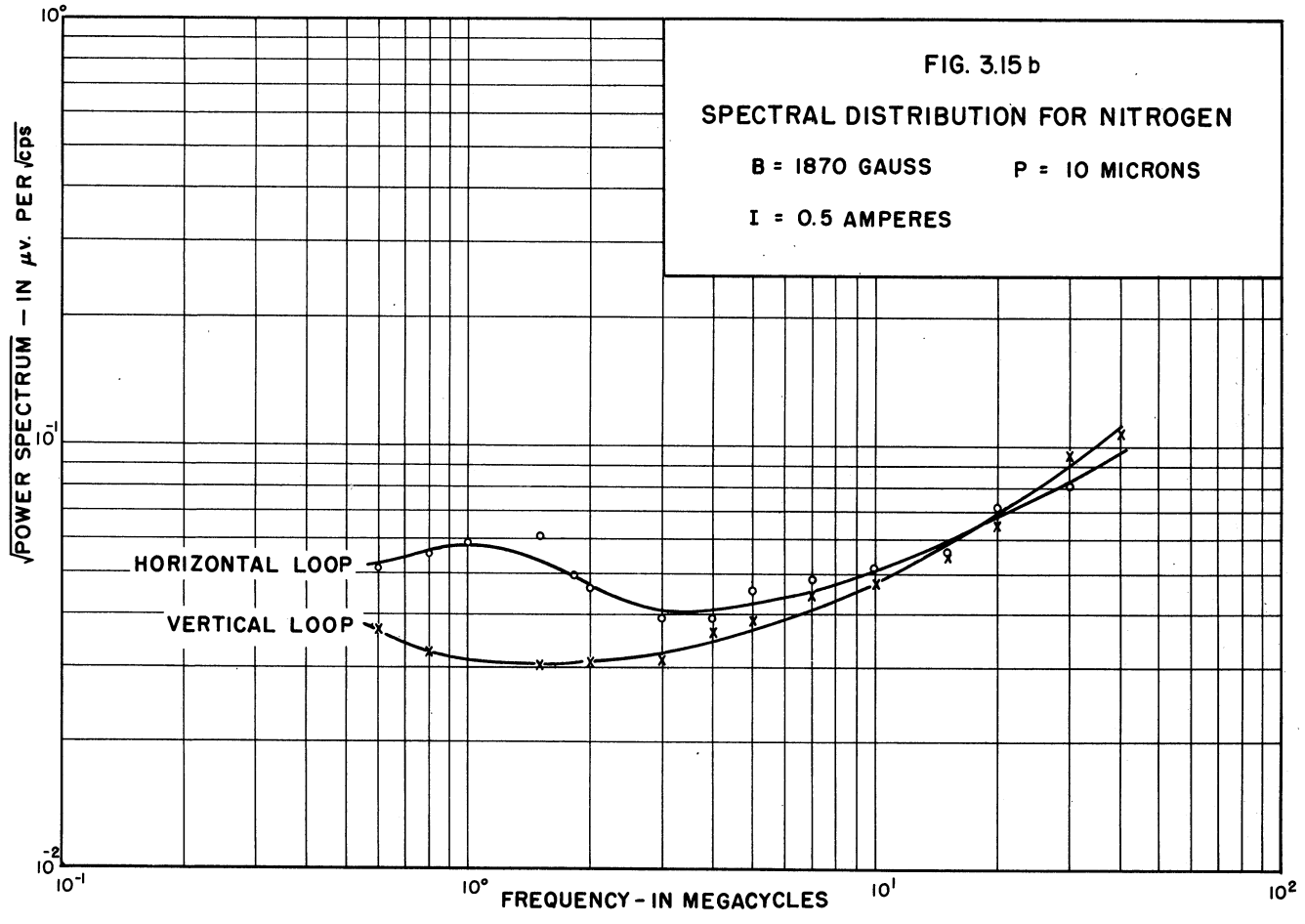
FIG. 3.15 b
SPECTRAL DISTRIBUTION FOR NITROGEN
B = 1870 GAUSS
P = 10 MICRONS
I = 0.5 AMPERES
HORIZONTAL LOOP
VERTICAL LOOP
√POWER SPECTRUM — IN μv. PER √cps
FREQUENCY - IN MEGACYCLES

Chapter IV

AN EXPERIMENTAL STUDY OF THE LOW FREQUENCY PROPAGATION NORMAL TO THE MAGNETIC FIELD

The last chapter was a study of the distribution of the power in the fluctuation with frequency. This chapter is an examination of the fluctuations in time; the objective is to answer the following questions:

(1) How fast do the fluctuations propagate?

(2) In what direction do the fluctuations propagate?

(3) Do the fluctuations amplify or attenuate as they propagate?

4.1 The low-frequency fluctuations

The experiments of this study were performed in the gas diode described in the last chapter, but the probe structure was modified from that previously discussed. The probe was merely a bare wire in a fine ceramic tube with the wire extending a quarter of an inch beyond the ceramic as sketched in Figure 4.1. The probe is midway between the mycalex plates and extends half an inch into the discharge. The other end of the wire was returned through a 300K ohm resistor to the plate.[1] The average potential on such a probe is typically 400 volts below the plate potential. Photographs of the fluctuating potential on such a probe are shown in Figure 4.2. The high intensity and random nature of this disturbance should be noted.

[1] A particular merit of biasing the probe in this way is that it avoids the rectifying action of a floating probe. See References 22 and 41.

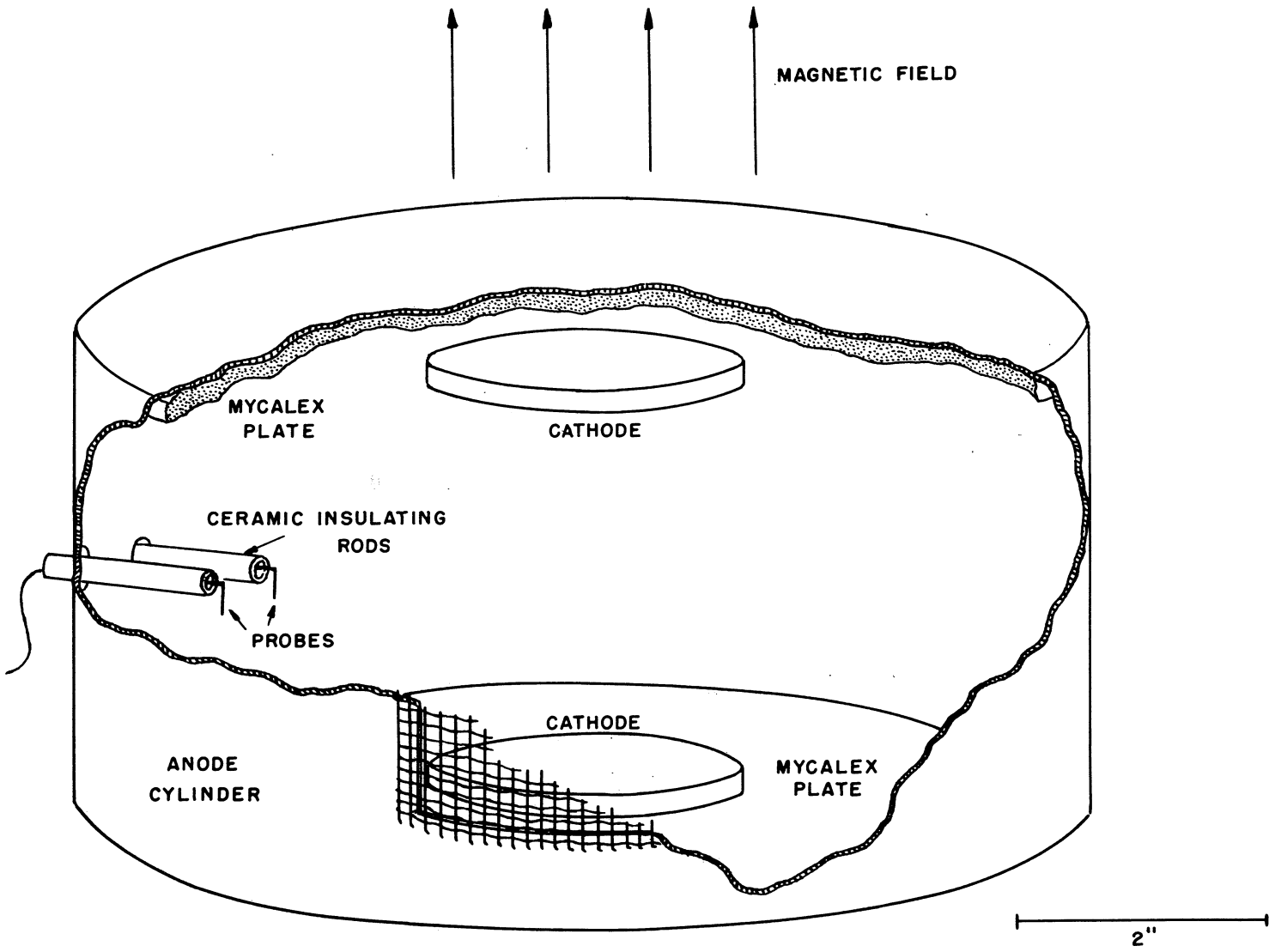

FIG. 4.1 ELECTRODE STRUCTURE AND TYPICAL PROBE ARRANGEMENT FOR THE STUDY OF PROPAGATION VELOCITY.

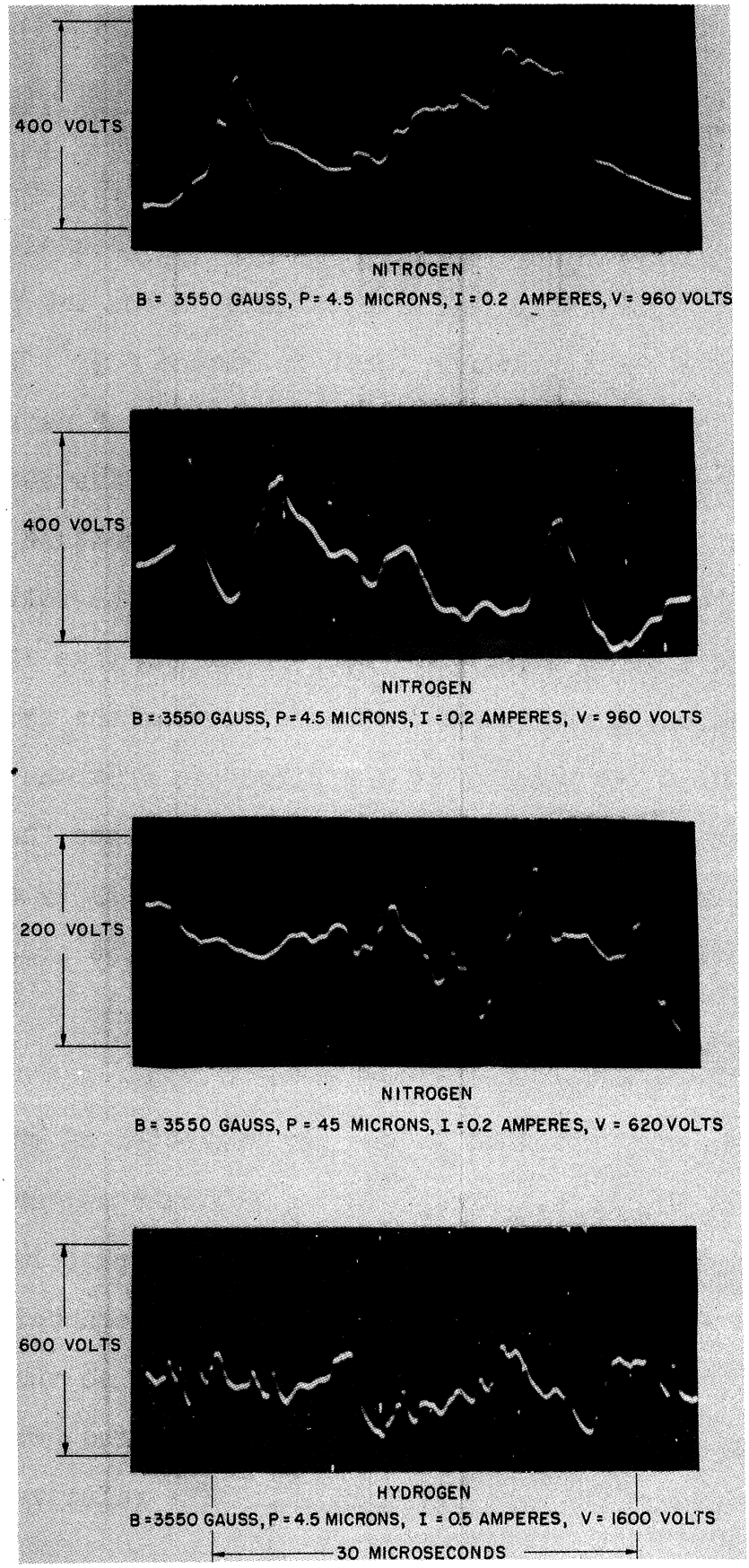

FIG. 4.2

POTENTIAL FLUCTUATIONS ON A PROBE
IN A GAS DISCHARGE

4.2 A comparison of the fluctuations on two neighboring probes

If a second probe is placed in the discharge one inch from the first and at the same distance from the anode, as indicated in Figure 4.1, the fluctuations on the two probes typically have the appearance shown in Figure 4.3.[1] The corresponding potentials on the two probes appear remarkably alike with two important exceptions: (a) the fine structure is different in the two fluctuations, (b) the voltage on probe 2 seems to be delayed in time with respect to the voltage on probe 1. This delay apparently represents the time it takes the fluctuation to propagate from a point near the one probe to a point near the other. If the direction from one probe to the other is the direction of propagation, then the velocity of propagation can evidently be determined merely by dividing this time delay into the distance between the two probes.

4.3 The methodology

The data were obtained in the way suggested in the discussion of Figure 4.3 except that a reticule appears on the photographs of the working data and the average level of the voltage was carefully noted. Also a half-megacycle signal was placed on the oscilloscope and photographed so that any nonlinearity in the sweep-rate could be calibrated out. About 200 photographs were taken in all. The relative probe

[1] These photographs were obtained using Polaroid Land cameras mounted on two Tektronix 513 oscilloscopes. The common time base was determined by intensity modulating the beam at the point t = 0 shown in Figure 4.3. The sweep-rates were set at four microseconds per centimeter.

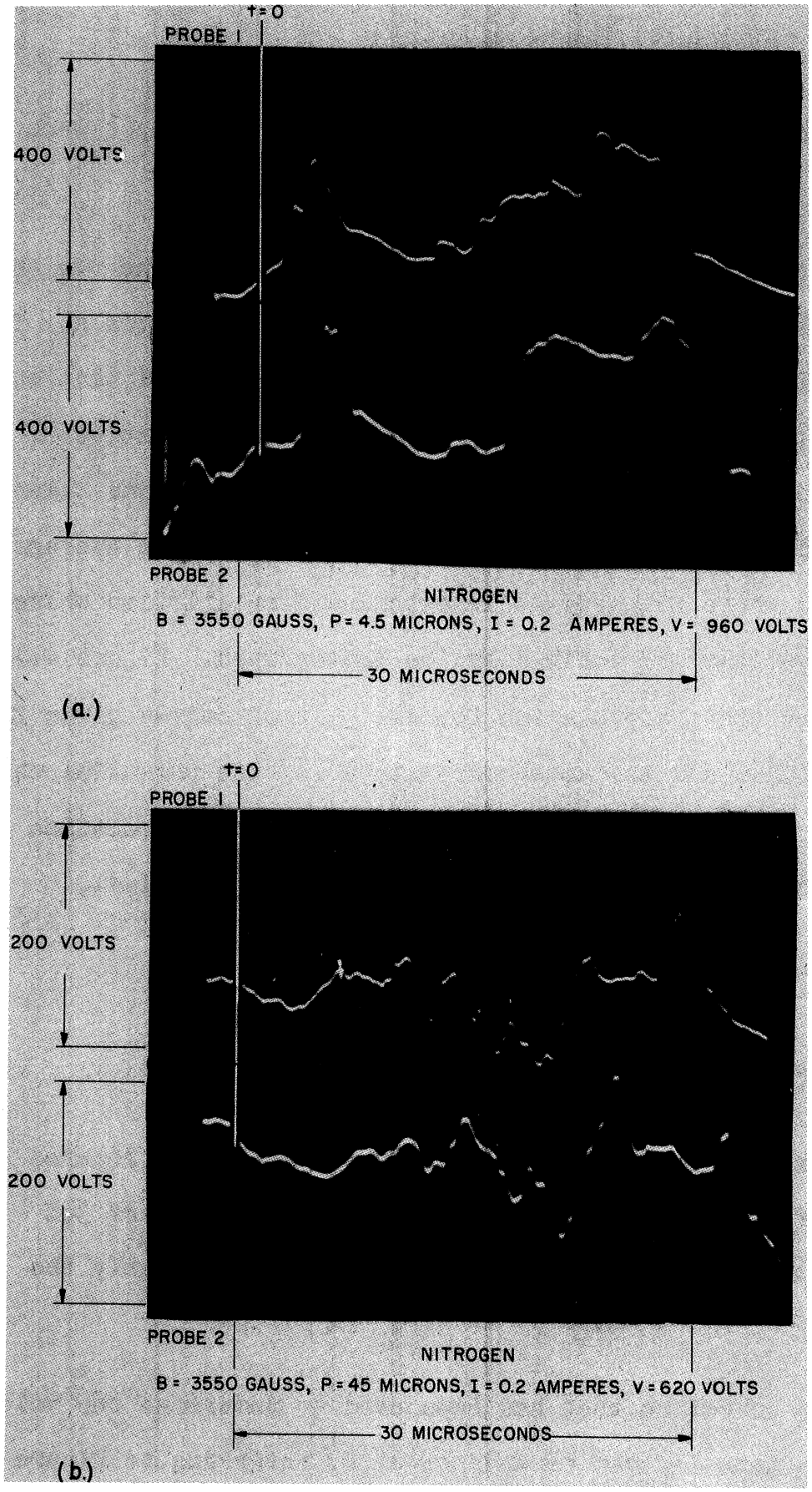

FIG. 4.3

POTENTIAL FLUCTUATIONS
ON TWO NEIGHBORING PROBES

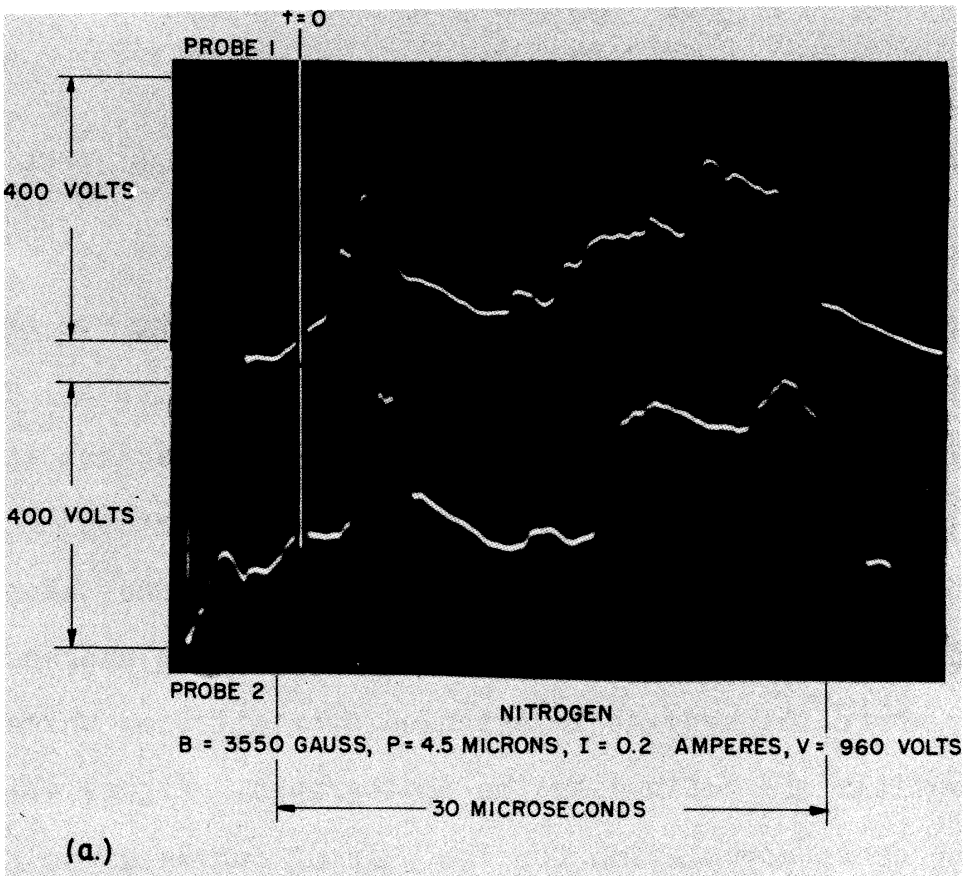

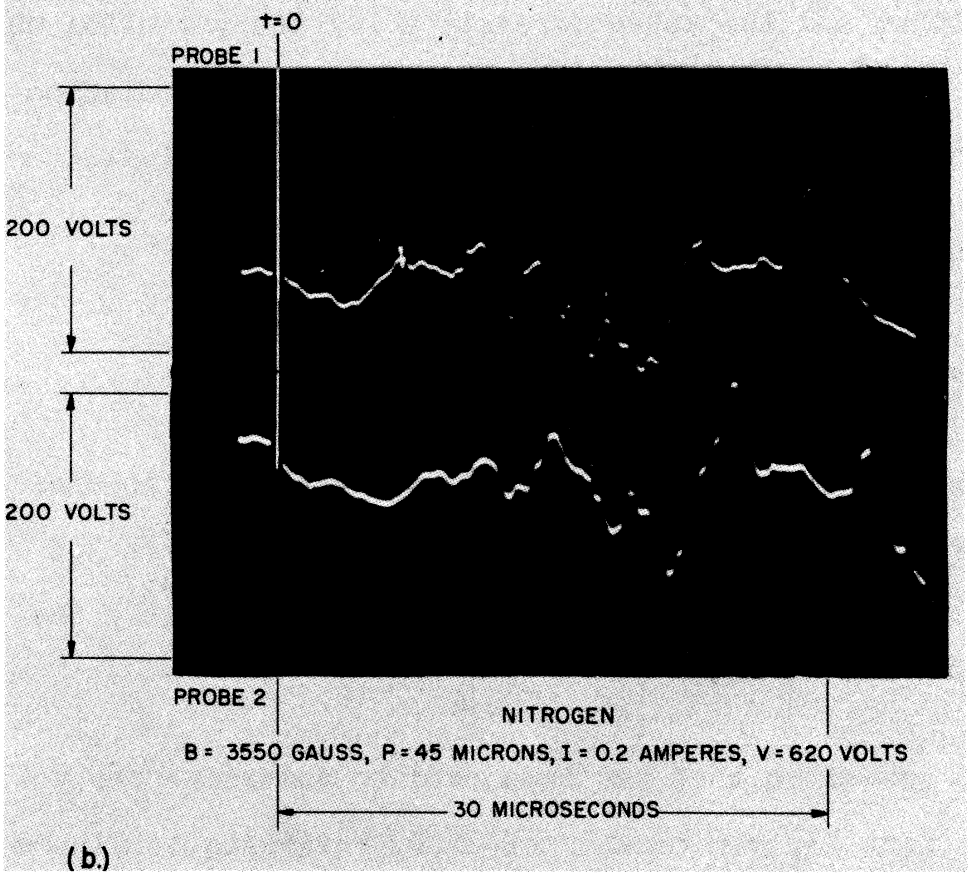

FIG. 4.3

POTENTIAL FLUCTUATIONS

ON TWO NEIGHBORING PROBES

positions, magnetic field, pressure, and power input were changed during this study.

The time delay between the fluctuations on the two probes was determined by cross-correlating the two potentials. That is, calling the potential on probe 1, $\phi_1(t)$, and that on probe 2, $\phi_2(t)$, the value of τ where the correlation function, $\overline{\phi_2(t+\tau)\,\phi_1(t)}$, reached its maximum was taken as the delay. The bar over this product means the average in time, where the average is extended over all time where the potentials are defined by the photographs. Figure 4.4 shows the cross-correlation for the pair of curves given in Figure 4.3a, and the auto-correlation for the potential on probe 1 of the same Figure. In this case the correlation functions have been normalized in the usual way, i.e.,

$$\text{cross-correlation} = \frac{\overline{\phi_2(t+\tau)\phi_1(t)}}{\sqrt{\overline{\phi_1^2(t)}\;\overline{\phi_2^2(t)}}}$$

$$\text{auto-correlation} = \frac{\overline{\phi_1(t+\tau)\phi_1(t)}}{\overline{\phi_1^2(t)}}\,.$$

The fact that the cross-correlation of Figure 4.4 reaches a value of 0.99 indicated that apart from the delay of 3.8 microseconds the potentials of Figure 4.3a are nearly the same.

The procedure that has been used to determine the velocity from the time lag can be understood by referring to Figure 4.5. Suppose the fluctuation is propagating in the direction P–P' with the probes in the positions shown. We now assume that the delay τ measures the time it takes the

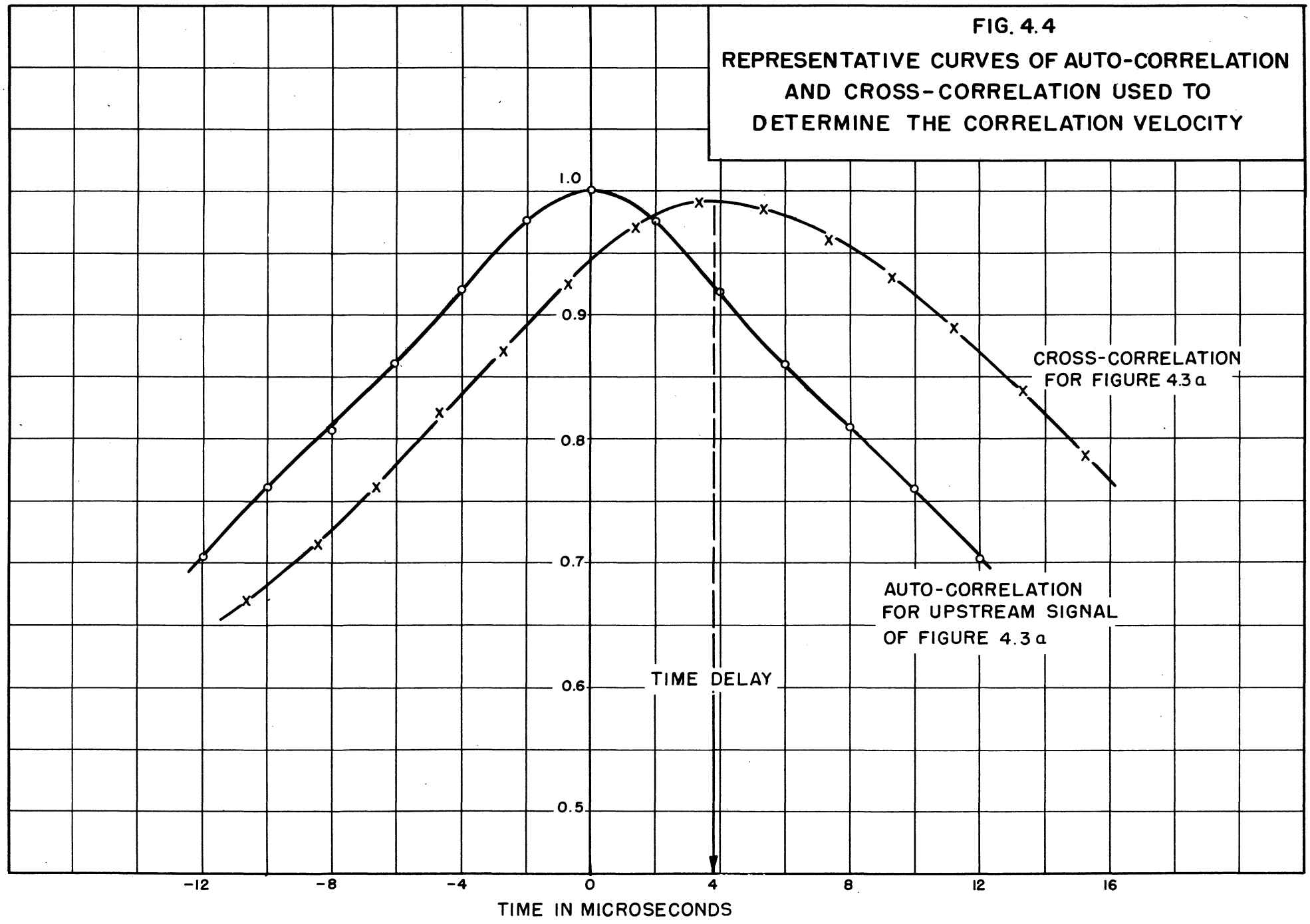
FIG. 4.4
REPRESENTATIVE CURVES OF AUTO-CORRELATION AND CROSS-CORRELATION USED TO DETERMINE THE CORRELATION VELOCITY
1.0
0.9
0.8
0.7
0.6
0.5
CROSS-CORRELATION FOR FIGURE 4.3 a
AUTO-CORRELATION FOR UPSTREAM SIGNAL OF FIGURE 4.3 a
TIME DELAY
-12
-8
-4
0
4
8
12
16
TIME IN MICROSECONDS

electrical disturbance to propagate from a point nearest probe 1 to a point nearest probe 2 along the direction of propagation. This time is

$$\tau = \frac{\ell \cos \alpha}{v}$$

where ℓ is the distance between the probes, v is the velocity of propagation, and α is the angle as shown in Figure 4.5. The delay τ is given by the correlation-function, and the distance ℓ between the probes is known, so that by taking data for two different relative probe positions the unknown velocity and direction of propagation can be calculated. In practice three different relative positions of the probes were taken so that there was a check on the answer. For all three positions the probes were one inch apart and in the same horizontal plane, but the direction between the probes was altered. In one case the probes were equidistant from the anode; in a second they were on the same radial line; in the last case the relative position was between these two.

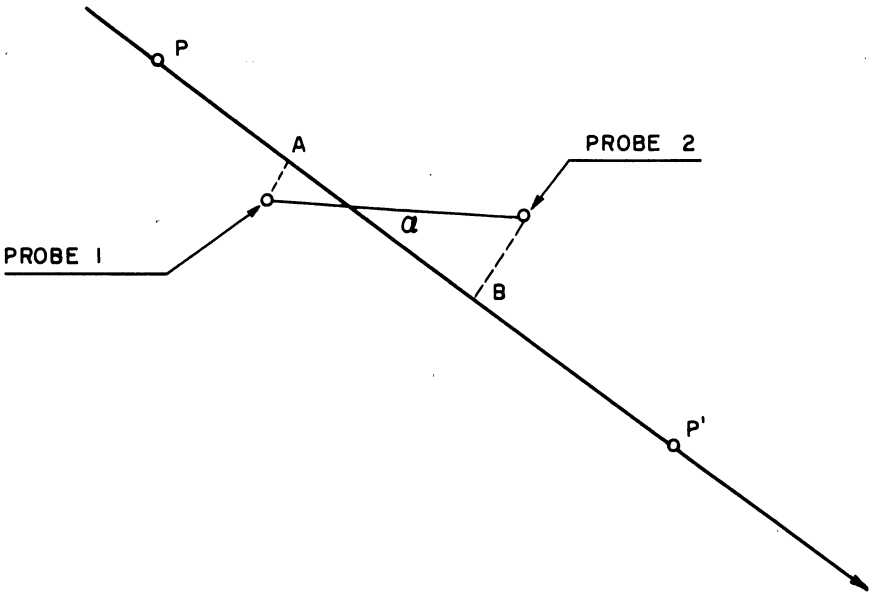

FIGURE 4.5

DIAGRAM SHOWING THE METHOD USED TO DETERMINE THE VELOCITY OF PROPAGATION.

4.4 An argument that the correlation velocity and group velocity are the same

The last section showed that a "correlation" velocity for the propagation could be obtained by cross-correlating the fluctuations on two neighboring probes. The question arises as to the relation between this velocity and the more familiar group, phase, or signal velocity. In this section a formal proof is given that

The correlation velocity is equal to the group velocity whenever a single group velocity exists.

As corollary we have that

The group velocity is the velocity of maximum correlation.

The phrase, "whenever a single group velocity exists," will be taken to mean that the disturbance can be expressed in the form

$$f(t,z) = \int_{-\infty}^{\infty} F(\omega)\, e^{i[\omega t - \beta(\omega) z]}\, d\omega \qquad (4.1)$$

with a group velocity independent of frequency.

It is to be understood that $F(\omega)$ is a function of ω which changes slowly with ω compared to $e^{i[\omega t-\beta(\omega)z]}$. Under these circumstances the group velocity, v_g, is given by

$$v_g = \frac{1}{\frac{d\beta}{d\omega}} \cdot \qquad (4.2)$$

The fact that the group velocity represents the velocity of propagation of $f(t,z)$ is often argued using Lord Kelvin's "principle of stationary phase." This principle effectively states that $f(t,z)$ as given in (4.1) reaches its greatest value as a function of t and z where there is stationary

phase, i.e., where

$$\frac{d}{d\omega}\left[\omega t - \beta(\omega)\, z\right] = 0 .$$

Carrying out the differentiation

$$t - \frac{d\beta}{d\omega} z = 0,$$

so that

$$\frac{dz}{dt} = \frac{1}{\frac{d\beta}{d\omega}},$$

and the disturbance travels with the group velocity.

The correlation velocity in this notation can be represented in the following way. Probes are located at z_1 and z_2 ; the fluctuations on these two probes are $f(t, z_1)$ and $f(t, z_2)$ respectively. Forming the product, $f(t + \tau, z_2)\, f(t, z_1)$, the cross-correlation is defined by

$$\Phi(\tau) = \lim_{T \to \infty} \frac{1}{2T} \int_{-T}^{T} f(t + \tau, z_2)\, f(t, z_1)\, dt. \qquad (4.3)$$

Taking the delay where this correlation function has its maximum as $\tau = \tau_m$, the correlation velocity is given by

$$\frac{z_2 - z_1}{\tau_m} .$$

We now want to show that this correlation velocity and the group velocity are equal, i.e.,

$$\frac{1}{\frac{d\beta}{d\omega}} = \frac{z_2 - z_1}{\tau_m} . \qquad (4.4)$$

Substituting into the integral of (4.3) from (4.1) gives

$$\Phi(\tau) = \lim_{T \to \infty} \frac{1}{2T} \int_{-T}^{T} dt \int_{-\infty}^{\infty} d\omega \int_{-\infty}^{\infty} d\zeta\, F(\omega) F^{*}(\zeta) e^{i\left[\omega\tau + \omega t - \zeta t - \beta(\omega) z_2 + \beta(\zeta) z_1\right]} \qquad (4.5)$$

where the star indicates the complex conjugate. Freely interchanging the order of integration and carrying the limit under the integrals gives a form

$$\lim_{T\to\infty} \frac{1}{2T}\int_{-T}^{T} e^{i(\omega-\zeta)t}\,dt = \delta(\omega-\zeta) \tag{4.6}$$

where δ is the Kronecker δ function defined by

$$\delta(\chi) = \begin{cases} 0 & \text{if } \chi \neq 0 \\ 1 & \text{if } \chi = 0. \end{cases} \tag{4.7}$$

Then (4.5) becomes

$$\Phi(\tau) = \int_{-\infty}^{\infty} d\omega \int_{-\infty}^{\infty} d\zeta\, F(\omega)F^{*}(\zeta)\,\delta(\omega-\zeta)\, e^{i\left[\omega\tau-\beta(\omega)z_2+\beta(\zeta)z_1\right]} \tag{4.8}$$

$$= \int_{-\infty}^{\infty} |F(\omega)|^2 e^{i\left[\omega\tau-\beta(\omega)z_2+\beta(\omega)z_1\right]} d\omega.$$

Now applying Kelvin's principle of stationary phase to determine the value of τ that maximizes this function,

$$\frac{d}{d\omega}\left[\omega\tau_m - \beta(\omega)z_2 + \beta(\omega)z_1\right] = 0.$$

On differentiating, one obtains

$$\tau_m - (z_2 - z_1)\frac{d\beta}{d\omega} = 0, \text{ or}$$

$$\frac{z_2 - z_1}{\tau_m} = \frac{1}{\frac{d\beta}{d\omega}}, \tag{4.4}$$

which is what was to be proved.

4.5 The velocity of propagation

Figure 4.6 summarizes the important results of the velocity measurements. The figure shows the direction and magnitude for the velocity of propagation in nitrogen gas for various conditions of operation. The directions of these vectors are probably reliable to $\pm 15^{\circ}$ and the magnitudes to $\pm 30\%$. This sizable error seems to be due to three effects. (1) The correlation calculation was made by averaging over about forty microseconds of the fluctuations. This period was evidently not long enough to insure accurate reproducibility. (2) The cross-correlation function was calculated from enlargements of the original photographs. The drying of the enlargements introduced nonuniform shrinking. (3) The direction of propagation was incorrectly estimated at the beginning of the study, and consequently the choice of relative probe positions was not the most satisfactory. The errors due to these three difficulties could certainly be reduced by: (1) taking several photographs with the same conditions of operation and consequently increasing the period of averaging, (2) exercising more care in the drying of enlargements, and (3) selection of new relative probe positions in view of the result already obtained. It should be easily possible to halve the errors in this way.

4.6 The amplification of propagated waves

The argument of Bailey that the fluctuations are to be identified with those waves that amplify as they propagate

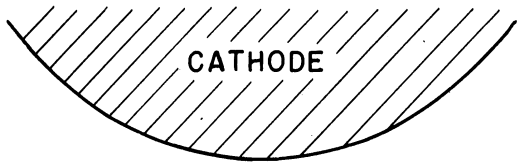

STANDARD CONDITIONS:

B = 3550 GAUSS

I = 0.2 AMPERES

p = 4.5 MICRONS

INCREASED CURRENT: I = 0.5 AMPERES

INCREASED PRESSURE: p = 45 MICRONS

DECREASED FIELD: B = 1870 GAUSS

VELOCITY SCALE IN cm/sec

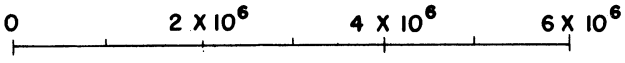

THE LORENTZ VELOCITY IS THE AVERAGE ELECTRIC FIELD DIVIDED BY THE MAGNETIC FIELD

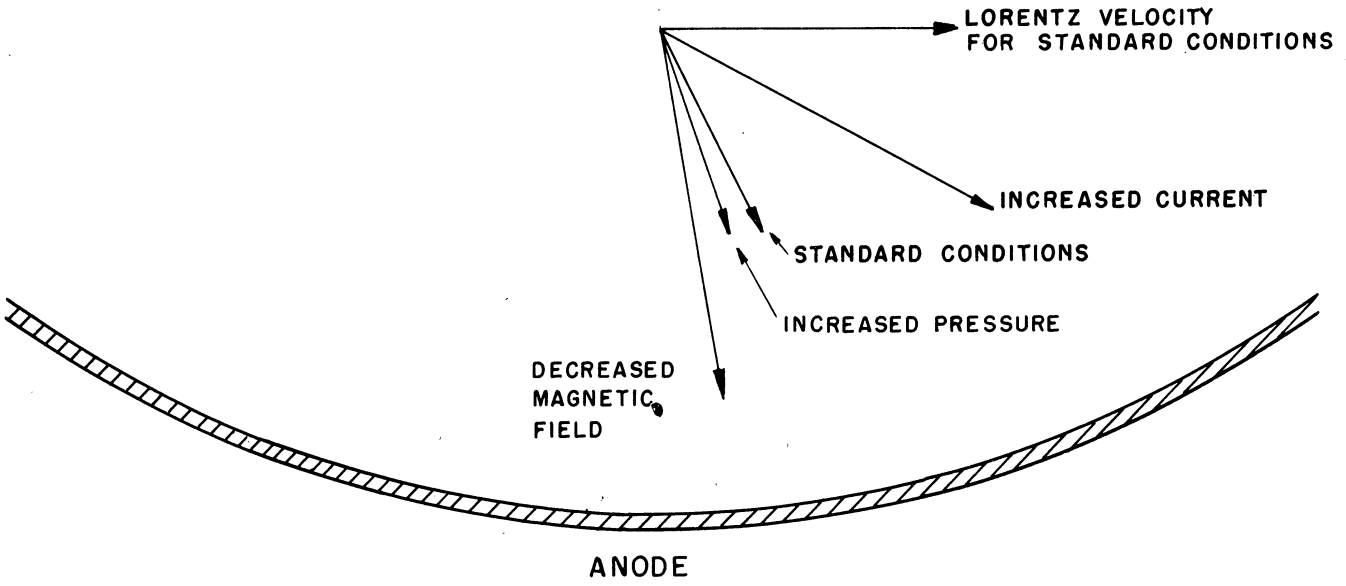

FIG. 4.6

VECTORS SHOWING THE DIRECTION AND AMPLITUDE OF THE PROPAGATION VELOCITY

has been mentioned many times in the earlier chapters. This chapter has demonstrated experimentally that there are high intensity waves propagating from cathode to anode, and it is natural to investigate whether there is amplification associated with these waves. This has been done in the following way. The two probes already discussed were placed midway between the mycalex insulating plates (see Figure 4.1); these probes were one-half inch apart and on the same radial line. By connecting their output to the input of a pulse transformer which isolated the probes from ground it was possible to obtain the fluctuating difference voltage between the two probes. This was accomplished by connecting a 100-ohm resistance across the secondary of the transformer and determining the effective voltage on this resistance by using a crystal rectifier and microammeter. Just as in the experiments on the velocity of propagation discussed earlier in this chapter, the probes were connected to the anode through resistances so that a direct current was carried by the probes. This current was maintained constant when the probes were moved to new positions by changing the resistances between the probes and the anode.

The results of this experiment are shown in Figure 4.7 where the voltage between the probes is plotted as a function of the distance from the probes to the cathode axis. The position of probes is taken as the point halfway between them. The increase in the curve of Figure 4.7 with distance from the cathode supports the idea that the waves amplify as they propagate from cathode to anode.

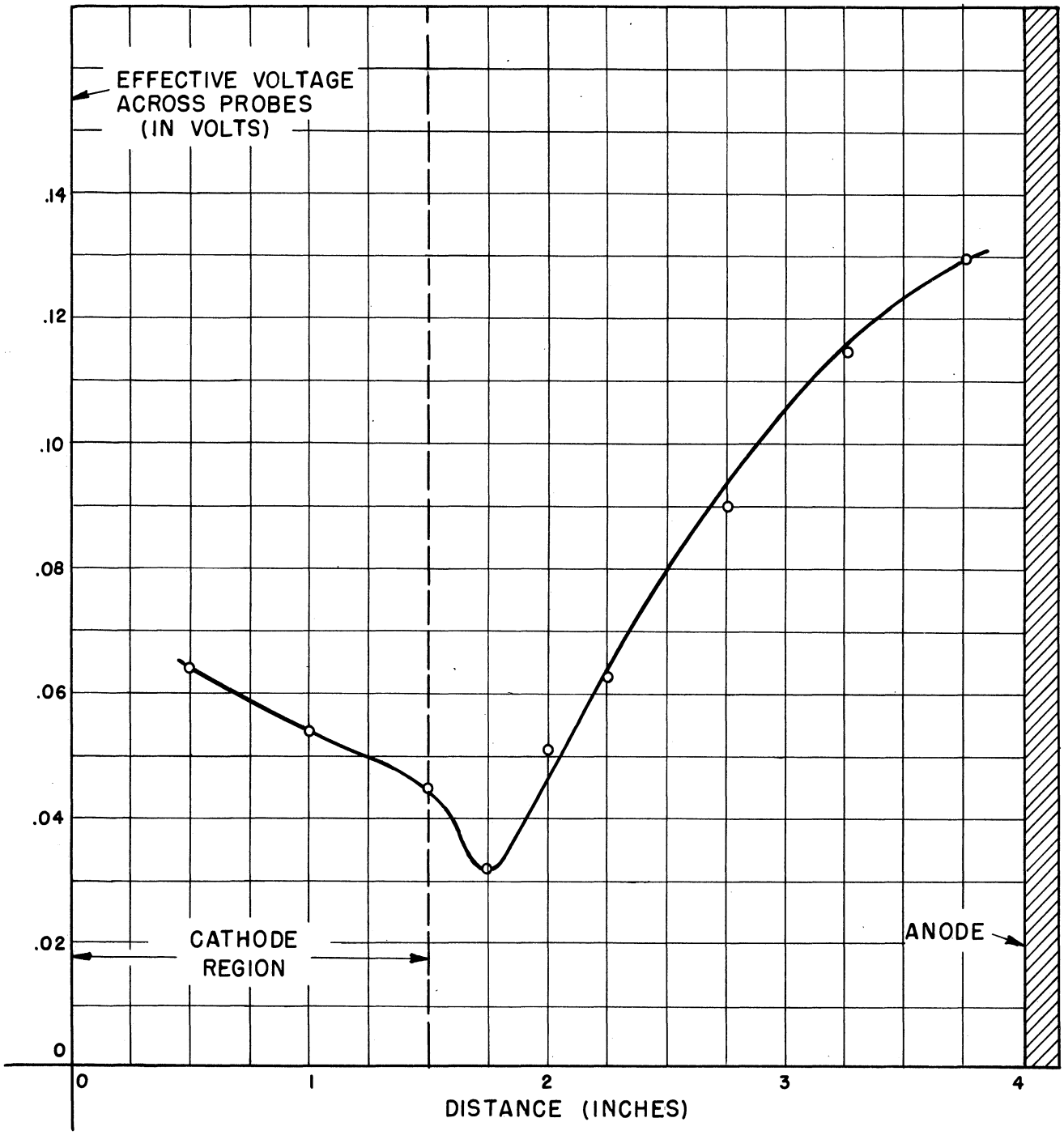

FIG. 4.7 CURVE SHOWING THE AMPLITUDE OF FLUCTUATIONS BETWEEN PROBES AS A FUNCTION OF THE POSITION OF THE PROBES.

This chapter was a study of the velocity of propagation for the low-frequency fluctuations. The observations on the amplification of propagated waves arose as a by-product of the study, and the data on amplification were quite limited. However, it seems worth emphasizing that the important and controversial problem of growing waves in a plasma can be experimentally investigated more thoroughly using a two-probe (or multi-probe) study similar to that outlined in this chapter.

Chapter V

A COMPARISON OF THEORY AND EXPERIMENT

The theoretical studies of Chapter I and II are largely an examination of particular solutions for the differential equations used to describe the electrical character of the plasma. These solutions also satisfy the wave equation and consequently represent the propagation of electrical disturbances through the medium. An important result of this theory is the determination of a dispersion relation which relates the frequency of propagation and the wave length. Unfortunately neither the dispersion relation nor the other results of the theory permit an explicit prediction on most of the experimental data. However there are several consequences of the theory that can be checked experimentally and likewise implications of the experiments that can be tested in the theory. This last chapter compares the theoretical and experimental studies of the earlier chapters in five ways: (1) by examining the power spectrum near the ion cyclotron frequency, (2) by studying the experimental data on the power spectrum for the ion cut-off frequency predicted by the theory, (3) by checking the Bailey amplification bands, (4) by examining the amplification of propagating waves, and (5) by noting the velocity of low-frequency propagation.

5.1 The power spectrum near the ion cyclotron frequency

Chapter III is an experimental study of the power spectrum.

In principle one might take the particular solutions of the theory, assign a particular weighing function to them, and represent a theoretical spectrum by a sum over these weighed solutions. However there is apparently no convenient way to determine such a weighing function, and only in a narrow frequency range near the ion cyclotron frequency will this technique be employed.

It is shown in Chapter I that the electric energy in the propagated waves approaches zero as the frequency approaches the ion cyclotron frequency. In Chapter III the experimental data revealed a sharp dip at the ion cyclotron frequency. These two observations seem to support one another; the point can be made more concretely in the following way. Suppose the power spectrum on the probe at a given frequency is assumed proportional to the average electric energy per unit volume in the gas at that frequency. In Chapter I the ratio of this electric energy density to the average kinetic energy density for the ions is determined; this ratio, $R(\omega, \theta)$, is given in equation (1.43), and graphically presented in Figure 1.6. Under the identification of the power spectrum on the probe with the average electric energy per unit volume, the spectrum can be written,

$$\int_0^{2\pi} W(\omega, \theta) \cdot R(\omega, \theta)\, d\theta \qquad (5.1)$$

where W represents the average ion kinetic energy per unit volume for those waves propagated in the directions between θ and $\theta + d\theta$ with frequencies between ω and $\omega + d\omega$.

An estimate of the weighting function W in (5.1) leads to a spectrum; for want of a better choice suppose W is assumed constant; that is, assume that all permitted waves are present and that their total ion kinetic energy is evenly distributed among them. The spectrum in this case is proportional to an integral of the known function $R(\omega, \theta)$. This integral was evaluated graphically; it is plotted in Figure 5.1. The similarity of this curve near the ion cyclotron frequency to the experimental curves in Figures 3.5 to 3.8 is taken as support of the theory. Of course, the assumption that the weighting function W is independent of frequency and the direction of propagation is an oversimplification, but for any sensible choice of W the integral of (5.1) would dip at the cyclotron frequency.

There is one further check on the theory of Chapter I. In Section 1.3 it is shown that the dispersion relation implies a greatest unattenuated frequency for the ion fluctuations given by

$$\omega_{max} = \sqrt{\omega_p^2 + \omega_c^2} \qquad (5.2)$$

where ω_p is the plasma ion frequency and ω_c is the ion cyclotron frequency. This frequency might typically be 30 megacycles per second for the choice of parameters in Chapter III. The curves for hydrogen and helium in Figures 3.5 to 3.8 lend support to this idea of a cut-off, but the curves for nitrogen in Figures 3.10 to 3.12 show no sign of any cut-off frequency below about 100 megacycles per second at the lower pressures. To identify the minimum at 100 megacycles per second

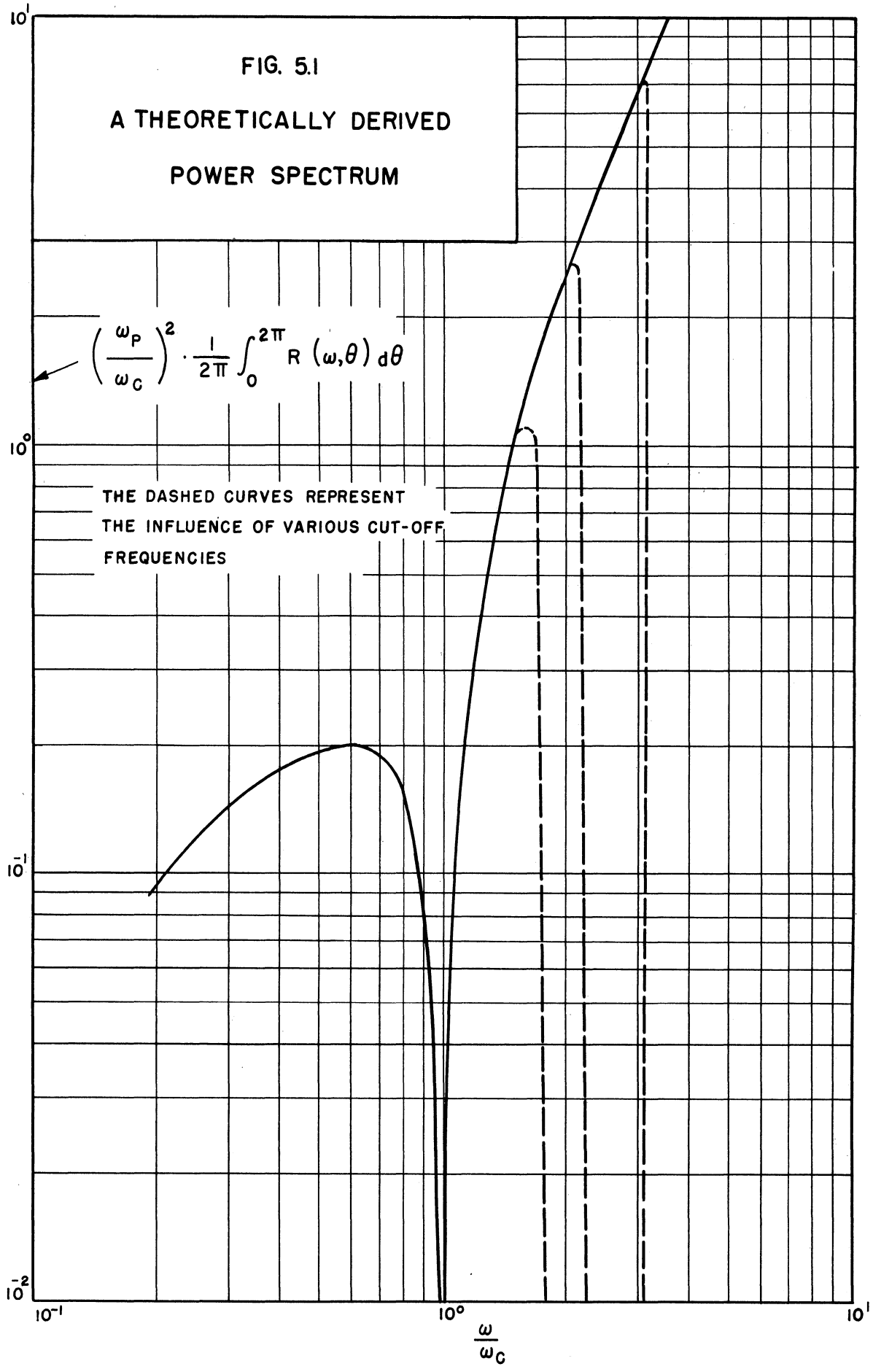
FIG. 5.1
A THEORETICALLY DERIVED
POWER SPECTRUM
$\left(\frac{\omega_P}{\omega_C}\right)^2 \cdot \frac{1}{2\pi}\int_0^{2\pi} R(\omega,\theta)\, d\theta$
THE DASHED CURVES REPRESENT
THE INFLUENCE OF VARIOUS CUT-OFF
FREQUENCIES
10^1
10^0
10^{-1}
10^{-2}
10^{-1}
10^0
10^1
$\frac{\omega}{\omega_C}$

with the maximum frequency given by equation (5.2) would require about 13% ionization at a pressure of 4 microns and a gas temperature of 1800° Kelvin. Stated another way, this would imply a plasma electron frequency of 1.6×10^{10} cycles per second. These values of percent ionization and plasma frequency are too high, so that it seems impossible to attribute the broad noise band of nitrogen below 100 megacycles per second with ion fluctuations.

A more successful explanation of this noise is given by the Bailey amplification bands discussed in Section 2.6. According to Bailey's argument this low-frequency noise band is attributed to electronic disturbances, which extend from $\omega = 0$ to $\omega_2 = \frac{1}{2}\left[\sqrt{\omega_c^2 + 4\omega_p^2} - \omega_c\right]$, where these plasma and cyclotron frequencies are for the electrons. Solving this last expression for the plasma electron frequency gives

$$\omega_p = \sqrt{\omega_c\ \omega_2 + \omega_2^2} \quad . \tag{5.3}$$

Taking values from the 4 micron curves of Figure 3.9 one has

$$\omega_2 = 2\pi\,(1.50)10^8 \qquad \text{radians per second}$$

$$\omega_c = 2\pi\,(1.28)10^{10} \qquad \text{radians per second.}$$

Putting these numbers into (5.3) gives $\omega_p = 2\pi\,(1.38)\,10^9$ radians per second, which is a very reasonable value for the electron plasma frequency.

5.2 The low-frequency propagation normal to the magnetic field

Chapter IV is an experimental study of the low frequency

propagation normal to the magnetic field. The group velocity for these propagations was determined experimentally, and an estimate of the gain associated with the propagating waves was made. These experimental results can be compared with the theoretical work in Section 2.7.

5.2.1 The velocity of propagation

The experimental results for the direction and amplitude of the propagation velocity are summarized in Figure 4.6. This velocity was determined by a correlation method, but it is shown in Section 4.4 that this correlation velocity is equal to the group velocity of the propagating waves. The theoretical studies in Section 2.7 argue that these low frequency waves, propagating normal to the magnetic field, have a group velocity that is approximately equal to the component of electron drift velocity parallel to the direction of propagation, and further that any electron drift normal to the propagation direction introduces attenuation, so that the preferred direction of propagation is parallel to the direction of electron drift.

These theoretical and experimental observations can be compared qualitatively, but it is difficult to check the agreement exactly since neither the amplitude nor the direction of the electron drift velocity is known independently. The direction of the velocities in Figure 4.6 must be nearly that of the electron drift velocity, for the electrons tend to move from the cathode to the anode, but the Lorentz force

deflects them counterclockwise. Also, one would expect this drift direction more nearly from cathode to anode for a reduction of the magnetic field, and rotated farther counterclockwise for an increase in power input. Figure 4.6 shows just this behavior; it seems likely that the theory and experiment are in good agreement on this point.

Checking the magnitude of the group velocities in Figure 4.6 with the theoretical observation that this magnitude should be approximately equal to the drift velocity is more difficult. The speeds of Figure 4.6 correspond to about 0.04 volts which certainly does not seem like too high a value to identify with the velocity of the electrons. Also these velocities are somewhat less than the Lorentz velocity which is sometimes taken as an approximate velocity for the electron drift. On the other hand, if the density of electrons is estimated by dividing the direct current delivered to the anode by the anode area, the electron charge, and the component of group velocity normal to the anode as given in Figure 4.6, the value seems quite small. Thus, taking this velocity as 10^4 meters per second, the anode area as 4×10^{-2} square meters, and the current as 0.2 amperes, the density is given by

$$N_o = \frac{0.2}{\left(1.6 \cdot 10^{19}\right) 10^4 \left(4.10^{-2}\right)} = 3.13 \cdot 10^5 \quad \text{electrons per cubic meter .} \qquad (5.4)$$

This number can be compared with 2.66×10^{19} which represents the particles per cubic meter for an ideal gas at 4.5 microns pressure and 1800° Kelvin. This gives an ionization of about

$100 \frac{3.13 \cdot 10^{15}}{2.66 \cdot 10^{19}} = .012\%$ which seems low. The corresponding electron plasma frequency is $\frac{\omega_p}{2\pi} = 505$ megacycles per second. It is likely that this plasma frequency is too low by a factor of about four and that the corresponding density of charged particles given in equation (5.4) is low by the square of this, or sixteen. This apparent discrepancy can be explained away by noting that the "effective" area of the anode is likely to be much less than the geometric area and also that the electron drift velocity is likely to be much higher near the middle of the anode where the data were taken than at the top or bottom. Both these considerations would reduce the denominator of (5.4) and provide a more satisfactory answer for the density of charged particles.

5.2.2 The gain with propagation

It is argued theoretically in Section 2.7.2 that the low frequency propagations normal to the magnetic field can experience gain. The value of gain is calculated in that section, and the result is presented graphically in Figure 2.4. This result can be compared with the gain that was observed experimentally. The approximate value of the experimental gain is given in Section 4.6 as 1.2 db per centimeter. For the parameters used in that experimental study the abscissa of Figure 2.4 would be less than unity and the theoretical gain would be approximately given by its asymptotic value of $8.7 \frac{\omega_p^2}{\omega_c C}$. The magnetic field for the experimental studies of Section 4.6 was 3550 gauss which

corresponds to a cyclotron frequency of $\omega_c = 2\pi \cdot 10^{10}$. If this value is used and the theoretical gain identified with the experimental gain, a plasma frequency can be calculated; that is,

$$8.7 \quad \frac{\omega_p^2}{\omega_c C} = 1.2.$$

Solving for the plasma frequency

$$\omega_p = \sqrt{\frac{(1.2)(2\pi \cdot 10^{10})(3 \cdot 10^{10})}{8.7}} = 2\pi\,(2.8)10^9 \text{ radians per second.}$$

This is a very reasonable value for the plasma electron frequency.

5.3 Concluding remarks

Much of the data that have been presented in this paper must be regarded as qualitative, and the interpretation given to that data in certain instances may be subject to serious criticism. The theory too has shortcomings, for it is essentially a small-amplitude study of a high-amplitude phenomena. Also the theory contains parameters such as the density of the charged particles and the temperature of the electrons which have not been independently determined and indeed cannot be determined by any familiar method. For these reasons the concluding remarks should be looked on as the author's impressions and not as facts; these remarks are an attempt to explain the high-intensity fluctuations that were observed in the experimental studies of this report.

It seems likely that most of the fluctuations described

in this report are attributable to electron behavior. The low frequency disturbances appear to have their origin near the cathode; very likely they are generated by cathode sputtering. This embryonic disturbance is probably several volts in amplitude. Much of this early disturbance is likely attenuated but certain components are amplified. The greatest gain is experienced by the waves propagating parallel to the electron drift velocity. These waves grow at about two decibels per centimeter, reaching their maximum near the anode. The velocity of these waves is very nearly that of the average electron velocity. These waves grow by taking kinetic energy out of the electron stream which in turn take energy from the average electric gradient established by the potential on the electrodes.

These electronic disturbances cannot explain all of the fluctuations at the low frequencies. The power spectrum curves of the hydrogen and helium discharges discussed in Chapter III are certainly not to be interpreted without admitting ion fluctuations. However, it seems likely that the prominent contribution of the ions in the spectrum of hydrogen is local to the cyclotron resonant frequency and merely adds to the broader spectrum due to the electrons. Also it appears that gases heavier than hydrogen have a reduced ion contribution in the spectrum, and it is likely that the broad spectrum of nitrogen discussed in Chapter III is entirely due to the electron fluctuations.

Appendix 1

LIST OF REFERENCES

1 Appleton, E.V., "Wireless Studies of the Ionosphere," Jour. I. E. E., 71, 642; (1932).

2 Appleton, E.V. and Builder, G., "The Ionosphere as a Doubly-Refracting Medium," Phy. Soc. of London, 45, 208; (1933).

3 Attwood, S.S., Electric and Magnetic Fields, Wiley and Sons; (1949).

4 Bailey, V.A., "Plane Waves in an Ionized Gas with Static Electric and Magnetic Fields Present," Australian Jour. of Sci. Res. (A), 1, 351; (1948).

5 Bailey, V.A., "Spontaneous Waves in Discharge Tubes and in the Solar Atmosphere," Nature, 161, 600; (1948).

6 Bailey, V.A., "Space-charge Wave Amplification Effects," Phy. Rev., 75, 1104; (1949).

7 Bailey, V.A., "On the Relativistic Electromagneto-Ionic Theory of Wave Propagation," Phy. Rev., 77, 418; (1950).

8 Bailey, V.A., "Growth of Circularly Polarized Waves in the Sun's Atmosphere and their Escape into Space," Phy. Rev., 78, 428; (1950).

9 Bakker, C.J. and Heller, G., "On the Brownian Motion in Electric Resistances," Physica, 6, 262; (1939).

10 Ballantine, S., "Fluctuation Noise Due to Collision Ionization in Electronic Amplifier Tubes," Physics, 4, 294; (1933).

11 Bell, D.A., "A Theory of Fluctuation Noise," Jour. I. E. E., 82, 522; (1933).

12 Biondi, M., "Measurement of the Electron Density in Ionized Gases by Microwave Techniques," Rev. of Sci. Instruments, 22, 500; (1951).

13 Bohm, D. and Gross, E.P., "Theory of Plasma Oscillations. A. Origin and Medium-Like Behavior; B. Excitation and Damping of Oscillations," Phy. Rev., 75, 1851, (1949).

14 Bohm, D. and Gross, E.P., "Effects of Plasma Boundaries in Plasma Oscillations," Phy. Rev., 79, 992; (1950).

15 Burgess, R.E., "Noise in Receiving Aerial Systems," Phy. Soc. of London, 53, 293; (1941).

16 Cobine, J.D. and Gallagher, C.J. and Weinstock, R. and Block, F., "Oscillations and Noise in Hot-Cathode Arcs," Harvard Res. Lab., 411-232, (PB-60992); (1945).

17 Cobine, J.D. and Gallagher, C.J., "Noise and Oscillations in Hot Cathode Arcs," Jour. Franklin Inst., 243, 41; (1947).

18 Cobine, J.D. and Gallagher, C.J., "Effects of a Magnetic Field on Oscillations and Noise in Hot-Cathode Arcs," Jour. of App. Phy., 18, 110; (1947).

19 Doob, J.L., Stochastic Processes, Wiley and Sons; (1953).

20 Dow, W.G., Fundamentals of Engineering Electronics, Wiley and Sons; (1952).

21 Dryden, H.L., "A Review of the Statistical Theory of Turbulence," Quarterly of App. Math., 1-2, 7; (1943).

22 Early, H.C. and Smith, H.L. and Lu, D.C., "Electrical Wind Phenomena," Summary Report No. 1, University of Michigan; (1952).

23 Gabor, D., "Plasma Oscillations," Brit. Jour. of App. Phy., 22, 209; (1951).

24 Gabor, D., "Wave Theory of Plasmas," Proc. Roy. Soc. (A), 213, 73; (1952).

25 Giovanelli, R.G., "Emission of Enhanced Microwave Solar Radiation," Nature, 161, 133; (1948).

26 Goldstein, L. and Cohen, N.L., "Behavior of Gas Discharge Plasma in High-Frequency Electromagnetic Fields," Elec. Comm., 28, 305; (1951).

27 Gross, E.P., "Plasma Oscillations in a Static Magnetic Field," MIT (Laboratory for Insulation Research), Tech. Rep. 39; (ATI-92338).

28 Haeff, A.V., "Space-Charge Wave Amplification Effects," Phy. Rev., 74, 1532; (1948).

29 Haeff, A.V., "The Electron-Wave Tube--A Novel Method of Generation and Amplification of Microwave Energy," I. R. E., 37, 4; (1949).

30 Hartree, D.R., "The Propagation of Electromagnetic Waves in a Refracting Medium in a Magnetic Field," Cambridge Phil. Soc., 27, 143; (1931).

31 Hastings, C. and Marcum, J.I., "Tables of Integrals Associated with the Error Function of a Complex Variable," RAD-284, Douglas Aircraft Co; (1948).

32 Huxley, L.G.H., "A General Formula for the Conductivity of a Gas Containing Free Electrons," Phy. Soc. of London (Proc.)-Sec. B, 64, 844; (1951).

33 Jen, C.K., "On the Induced Current and Energy Balance in Electronics," I. R. E., 35, 357; (1947).

34 Johnson, E.O. and Webster, W.M., "The Plasmatron, a Continuous Controllable Gas-Discharge Developmental Tube," I. R. E., 40, 645; (1952).

35 Johnson, J.B., "Thermal Agitation of Electricity in Conductors," Phy. Rev., 32, 97; (1928).

36 Knol, K.S., "Determination of the Electron Temperature in Gas Discharges by Noise Measurements," Philip's Res. Rep., 6, 288; (1951).

37 Labrum, N.R. and Bigg, E.K., "Observations on Radio-Frequency Oscillations in Low-Pressure Electrical Discharges," Phy. Soc. of London (Proc.)-Sec. B, 65, 356; (1952).

38 Lampert, M.A. and Goldstein, L., "Microwave Propagation in an Anisotropic Electron Gas," Federal Telecommunication Lab., (NDQCPR No. 1-B), (ATI-91288); (1950).

39 Lawson, J.L. and Uhlenbeck, G.E., Threshold Signals, McGraw-Hill; (1950).

40 Makinson, R.E.B. and Thonemann, P.C. and King, R.B. and Ramsay, J.V., "Dielectric Constant and Electron Density in a Gas Discharge," Phy. Soc. of London (Proc.)-Sec. B, 64, 665; (1951).

41 McBee, W.D. and Dow, W. G., "The Influence of a Transverse Magnetic Field on an Unconfined Glow Discharge," Trans. I. E. E.; (1953).

42 Moullin, E.B., Spontaneous Fluctuations of Voltage, Clarendon Press; (1938).

43 Moullin, E.B. and Ellis, H.D.M., "The Spontaneous Background Noise in Amplifiers Due to Thermal Agitation and Shot Effect," Jour. I. E. E., 74, 323; (1934).

44 Mumford, W.W., "A Broad-Band Microwave Noise Source," Bell Sys. Tech. Jour., 28, 608; (1949).

45 Nyquist, H., "Thermal Agitation of Electric Charge in Conductors," Phy. Rev., 32, 110; (1928).

46 Pardue, L.A. and Webb, J.S., "Ionic Oscillations in a Glow Discharge," Phy. Rev., 32, 946; (1928).

47 Parzen, P. and Goldstein, L., "Current Fluctuations in a Direct-Current Gas Discharge Plasma," Phy. Rev., 82 724; (1951).

48 Pierce, J.R., "Theory of the Beam-Type Traveling-Wave Tube," I. R. E., 35, 111; (1947).

49 Pierce, J.R., "Possible Fluctuations in Electron Streams Due to Ions," Jour. App. Phy., 19, 231; (1948).

50 Planck, M., "Distribtuion of Energy in the Spectrum," Ann. Phy., 4, 553; (1901).

51 Planck, M., "Laws of Vibration of a Linear Resonator in a Field of Steady Radiation," Phys. Zeitschr, 2, 530; (1901).

52 Roberts, J.A., "Wave Amplification by Interaction with a Stream of Electrons," Phy. Rev., 76, 340; (1949).

53 Schremp, E.J., Chapter 12 from Vacuum Tube Amplifiers, MIT, 18; (1948).

54 Senitzky, I.R., "A High Vacuum Cold Cathode Gaseous Discharge: A Cyclotron Effect," Signal Corp Pub., Eng. Rep. No. E-1067, (ATI-90066).

55 Simmons, L.F.G. and Salter, C., "An Experimental Determination of the Spectrum of Turbulence," Proc. Roy. Soc. (A), 165, 73; (1938).

56 Taylor, G.I., "The Spectrum of Turbulence," Proc. Roy. Soc. (A), 164, 476; (1938).

57 Thomson, J.J., "Oscillations in Discharge-Tubes and Allied Phenomena," Phil. Mag., 11, 697; (1931).

58 Thomson, J.J., "Electronic Waves and the Electron," Phil. Mag., 6, 1254; (1928).

59 Tonks, L. and Langmuir, I., "Oscillations in Ionized Gases," Phy. Rev., 33, 195; (1929).

60 Twiss, R.Q., "On Oscillations in Electron Streams," Phy. Soc. of London (Proc.)-Sec. B, 64, 654; (1951).

61 van der Ziel, "Thermal Noise at High Frequencies," Jour. App. Phy., 21, 399; (1950).

62 Von Lassen, H., "Zur Theorie der Doppelbrechung electromagnetischer Wellen in einem ionisierten Gas unter dem Einfluss eines konstanten Magnet feldes (Ionosphare)," Ann. Phy., 436, 415; (1947).

63 Wehner, G., "Plasma Oscillations," AMC Wright Patterson Air Force Base, (ATI-77090); (1950).

64 Wehner, G., "Plasma Oscillator," Jour. of App. Phy., 21, 62; (1950).

Appendix 2

LIST OF SYMBOLS

A , a constant

$\vec{A}$, the vector potential

a , a constant

$\vec{B}$, $\vec{B}_o$, the magnetic flux density

b , a constant

c , a constant

C , the velocity of light

$\vec{E}$, the electric field

$\vec{E}_o$, the electric field of the undistrubed stream

$\vec{\xi}$, the perturbed electric field

e , the fundamental charge

I , the direct current

$\vec{J}$, the current density

k , the Boltzmann constant

m , the electron mass

m_p , the ion mass

N_e , the density of electrons

N_o , the density of ions or of electrons in the undisturbed plasma

N_p , the ion density

n_e , the perturbed electron density

n_p , the perturbed ion density

P , the pressure

$\vec{S}$, the total stream vector

$\vec{S}_r$, the stream vector of the r'th stream

$\vec{\mathcal{S}}$, the total perturbed stream vector

$\vec{\mathcal{S}}_r$, the perturbed stream vector of the r'th stream

T , the electron temperature

$\vec{u}$, the perturbed velocity of the ions

u_0 , the ion drift velocity in the direction of propagation

$\vec{v}$, the electron velocity

v_g , the group velocity

$\vec{v}_p$, the ion velocity

$\vec{v}_{p_0}$, the ion velocity of the undistrubed plasma

$\vec{v}_0, \vec{v}^\circ$, the drift velocity of the electrons

$\vec{v}_r$, the electron velocity in the r'th stream

U_T , the most probable thermal speed

$\vec{\beta}, \beta$, the propagation constant

ϵ_0 , the free-space dielectric constant

θ , the angle between the direction of propagation and the direction of the magnetic field

$\lambda = \frac{2\pi}{\beta}$, the wave length

λ' , a normalizing constant

μ_0 , the permeability of free-space

υ , a constant approximately equal to the collision rate of the charged particles

ρ , an angle

ρ , the space charge density

ρ_r , the space charge density of the r'th stream

Φ , the electric potential

Φ_0 , the electric potential of the undistrubed plasma

ϕ , the perturbed electric potential

ϕ , the fluctuating potential on a probe

ω , the radian frequency

$\vec{\omega}_c$, the cyclotron frequency vector for ions or for electrons

$\omega_c = |\vec{\omega}_c|$

ω_{max} , the upper frequency limit for the ion noise spectrum

ω_0 , the Tonks-Langmuir ion frequency defined by (1.17)

ω_p , the ion or electron plasma frequency

ω_r , the characteristic frequency of the r'th stream

ω_1 , the ratio of the frequency to the cyclotron frequency

Appendix 3

A GENERALIZED ION DISPERSION RELATION

An extension of some of the material in Chapter I is made in this appendix to include the role of ion drift and attenuation due to ion collisions.

The general differential equations (1.1-1.5) embrace the effect of ion collisions and permit a drift in the ion stream. However, the perturbation equations (1.7-1.10) neglect these factors. If we rewrite the perturbation equations including these factors only the Lorentz law is changed. It now has the form,

$$\frac{e}{m\rho}(-\nabla\phi + \vec{u}\times\vec{B}_0) = \frac{\partial\vec{u}}{\partial t} + (\vec{v}_{p_0}\cdot\nabla)\vec{u} + \nu\vec{u}. \qquad (3.1)a$$

Equations (1.11) and (1.12) remain unchanged under the generalization since neither of these involves the Lorentz equation. Taking the gradient of (1.12), as before, and eliminating the potential by using (3.1)a gives

$$\left(\nabla^2 - \frac{\omega_p^2 m\rho}{kT}\right)\left[\frac{\partial^2\vec{u}}{\partial t^2} + \left(\vec{v}_{p_0}\cdot\nabla\right)\frac{\partial\vec{u}}{\partial t} + \nu\frac{\partial\vec{u}}{\partial t} - \frac{\partial\vec{u}}{\partial t}\times\vec{B}_0\right] = -\omega_p^2\nabla(\nabla\cdot\vec{u}) \qquad (3.2)a$$

where $(\nabla^2 - \frac{\omega_p^2 m_p}{kT})$ is understood to be a distributive operator. Just as in the discussion of the less general form in Chapter I, we seek solutions to this equation in the form of propagating waves,

$$\vec{u} = [u_1, u_2, u_3,]\, e^{i(\omega t - \beta z)}. \qquad (3.3)a$$

Adopting the convention of (1.15) the equations of (1.16) now have the form

$$\left(\beta^2+\frac{\omega_p^2 m_p}{kT}\right)\left[(\omega^2-i\omega\nu-\omega\beta u_0)u_1+i\omega(u_2\omega_c\cos\theta-u_3\omega_c\sin\theta)\right]=0, \tag{3.4a)a}$$

$$\left(\beta^2+\frac{\omega_p^2 m_p}{kT}\right)\left[(\omega^2-i\omega\nu-\omega\beta u_0)u_2-i\omega u_1\omega_c\cos\theta\right]=0, \text{ and} \tag{3.4b)a}$$

$$\left(\beta^2+\frac{\omega_p^2 m_p}{kT}\right)\left[(\omega^2-i\omega\nu-\omega\beta u_0)u_3+i\omega u_1\omega_c\sin\theta\right]-\omega_p^2\beta^2 u_3=0 \tag{3.4c)a}$$

where u_0 represents the ion drift velocity in the direction of propagation z. Just as before a solution for u_1, u_2, and u_3 implies that the determinant of the coefficients vanish and adapting the notation previously used the dispersion relation becomes,

$$\left[(\omega-i\nu-\beta u_0)^2-(\omega_c\cos\theta)^2\right](\omega^2-i\nu\omega-\beta u_0\omega-\omega_0^2)$$
$$-(\omega_c\sin\theta)^2(\omega^2-i\nu\omega-\beta u_0\omega)=0. \tag{3.5)a}$$

This is the more general form of (1.18a). This expression is considerably more complicated than the form which neglects ion drift and the damping due to collisions, but certain interesting observations are readily made:

a. <u>The dispersion relation is independent of the components of ion drift normal to the direction of propagation.</u>

b. $\omega_0 \to 0$. If the ion density approaches zero the dispersion relation becomes

$$(\omega^2-i\nu\omega-\beta u_0\omega)\left[(\omega-i\nu-\beta u_0)^2-\omega_c^2\right]=0;$$

there are three solutions

$$\omega=\beta u_0+i\nu \text{ and} \tag{3.6)a}$$

$$\omega = \beta u_0 + i\nu \pm \omega_c . \qquad (3.7)a$$

Here the ions are so loosely coupled that waves can propagate in the medium only by being carried with the drift velocity of the ions in the direction of propagation. In (3.6)a the ion motion is in the direction of propagation, and the frequency is given by the doppler shift. In (3.7)a the perturbed ion motion is normal to the propagation direction and the doppler frequency is modified by the cyclotron frequency.

c. $\omega_c = 0$. If the magnetic field vanishes

$$(\omega - i\nu - \beta u_0)^2 (\omega^2 - i\nu\omega - \beta u_0 \omega - \omega_0^2) = 0,$$

and again the doppler shift gives one solution. For the other,

$$\omega = \frac{\beta u_0 + i\nu}{2} \pm \sqrt{\frac{(\beta u_0 + i\nu)^2 + \omega_0^2}{2}}, \qquad (3.8)a$$

the more general form of the Tonks and Langmuir solution that embraces the damping due to collisions and the effect of ion drift.

d. If the propagation is parallel to the magnetic field, $\sin\theta = 0$, and

$$\left[(\omega - i\nu - \beta u_0)^2 - \omega_c^2\right](\omega^2 - i\nu\omega - \beta u_0 \omega - \omega_0^2),$$

which gives two solutions already discussed above. For the one, ion perturbation is normal to the field, for the other, parallel to the field.

e. If propagation is normal to the field, $\cos\theta = 0$, and one solution is given by the doppler shift (3.6)a; the other solutions are quite complicated.

Appendix 4

THE INTEGRAL, $p(a) = \int_{-\infty}^{\infty} \frac{e^{-(x-a)^2}}{x}\,dx$

The value of the integral p(a) is determined formally in the text. In this appendix, the integral is properly defined and its value determined more carefully.

It is evident that p(a) does not exist as a Riemann integral. As in many problems in physics, the integral must be interpreted in the Cauchy sense if the answer is to have any meaning. We therefore write,

$$p(a) = \lim_{b\to\infty}\lim_{\epsilon\to 0^+}\left\{\int_{-b}^{-\epsilon}\frac{e^{-(x-a)^2}}{x}\,dx + \int_{\epsilon}^{b}\frac{e^{-(x-a)^2}}{x}\,dx\right\}. \qquad (4.1)a$$

Introducing a new function,

$$f(a) = \lim_{b\to\infty}\lim_{\epsilon\to 0^+}\left\{\int_{-b}^{-\epsilon}\frac{e^{-x^2+2ax}}{x}\,dx + \int_{\epsilon}^{b}\frac{e^{-x^2+2ax}}{x}\,dx\right\};$$

we note that if f(a) exists, then p(a) exists and has the value,

$$p(a) = e^{-a^2} f(a). \qquad (4.2)a$$

Now by changing the sign of x in the first integral of f(a),

$$f(a) = \lim_{b\to\infty}\lim_{\epsilon\to 0^+}\int_{\epsilon}^{b} e^{-x^2}\,\frac{e^{2ax} - e^{-2ax}}{x}\,dx. \qquad (4.3)a$$

The integrand in this expression has a removable singularity at x = 0, and by defining the value of the integrand at

$x = 0$ as (4a), it becomes continuous on $[o, b]$, and we have unambiguously

$$f(a) = \lim_{b\to\infty} \int_0^b e^{-x^2} \frac{e^{2ax} - e^{-2ax}}{x}\, dx. \qquad (4.4)a$$

The next step is to show that the derivative of f(a) can be obtained by differentiating this expression under the integral sign. After that, the value of p(a) is established just as in the text. The proof that the differentiation can be carried under the integral sign follows the conventional development except that here the interval is infinite and this imposes a more severe restriction on the integrand.

From (4.4)a,

$$\frac{f(a) - f(a_0)}{a - a_0} = \lim_{b\to\infty} \int_0^b \frac{e^{-x^2}}{x} \left\{ \frac{e^{2ax} - e^{2a_0x}}{a - a_0} - \frac{e^{-2ax} - e^{-2a_0x}}{a - a_0} \right\} dx.$$

Now employing the mean value theorem, one has

$$\frac{e^{2ax} - e^{2a_0x}}{a - a_0} - \frac{e^{-2ax} - e^{-2a_0x}}{a - a_0} = 2x\left(e^{2a_1x} + e^{-2a_2x}\right)$$

where a_1 and a_2 are on $[a, a_0]$. Then

$$\frac{f(a) - f(a_0)}{a - a_0} = 2\lim_{b\to\infty} \int_0^b e^{-x^2}\left(e^{2a_1x} + e^{-2a_2x}\right) dx .$$

Whence,

$$\left| \frac{f(a) - f(a_0)}{a - a_0} - 2\lim_{b\to\infty} \int_0^b e^{-x^2}\left(e^{2ax} + e^{-2ax}\right) dx \right|$$

$$\leq \left| 2\lim_{b\to\infty} \int_0^b e^{-x^2}\left(e^{2a_1x} - e^{2ax} + e^{-2a_2x} - e^{-2ax}\right) dx \right| .$$

This expression can be made arbitrarily small by taking a_0 sufficiently close to a. Therefore,

$$f'(a) = 2 \lim_{b \to \infty} \int_0^b e^{-x^2} (e^{2ax} + e^{-2ax})\, dx,$$

and we have established the right to differentiate under the integral sign. The rest of the argument follows as in the text.

$$f'(a) = 2e^{a^2} \lim_{b \to \infty} \int_{-b}^{b} e^{-(x-a)^2}\, dx = 2\sqrt{\pi}\, e^{a^2}.$$

Integrating, $$f(a) = 2\sqrt{\pi} \int_0^a e^{\eta^2}\, d\eta,$$

the constant of integration necessarily being zero, and then,

$$p(a) = 2\sqrt{\pi}\, e^{-a^2} \int_0^a e^{\eta^2}\, d\eta.$$

This is the result formally derived in the text.

Appendix 5

THE EXPERIMENTAL DETERMINATION OF THE POWER SPECTRUM

The experimental method for observing the power spectrum in this study has been to employ superheterodyne receivers to convert, filter, amplify, and detect the incoming noise. The relation between the output of the receiver with noise at the input and the power spectrum of the noise source is discussed in this appendix.

Input Quantities	Output Quantities
Potential: $\Phi(t)$	Potential: $\phi(t)$
Transform: $S(f)$	Transform: $s(f)$
Power spectrum: $G(f)$	Power spectrum: $g(f)$

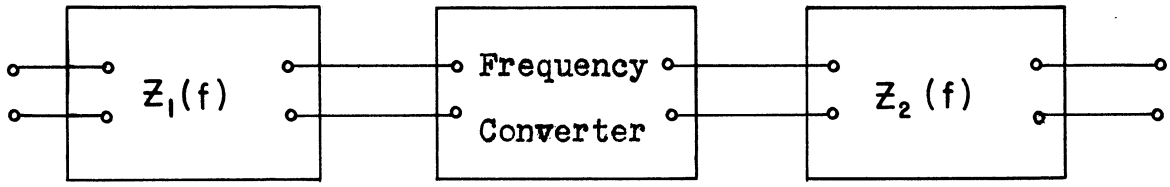

Figure 5.1a

Consider Figure 5.1a which shows an idealized receiver that amplifies, converts, and filters. It is assumed that the potential $\Phi(t)$ at the input is amplified and filtered by the

linear transfer function $Z_1(f)$, the result translated f_0 in frequency by the converter, and then amplified and filtered by the transfer function $Z_2(f)$ which represents the intermediate frequency stages with f_i as the intermediate frequency. Using this idealization and the notation of Figure 5.1a the Fourier transform for the output of the first stage is $S(f)\cdot Z_1(f)$. After the converter stage this has the form $S(f+f_0)Z_1(f+f_0)$, and after the i-f stages, $S(f+f_0)Z_1(f+f_0)Z_2(f)$.

Now we write without proof the expression relating the auto-correlation function of the output potential with its power spectrum,[1]

$$\overline{\phi(t)\,\phi(t+\tau)} = \int_0^\infty g(f)\cos(2\pi f\tau)\,df. \qquad (5.1)a$$

As a special case of this,

$$\overline{\phi^2(t)} = \int_0^\infty g(f)\,df. \qquad (5.2)a$$

But the output spectrum is related to the input spectrum by

$$g(f)=G(f+f_0)\left|Z_1(f+f_0)\,Z_2(f)\right|^2.$$

Putting this in (5.2)a gives

$$\overline{\phi^2(t)} = \int_0^\infty G(f+f_0)\left|Z_1(f+f_0)Z_2(f)\right|^2 df. \qquad (5.3)a$$

Now the function Z_2 in the integrand of this expression

---

[1]For a proof, see Reference 39, p. 40.

represents the intermediate frequency stages; this function peaks sharply where the argument is f_i and is very small except near this frequency. Assuming that the change in the power spectrum of the input is slight where the intermediate frequency gain is appreciably different from zero, equation (5.3)a can be approximated

$$\overline{\phi^2(t)} = G(f_i + f_0)\int_0^\infty \left|Z_1(f+f_0)\,Z_2(f)\right|^2 df. \qquad (5.4)a$$

Defining a noise bandwidth by

$$B = \frac{\int_0^\infty \left|Z_1(f+f_0)Z_2(f)\right|^2 df}{\left|Z_1(f_i+f_0)Z_2(f_i)\right|^2}, \qquad (5.5)a$$

equation (5.4)a has the form

$$\overline{\phi^2(t)} = B\cdot G(f_i+f_0)\left|Z_1(f_i+f_0)Z_2(f_i)\right|^2. \qquad (5.6)a$$

$\overline{\phi^2(t)}$ represents the average power output of this idealized system,[1] and $\left|Z_1(f_i+f_0)Z_2(f_i)\right|^2$ represents the peak power gain at the frequency (f_i+f_0). Then the ratio of these two quantities,

$$\frac{\overline{\phi^2(t)}}{\left|Z_1(f_i+f_0)Z_2(f_i)\right|^2},$$

is equal to the minimum average power input (centered on the pass-band) required to give the same power output $\overline{\phi^2(t)}$.

[1] The word power is conventionally but abusively used in this way. Actually this is a mean-squared voltage and represents power only in the sense that it works into a unit resistance.

Returning this result to equation (5.6)a, we have that

$$\text{(amplitude of the power spectrum)} = \frac{\text{(minimum input power for the given output)}}{\text{(noise bandwidth)}} . \qquad (5.7)a$$

Thus the power spectrum at a given frequency is obtained by dividing the input power of a calibrating signal generator (which gives the same output as the noise source) by the noise bandwidth of the receiver.

The following receivers were used in this study.

Receiver	Tuning unit	Frequency range (in mc/sec)	Noise bandwidth (in kc/sec)
Hallicrafter (SX71U)		0.56 - 34 47. - 55	2.83
APR - 4	TN - 16	38. - 95	169.
	TN - 17	74. - 320	
	TN - 18	300. - 1000	
	TN - 19	975. - 2200	
	TN - 54	2150. - 4000	

The following signal generators were used in this study.

Signal generator	Type	Frequency Range
General Radio	Standard Signal Generator 1001A	5 kc - 50 mc/sec
General Radio	VHF Signal Generator	50 - 930 mc/sec
Hewlett-Packard	UHF Signal Generator Model 614A	800 - 2100 mc/sec

Equation (5.7)a makes it clear that the output of the receiver must be metered using a square-law device. The method adopted in this study was to use the filtered output

of the second detector. For low power input this is square-law; for high power it is more nearly linear. Many of the data were taken in the square-law region, but part of the data were taken in the region where the second detector was nearly linear. It will be assumed that the greatest error in the spectrum does not exceed that which would be produced by a linear detector and an estimate of that error will be obtained.

The procedure in determining the spectrum with a square-law device is as follows. The noise potential $\Phi(t)$ at the input of the receiver of Figure 5.1a gives an output $\phi(t)$. A calibrating signal $A \cos \omega t$ is fed into the receiver in place of the noise; its output is $a \cos(\omega t + \alpha)$. A is chosen so that

$$\overline{\phi^2(t)} = \overline{\left[a \cos(\omega t + \alpha)\right]^2} = \frac{a^2}{2} . \qquad (5.8)a$$

Then the power spectrum at the frequency $f = \frac{\omega}{2\pi}$ is given by

$$G(f) = \frac{A^2}{2B}$$

where B is the noise bandwidth.

Now if the recifier is linear and not square-law one mistakenly gets

$$G_1(f) = \frac{A_1^2}{2B}$$

for the power spectrum. A_1 is now determined by

$$\overline{|\phi(t)|} = \overline{|a_1 \cos(\omega t + \alpha_1)|} = \frac{2}{\pi} a_1 \qquad (5.9)a$$

with the calibration input $A_1 \cos \omega t$ and its output $a_1 \cos(\omega t + a_1)$. Thus the ratio of the correct power spectrum to that which would be observed with a linear rectifier is

$$\frac{G(f)}{G_1(f)} = \frac{A^2}{A_1^2} = \frac{a^2}{a_1^2} \quad . \tag{5.10)a}$$

By equations (5.8)a and (5.9)a

$$\frac{a^2}{a_1^2} = \frac{8}{\pi^2} \cdot \frac{\overline{\phi^2(t)}}{\overline{|\phi(t)|}^2} \quad ,$$

so that

$$\frac{G(f)}{G_1(f)} = \frac{8}{\pi^2} \cdot \frac{\overline{\phi^2(t)}}{\overline{|\phi(t)|}^2} \quad . \tag{5.11)a}$$

This equation indicates the error that can be introduced by a linear detector.

Since it is always true that

$$\overline{\phi^2(t)} \geq \overline{|\phi(t)|}^2 ,$$

$$\frac{G(f)}{G_1(f)} \geq \frac{8}{\pi^2} ,$$

and the power spectrum as determined is never greater than the true power spectrum by more than

$$100\left(\frac{\pi^2}{8} - 1\right) = 24\% .$$

Actually it is the square root of the power spectrum that is studied in Chapter III, and this will not be too high by more and 11%.

No such general argument limits the observed power

spectrum from being much too small since the ratio on the right of (5.11)a can get arbitrarily large if any choice of output potential $\phi(t)$ is tolerated. However, it is often reasoned that the output of a narrow band filter with a broad band noise input has a gaussian amplitude distribution in time. For such a distribution

$$\frac{\overline{\phi^2(t)}}{\overline{|\phi(t)|}^2} = \frac{\pi}{2},$$

and

$$\frac{G(f)}{G_1(f)} = \frac{8}{\pi^2} \cdot \frac{\overline{\phi^2(t)}}{\overline{|\phi(t)|}^2} = \frac{4}{\pi} .$$

The corresponding error in the square root of the power spectrum is about 11%.

We summarize these arguments by noting that many of the data were taken in the range where the detector was square-law. However some of the data were taken where the detector was more nearly linear. The error introduced by this departure from square-law does not likely exceed 24% in power or 11% in voltage. This error is of the same magnitude as that introduced by the mismatch on the line and the general reproducibility of data. Therefore no attempt has been made to adjust the data to compensate for this error.

Appendix 6

A PROOF OF THE NYQUIST NOISE FORMULA USING PLANCK HARMONIC OSCILLATORS

6.1 Introduction

The theoretical study of noise in a linear electrical circuit has been a popular one since the classic work of Nyquist.[1] Such studies have usually attempted a derivation of the Nyquist formula for the noise spectrum of a linear resistance, either by thermodynamic or kinetic theory arguments. The formula applies to a gas discharge tube. Indeed Knol has shown that the electron temperature in a gas discharge can be determined by identifying the experimentally determined power spectrum with the value from the Nyquist formula.

The Nyquist result can be summarized in the following theorem:

Every linear frequency dependent conductance g(f) in thermal equilibrium at temperature T has associated with it a noise source which can be represented by a shunting current generator with the power spectrum

$$4g(f)\,\overline{\mathcal{E}(f)}\quad, \tag{6.1}$$

where

$$\overline{\mathcal{E}(f)} = \frac{hf}{e^{\frac{hf}{kT}} - 1}\quad, \tag{6.2}$$[2]

[1] Reference 43.

[2] This form is often approximated $\overline{\mathcal{E}(f)} = kT$ since hf/kT is usually very small for the frequencies encountered in electric circuits.

h is Planck's constant, k is the Boltzmann constant, and f the frequency.

This theorem is stated in its generality by Nyquist in his original paper, but his proof has a serious shortcoming; implicit in his argument of a resistor matched to a lossless transmission line is the assumption that the resistance does not depend on frequency. Subsequent articles have avoided this difficulty, but not without other limiting assumptions, and the theorem has apparently never been established in its generality. The following seem to be the principal assumptions that have limited previous proofs.

(1) The conductance is taken independent of frequency. (See Moullin,[1] Nyquist,[2] Schremp,[3] and van der Ziel.[4])

(2) Equipartition of the energy in electric circuit elements is employed. (See Uhlenbeck,[5] Moullin,[1] and van der Ziel.[4]) The difficulty here is that the theoretical proofs of equipartition rely on the Nyquist formula, and therefore equipartition cannot be used in the proof of the Nyquist theorem.

(3) The kinetic theory models are one dimensional. (See Bakker and Heller,[6] Bell,[7] and Schremp.[3]) Apparently

---

[1]References 42 and 43.

[2]Reference 45.

[3]Reference 53.

[4]Reference 61.

[5]Reference 39.

[6]Reference 9.

[7]Reference 11.

all kinetic theory models have been one dimensional. The early studies permitted only particle motion in one direction; more recent models have included velocity components in all directions but allowed only one of these to couple current into the conductance terminals.

(4) All kinetic theory arguments have assumed a mean-free time or a mean-free path independent of the particle velocity. (See Bakker and Heller,[1] Bell,[2] Schremp.[3]) This step seemed to be necessary since previous kinetic theory arguments have resorted to Fourier theory techniques.

All these assumptions are avoided in the present development of the Nyquist theorem.

Nyquist pointed out that two linear conductances that have the same value at all frequencies, in equilibrium at temperature T, necessarily have the same noise spectrum; for if their spectra differ, they can be connected together with a shunting lossless filter in such a way that a net power is transferred from one to the other, and this is a contradiction of thermal equilibrium.[4] From this we have that any kinetic theory model that established the Nyquist formula (6.1) for a general frequency dependent linear conductance g(f) necessarily establishes the formula for all linear conductances.

---

[1]Reference 9.

[2]Reference 11.

[3]Reference 53.

[4]Reference 45.

The argument developed below shows that the noise current delivered to the terminals of a resistance is given by a sum over the charged particles in the "interaction space." This expression is obtained for an N terminal structure since the derivation is no simpler if the number of terminals are restricted to two. The result is applied to a model where the charged particles are a system of Planck harmonic oscillators, homogeneously distributed in the interaction space. It is shown that the Nyquist formula applies rigorously for this model, and since any linear frequency dependent conductance can be constructed by a homogeneous distribution of Planck harmonic oscillators, the theorem is proven.

6.2 Induced Current Theory

The objective of the appendix is an expression for the spectrum of current flowing to each of N terminals. These currents have their origin in the motion of charged particles in the interaction space and are determined by the terminal geometry, the charge on the particles, and the particle motions. The Theory of Induced Currents provides the necessary quantative relation; but since this theory is not widely appreciated and never argued in its generality, a derivation of the formula for the induced current in a terminal will be included.[1]

Let q_j represent the charge inside a closed surface bounding the j'th terminal, then by the familar divergence

---

[1]See Reference 33. This article by Jen is perhaps the best published derivation, but it lacks the generality of the present argument.

relation

$$q_j = -\epsilon_0 \int E_N \, dS_j \quad , \text{ where} \tag{6.3}$$

E_N represents the normal component of the electric field at the surface, and ϵ_0 is the free-space dielectric constant. Taking the partial derivative of (6.3) with respect to time gives

$$\dot{q}_j = -\epsilon_0 \int \dot{E}_N \, dS_j \quad , \tag{6.4}$$

but from the conservation of charge one must have

$$\dot{q}_j = i_j + \int J_N \, dS_j \quad , \tag{6.5}$$

where i_j represents the current flowing to the j'th terminal through its connecting lead and the integral gives the current arriving from the interaction space. Substituting from (6.5) into (6.4) one has

$$i_j = -\int (J_N + \epsilon_0 \dot{E}_N) \, dS_j \quad . \tag{6.6}$$

Using this form, the current in the j'th terminal can easily be expressed as an intergral over the interaction space, for suppose we uniquely define a function ψ_j as follows: let

$$\psi_j = \begin{cases} 1 \text{ ON } S_j \\ 0 \text{ ON } S_m \, , \; m \neq j \end{cases} \quad , \tag{6.7}$$

and

$$\nabla^2 \psi_j = 0 \tag{6.8}$$

in the interaction space. Then clearly (6.6) can also be written

$$i_j = -\int \psi_j \left(J_N + \epsilon_0 \dot{E}_N\right) dS \qquad (6.9)$$

where $S = \sum_j S_j$, the surface of all terminals. Equation (6.9) can now be written as a volume integral over the interaction space.

$$i_j = -\int \nabla \cdot \left\{ \psi_j \left(\vec{J} + \epsilon_0 \dot{\vec{E}}\right)\right\} d\tau$$

$$= -\int \nabla \psi \cdot \left(\vec{J} + \epsilon_0 \dot{\vec{E}}\right) d\tau \qquad (6.10)$$

since $\nabla \times \vec{H} = \vec{J} + \epsilon_0 \dot{\vec{E}}$ is divergence free.

One more step remains before the current is in an appropriate form. This is accomplished by reducing the electric field of this expression to the sum of three terms.

$$\vec{E} = \vec{E}_1 + \vec{E}_2 + \vec{E}_3 \qquad (6.11)$$

defined as follows.

Let a scalar potential Φ_j be associated with each of the N terminals; then write

$$\vec{E}_1 = -\sum_j \Phi_j \nabla \psi_j \quad . \qquad (6.12)$$

In this manner we have defined a field that is associated with the interaction space if no space-charge is present. Also, $\vec{E}_1$ is irrotational and solenoidal, and its potential is

$$\phi_1 = \sum_j \Phi_j \psi_j \qquad (6.13)$$

Now $\vec{E}_2$ is to be defined so that it accounts for the remaining charges on the electrodes, and those in the interaction space. Likewise, it is to be irrotational and its potential added to that of $\vec{E}_1$ is to be the potential in the volume and on the bounding surface. Thus,

$$\nabla \times \vec{E}_2 = 0 , \tag{6.14a}$$

$$\nabla \cdot \vec{E}_2 = -\nabla^2 \phi_2 = \frac{\rho}{\epsilon_0} , \tag{6.14b}$$

$$\text{and } \phi_2 = 0, \text{ ON } S \tag{6.14c}$$

which uniquely defines the field $\vec{E}_2$. Then $\vec{E}_3$ is simply the difference

$$\vec{E}_3 = \vec{E} - \left(\vec{E}_1 + \vec{E}_2\right) . \tag{6.15}$$

The field $\vec{E}_3$ has the following two important properties. (1) It is solenoidal, a property evident if one takes the divergence of equation (6.15), and (2) the normal component of $\vec{E}_3$ vanishes on S .

This splitting of the field into these three components may seem somewhat artificial; its importance in induced current theory will be seen presently when we return to equation (6.10), but it is worth remarking in passing that <u>this division of the electric field corresponds to dividing the power originating in the interaction space into that delivered to the terminals, that radiated from the system, and that vested in the capacity of the electrode structure</u>.

Now returning to equation (6.10) and dividing the electric field into these three components gives

$$i_j = -\int \nabla\psi_j \cdot \vec{J} d\tau - \epsilon_0 \int \nabla\psi_j \cdot \vec{\dot{E}}_1 d\tau - \int \nabla\psi_j \cdot \vec{\dot{E}}_2 d\tau - \int \nabla\psi_j \cdot \vec{\dot{E}}_3 d\tau \quad . \tag{6.16}$$

The last two integrals of this expression vanish, for applying the divergence relation to the last integral one obtains

$$\int \psi_j \cdot \dot{E}_{3N}\, dS = \int \nabla\psi_j \cdot \vec{\dot{E}}_3 d\tau + \int \psi_j \nabla \cdot \vec{\dot{E}}_3 d\tau \quad , \tag{6.17a}$$

but $E_{3N} = 0$ on S and $\nabla \cdot \vec{E}_3 = 0$,

so that

$$\int \nabla\psi_j \cdot \vec{\dot{E}}_3 \, d\tau = 0 \quad . \tag{6.17b}$$

Similarly,

$$\int \dot{\phi}_2 \left(\nabla\psi_j\right)_N dS = \int \nabla\dot{\phi}_2 \cdot \nabla\psi_j \, d\tau + \int \dot{\phi}_2 \nabla^2\psi_j \, d\tau \, , \tag{6.18a}$$

but $\phi_2 = 0$ on S and $\nabla^2\psi_j = 0$,

so that

$$\int \dot{E}_2 \cdot \nabla\psi_j \, d\tau = 0 \quad . \tag{6.18b}$$

Thus equation (6.16) has the form

$$i_j = -\int \nabla\psi_j \cdot \vec{J} d\tau - \epsilon_0 \int \nabla\psi_j \cdot \vec{\dot{E}}_1 d\tau \quad . \tag{6.19}$$

Using (6.12) the second integral in this expression can be written

$$\epsilon_0 \int \nabla \psi_j \cdot \vec{E}_1 \, d\tau = - \sum_k \Phi_k \epsilon_0 \int \nabla \psi_j \cdot \nabla \psi_k \, d\tau \quad . \tag{6.20}$$

Clearly

$$C_{jk} = \epsilon_0 \int \nabla \psi_j \cdot \nabla \psi_k \, d\tau \tag{6.21}$$

is the matrix of capacities for the N terminal system; using this notation (6.19) can be written

$$i_j = - \int \nabla \psi_j \cdot \vec{J} \, d\tau + \sum_k C_{jk} \dot{\Phi}_k \quad . \tag{6.22}$$

Thus the current flowing to any terminal can be reduced to a capacitive current and an "induced current."

It is convenient conceptually to think of the induced currents as the only currents flowing to capacity free electrodes and to account for the capacitive effects by allowing for condensers C_{jk} near the electrodes. With this understanding, we write

$$i_j = - \int \nabla \psi_j \cdot \vec{J} \, d\tau \quad . \tag{6.23}$$

An alternative form for (6.23) is

$$\begin{aligned} i_j &= - \int \nabla \cdot \left(\psi_j \vec{J} \right) d\tau + \int \psi_j \nabla \cdot \vec{J} \, d\tau \\ &= - \int \psi_j J_N \, dS - \int \psi_j \dot{\rho} \, d\tau \\ &= - \int J_N \, dS_j - \frac{d}{dt} \int \psi_j \rho \, d\tau \quad . \end{aligned} \tag{6.24}$$

In this form the induced current in the j'th electrode has been reduced to the sum of the "arrival current" and the rate of change of induced charges where ψ_j represents the fraction of the charge $(\rho\, d\tau)$ in the volume element $d\tau$ induced on the j'th electrode.

From (6.23) it is evident that the contribution of a single particle to the induced current is

$$i_j = -q\vec{u}\cdot\nabla\psi_j \qquad (6.25)$$

where q is the charge on the particle and $\vec{u}$ its velocity. The integral of (6.23) can just as well be expressed as an integral over the charges as one over the volume,

$$i_j = -\int \nabla\psi_j \cdot \vec{u}\, dq \quad , \qquad (6.26)$$

where it is understood that the integration is over all the charge in the interaction space.

6.3 The Thermal Noise Spectrum

We imagine now that the charged particles of the interaction space have random motions, and we proceed to investigate a volume $d\tau$ of that space sufficiently small that $\nabla\psi_j$ is essentially constant over that volume but large enough that the distribution of particle velocities in the volume is representative of that region of the interaction space. Applying equation (6.25) to a particle in $d\tau$

$$i_j = -qu\left|\nabla\psi_j\right| \qquad (6.27)$$

where u is the component of $\vec{u}$ in the direction of $\nabla\psi_j$. Squaring (6.27) and taking the average in time for that particular particle.

$$\overline{i_j^2} = \frac{q^2(\nabla\psi_j)^2}{m} \cdot \overline{mu^2} \quad . \tag{6.28}$$

where $\overline{mu^2}$ is twice the average kinetic energy for the particle in question in the direction of $\nabla\psi_j$.

At this point the argument is specialized to a particular model. We choose a system of Planck harmonic oscillators for the particles. The merit of this particular choice will shortly appear. The choice really represents no loss of generality since, as will be argued later, every linear system is "equivalent" to a system of Planck harmonic oscillators.

For a Planck harmonic oscillator we have

$$\overline{mu^2} = \overline{\mathcal{E}(f)} = \frac{hf}{e^{\left(\frac{hf}{kT}\right)} - 1} \tag{6.29}$$

where $\overline{\mathcal{E}(f)}$ is the average energy of an oscillator of frequency f , and the other symbols have their familiar meanings. Now in the volume element $d\tau$ there are

$$n(f)\,df\,d\tau \tag{6.30}$$

particles with frequencies in the interval $(f, f+df)$ where $n(f)$ is the density of particles in frequency per unit volume. Using this expression and (6.29), the average of the square of the induced current for oscillators in the frequency range $(f, f+df)$ and the volume element $d\tau$ is

$$\frac{\left(q\nabla\psi_j\right)^2}{m}\, n(f)\,\overline{\mathcal{E}(f)}\,df\,d\tau \quad . \tag{6.31}$$[1]

Integrating this expression gives the current spectrum at the j'th electrode; in particular, if the Planck harmonic oscillators are homogeneously distributed, i.e., $n(f)$ is independent of the position in the interaction space,

$$G_j(f)\,df = \frac{q^2 n(f)}{m}\,\overline{\mathcal{E}(f)}\,df\int\left(\nabla\psi_j\right)^2 d\tau \quad . \tag{6.32}$$

For a homogeneous system the conductivity $\sigma(f)$ is the same at every point in the volume, and the conductance between the j'th electrode and all other electrodes tied together is given by

$$g_j(f) = \sigma(f)\int\left(\nabla\psi_j\right)^2 d\tau \quad . \tag{6.33}$$

Substituting the integral from this expression into (6.32) gives

$$G_j(f)\,df = \frac{q^2 n(f)\, g_j(f)}{m\sigma(f)}\,\overline{\mathcal{E}(f)}\,df \quad . \tag{6.34}$$

We proceed next to determine the conductivity of a system of Planck harmonic oscillators; this conductivity substituted into (6.34) will give the final relation.

The differential equation for the motion of a single harmonic oscillator can be written

---

[1]The justification for adding the squares of the particle currents is the assumption that the particle velocities are independently distributed with zero mean.

$$qE = m\frac{d^2x}{dt^2} + a\frac{dx}{dt} + bx \ ,$$

or in terms of current,

$$E = \frac{m}{q^2}\frac{di}{dt} + ri + S\int i\,dt \quad . \tag{6.35}$$

Under the influence of an electric field $E = E_0 e^{j2\pi ft}$ one has a solution of the form

$$i = I_0 e^{j2\pi ft}$$

such that

$$\frac{I_0}{E_0} = \frac{1}{r + j\left(\frac{2\pi mf}{q^2} - \frac{js}{2\pi f}\right)} = \frac{1}{r + j\frac{2\pi m}{q^2 f}\left(f^2 - f_0^2\right)} \tag{6.36}$$

where f_0 is the resonant frequency of the oscillator. Now if the density of resonant frequencies per unit volume of the harmonic oscillators is given by $n(f_0)$, then the conductivity can be written:

$$\sigma(f) = \int_0^\infty \text{REAL PART OF}\left(\frac{I_0}{E_0}\right) n(f_0)\,df_0$$

$$= \int_0^\infty \frac{r\,n(f_0)\,df_0}{r^2 + \left(\frac{2\pi m}{q^2 f}\right)^2 \left(f^2 - f_0^2\right)^2} \quad . \tag{6.37}$$

For Planck harmonic oscillators we are concerned with the conductivity for the case of very sharp resonance; that is, $r \longrightarrow 0$. In addition, for r small the principal contribution

to the integral of equation (6.37) is very near $f_0 = f$ so that for a system of Planck harmonic oscillators we have the conductivity:

$$\sigma(f) = n(f) \lim_{r \to 0} \int_0^{\infty} \frac{r\, df_0}{r^2 + \left(\frac{2\pi m}{q^2 f}\right)^2 \left(f^2 - f_0^2\right)^2}$$

$$= n(f) \lim_{r \to 0} \int_0^{\infty} \frac{r\, df_0}{r^2 + 4\left(\frac{2\pi m}{q^2}\right)^2 \left(f - f_0\right)^2}$$

$$= \frac{q^2\, n(f)}{4m} . \qquad (6.38)$$

Substituting from here into (6.34) gives

$$G_j(f)\, df = 4 g_j(f)\, \overline{\varepsilon(f)}\, df \quad . \qquad (6.39)$$

For a two terminal structure this is the celebrated equation of Nyquist; for more than two terminals the equation represents a generalization.

Conclusion

Nyquist pointed out in his original articles that any two terminal linear frequency dependent conductance in thermal equilibrium has associated with it a unique spectrum. The particular merit of a system of Planck harmonic oscillators can now be seen. From equation (6.38) one notes that any desired frequency dependent linear conductance $g(f)$ at any temperature T can be constructed from a collection of Planck harmonic oscillators, merely by choosing a suitable distribution $n(f)$, but we have proved that any such system satisfies

equation (6.39). Therefore, by the Nyquist argument every frequency dependent linear resistance must satisfy equation (6.39), and the argument is complete.

The similarity between the Planck radiation law and the Nyquist formula has often been noted in the literature. The nature of this derivation of the Nyquist theorem and its similarity to Planck's kinetic theory derivation of the radiation law leads to the following conclusion:

> All the electromagnetic energy delivered from a system of charged particles takes place either by radiation or by induction into terminals. If the system of particles is a linear black body in thermal equilibrium, which delivers energy to a nonreflecting load, then the radiation is given by Planck's law and the induction by the Nyquist formula.